On some thermally coupled systems in solid mechanics across various time scales

Thomas Heuzé

HABILITATION À DIRIGER DES RECHERCHES DE L'UNIVERSITÉ DE NANTES

présentée par

Thomas Heuzé

Spécialité

SCIENCES DE L'INGÉNIERIE ET DES SYSTÈMES

Sujet du mémoire

On some thermally coupled systems in solid mechanics across various time scales

Sur quelques systèmes couplés thermiquement en mécanique des solides à différentes échelles de temps

Présentée à l'École Centrale de Nantes le 13 juin 2023 devant le jury composé de:

Rapporteurs:	Gil Antonio	Swansea University
	Gravouil Anthony	INSA Lyon
	Mosler Jörn	Technische Universität Dortmund
Examinateurs:	Bergheau Jean-Michel	Université de Lyon, École Centrale de Lyon
	Gavrilyuk Sergey	Université d'Aix-Marseille
	Kondo Djimedo	Sorbonne Université
	Stainier Laurent	Université de Nantes, École Centrale de Nantes

Institut de Recherche en Génie Civil et Mécanique (GeM)
École Centrale de Nantes
1, rue de la Noë BP 92101
44321 Nantes Cedex 3

Contents

Acknowledgments

First of all, this work is the result of a personal journey carried out over decades, and has obviously benefited from the influence and contribution of many people, both personally and professionally.

I would like to express my gratitude to all the members of my accreditation jury. I thank first my reviewers Antonio Gil, Anthony Gravouil and Jörn Mosler, for agreeing to do this work but also for their very kind and encouraging comments on my work. I thank also my examinators (Jean-Michel Bergheau, Sergey Gavrilyuk, Djimedo Kondo and Laurent Stainier) for having accepted to participate as a jury member to this accreditation. Although you all come from various scientific communities, you each represent one of the facets of my work, and each contributed in one way or another to this work. Thanks to Jean-Michel for pushing me writing this manuscript and for your kind words on my old PhD thesis finished more than ten years ago; thanks to Sergey for the always fascinating and marvelous scientific discussions we have each time we meet; thanks to Djimedo for having accepted to be the president of this jury, for your kindness and for all your very kind and encouraging comments for the future; at last thanks to Laurent for all your contributions and for having been a scientific traveling companion for more than the past ten years as well as my jury guarantor, it seems this journey still goes on.

Of course, all these research works were not performed alone, and often result from collaborations and discussions with many people. Especially, I would like to thank all the PhD students I had the opportunity to co-supervise, for their scientific contributions but also for having gone a long way in research with me: in order of seniority Xiaoli Guo, Rohit Pethe, Jorge de Anda Salazar, Cheikh Tidiane Sow, Adrien Renaud, Ataollah Ghavamian, Abdullah Waseem, Alaa Lakiss and Benoit Lagain. I thank also all the master students which did their internship under my supervision. A big thank also to my colleague Guillaume Racineux for his constant kindness, thanks to whom I was able to come to Nantes more than ten years ago, and with whom I continued and I still continue to collaborate with great pleasure on applied subjects related to high pulsed power processes. Thanks also to my friend Nicolas Favrie for this scientific collaboration whose fruit are expected soon, for teaching me so many things, but essentially for these deep discussions which brought me a lot. Thanks also to external contributors to some common published works (Marc Geers, Varvara Kouznetsova, Antonio Gil, Michel Arrigoni), which all provided something to me.

I would also like to thank my colleagues of the (ex-)Modeling and Simulation research team for their friendliness in day-to-day life in the laboratory but also in work related to teaching, namely Patrice Cartraud, Laurent Stainier, Claude Stolz, Marie Billaud-Friess, Grégory Legrain, Nicolas Chevaugeon, Nicolas Moës, Patrick Rozycki, Pascal Cosson, Laurent Gornet, Julien Réthoré, Rian Seghir. Sorry to other colleagues of the GeM laboratory whose names cannot fit within these lines, but who are also thanked.

Last but not least, my deepest thanks go to my loved ones, family (parents and my parents-in-law) and friends, for their constant support and for all that they bring me on a daily basis. Thank you above all to my love Mélanie, who has courageously supported me day by day for almost ten years now, and to whom this manuscript is dedicated. Thanks to you, our family has grown and strongly gained in momentum with the arrival of Romane and Aubin, who one could say that they too participated in the construction of this work in their own way.

Forewords

This document is a resume of my research works carried out over these last fifteen years, from automn 2007 to automn 2022. On the one hand, this period covers my PhD thesis performed at Institut Jean Le Rond d'Alembert at University Pierre et Marie Curie over the years 2007-2011 (as a PhD student, then as lecturer or "ATER"), under the supervision of Professors Jean-Baptiste Leblond and Jean-Michel Bergheau, and in collaboration with the company ESI Group. On the other hand, the remaining eleven years were spent in the nice town of Nantes, at Ecole Centrale de Nantes at Institut de recherche en génie civil et mécanique (or in short, laboratory GeM). I came first to Nantes after my PhD as a post-doc, working with Professor Guillaume Racineux in the research team devoted to Materials and processes, then stayed in the same laboratory as assistant professor from automn 2012, which position I still hold. I joined at that time the research team "Modeling and simulation", especially working with professor Laurent Stainier.

During this large period, my research activities have mainly revolve around coupled thermo-mechanical phenomena occurring in metallic structures. I work on their modeling, on the development and/or the improvement of numerical methods providing approximations for the solution of these models, and on engineering applications in which these couplings appear naturally and whose numerical simulation requires the use of these advanced numerical methods. My research works are conducted on a broad scientific and technical spectrum, covering certain areas of theoretical mechanics and mathematics, computational mechanics and computer science, but also industrial technologies and processes.

My activities related to the modeling and numerical simulations follow an approach that consist in studying on the one hand a class of mathematical problems, whose solutions are generally useful in the description of some aspects of a given engineering problem of interest, and on the other hand its potential approximations mimicking various aspects of the solution, living in a reduced space or not. Some slow processes of diffusive nature have been studied, essentially governed by elliptic and parabolic equations and whose solutions are smooth, as well as faster ones linked to impacts on structure, which may involve hyperbolic equations whose solutions may not be smooth.

Although my contributions are mainly related to the modeling and computational areas, yet I had the pleasure to carry out a few contributions in experimental testing by either designing some new experiments by myself with the help of colleagues, or by participating or even following from afar experiments carried out by them. Although not in the majority, these activities had an important influence for me and especially on my modeling and computational activities. It helped me understand better what relationship recorded signals and simulated data can have, especially to what extent recorded signals can be usable to calibrate models, or to what extent simulated data can have a physical relevance. A last aspect of these works pertains to their relationship (even sometimes from very far) with very practical problems in mechanical engineering found in industrial technologies, such as material processing, assemblies of structures and so on. Since the beginning of my early studies, I had always the pleasure starting with some of such actual engineering problems associated with manufacturing or forming processes, from which aspects related to the process itself, the modeling of particular key phenomena involved in that process, and the numerical strategy followed for solving the model can be extracted and studied.

At last, this document has been written in a concise manner, and only describe and order the main ideas proposed during these last fifteen years, the details can be found within the papers and are not expanded here.

Autumn 2022, Thomas Heuzé

Introduction

0.1 On the interest of thermo-mechanical phenomena in solids

The study of coupled thermo-mechanical phenomena is a very old scientific topic, but still of much interest. Actually, it represents one instance among many others of multiphysic problems. The field of multiphysics is a branch of physics whose object is to couple at least two physical systems, each being governed by its own principles of evolution or equilibrium, such as balance laws or constitutive equations [106]. Many engineering problems as well as many physical phenomena can only be described correctly by coupling areas of physics that have historically been developed and taught separately. Certain physical phenomena indeed involve exchanges of energies that the history of science has classified into different types within different subfields of the physical sciences. These problems require on the one hand a good understanding of each physics governing the phenomena in presence, but especially an analysis of their coupling mechanisms, to propose relevant modelings, capable of describing these observed phenomena. The difficulty raised by such systems lies in that nonlinearities and the interaction between its different components often results in complexities. Coupled systems are systems whose behavior is driven by the interaction of functionally distinct components. Within that scope, the coupling between thermal and mechanical effects is widespread, and this is why it is still a very active research topic. The motion of the body combines with the generation and the flow of heat within it in such a way that a mutual influence between both components occur. In solid mechanics, such coupling can occur in different types of materials like metals or polymers, and through various mechanisms: temperature-dependence of elastic or inelastic properties, heating from dissipative micro-mechanisms, thermal softening (i.e. a thermally-induced reduction of the yield stress) eventually triggering thermally-induced deformation patterns such as shear banding, phase change and so on. Although much has been done in the study of thermo-mechanical phenomena in solids, and maybe some might think at first glance that everything or almost has been done in that domain, one could still mention at least three basic reasons supporting the idea that much remains to be developed in that research area.

First, it has interests related to many practical problems in engineering sciences, in which both thermal and mechanical phenomena may be coupled to each other. Applications may be linked to some well-known problems in mechanical engineering, especially related to the mechanical industry. Forging or casting processes, sheet metal forming like dreep drawing, joining heterogeneous structures through various technologies such as welding represent only a few examples of processes that rely on the exploitation of an external source of energy (it may be a mechanical or a thermal one) in order to process the matter in a desired way. But new processes involving coupled thermo-mechanical phenomena continue to be regularly proposed, as for instance additive manufacturing processes during which the material and the structure may be manufactured simultaneously. Applications may also be linked to sustainability of mechanical objects, especially to external loads like high-velocity impact which occurs during ballistic penetration. Other applications can also be found, for instance in the domain of energy. Without exhaustivity, some examples can be mentioned such as the design of materials with particular microstructures for heat storage or guidance purposes, or for the design of electrical batteries by describing the processes of charge and discharge in electrodes thanks to the analogy between heat transfer and diffusion of species.

Second, thermo-mechanics (and more generally multiphysic problems) has brought many mathematical modelings and computational methods of various complexities, whose developements are still very active. Although the basic isothermal split procedure [44] is now implemented in every finite element commercial codes to treat a basic class of coupled thermo-mechanical problems, novel formulations and associated computational methods

continue to be proposed which may be better suited, either for the numerical simulation of some particular applications which may require to account for some special coupling effect, for improving the accuracy and robustness of algorithms, or simply from the mathematical viewpoint. Regarding the latter, one good example is the use of the variational calculus [8] which has brought a very convenient and sound modeling framework, and allows in turn to naturally define efficient and consistent computational methods. The application of such approach to non-linear dissipative thermo-mechanical problems in the work of Yang et *al.* [72] represented an important step forward in this regard, providing thermodynamically consistent and numerically efficient constitutive updates, as well as a correct computation of the non-constant partition of plastic work into heat and stored energy [61]. Such variational framework calls for further developments, for instance towards gradient-enhanced theories [127, 136], or within the context of high-velocity impacts [174]. A second example pertains to thermo-mechanical multi-scale analyses which also represent a great challenge, in order to derive accurate models at higher scales while accounting for the microstructure, and to analyse the effective influence of microscopic features on the macroscopic response. Especially, investigating how local thermo-mechanical effects translate at a higher scale, the identification of enriched continua, and the definition of computationally efficient upscaling methods [161, 67] notably for non-linear problems have not yet finished to be explored. As a third example, one could also mention that the modeling of thermal effects has historically been made considering the temperature as the main thermal unknown, because it is a measurable quantity. This has led to solve thermal effects via the heat equation and to design constitutive updates driven by the temperature. However, formulations considering different primal unknowns have started to emerge recently for various reasons. The entropy may be preferred, especially in the context of large strain thermally-coupled fast transient dynamics [165], or to design unconditionally stable thermo-mechanical splitting schemes [39]. Others based on the conservation of the total energy are better suited when shocks occur, and can also be used to build dedicated constitutive updates [174].

Third, the validation of numerical simulations of various thermo-mechanical processes against experiments raises the question of the experimental characterization of these processes, and of technologies dedicated to acquiring experimental data. As a first example, much work was devoted to performing experimental energy balance, whatever at low [32] or high [57] strain rate, and determining the fractions of energy which are stored or dissipated as heat, as initially estimated in the pioneering works of Taylor and Quinney [4], and reviewed for instance in [22]. Various experimental testing apparatus were designed to this end, especially including thermal measurement through infrared thermography [49]. Though thermal cameras are now known to give quite accurate measurements for quasi-static processes when looking at plane surfaces, they are still too slow to envisage truly dynamic processes even though some attempts were performed in that direction [110]. Hence, infrared thermography is rather achieved through pyrometers which allows to get one (or few) point(s) of measurement, and whose setup is always delicate since it involves to handle parabolic mirrors [81, 84, 102]. Besides its intrinsic interest, such experimental energy balance also represent a discriminating criterion for building constitutive models, or any evolution laws describing dissipative processes which should correctly balance stored and dissipated energies. However, dedicated paths remain to be drawn in order to perform such balance in complex problems, as for instance interface problems at lower scales, in the presence of fractures, welded interface, spalling or fragmentation. Another example lies in the investigation at lower scales of the relation between thermally-induced mechanisms of change of microstructure and its mechanical loading conditions, especially in the dynamic context when strong waves propagate. Such investigation require dedicated experimental apparatus as well as highly accurate means of measurements, which can profit from ultra-high speed imaging techniques [169] for instance. As an opening, various new methods of acquiring thermal data begin to be developed, such as in-depth thermal measurement [162], or simultaneous temperature and strain measurements via thermographic phosphor coupled Digital Image Correlation [166] rather infra-red measurement, which ultimately will profit to calibration, characterization testing and energy balance purposes.

0.2 Thermo-mechanical systems across various time scales

In this manuscript, we will talk about a thermo-mechanical system as a general view of a material or an immaterial object within which both thermal and mechanical phenomena occur and interact with each other. It could just as well be a (sub)part of an experimental device or a continuous or discrete modeling of an arbitrary domain. In the latter case, a system will consist of several entities (or fields here) whose interaction and evolutions are governed by a set of equations. However, only systems lying in the field of solid mechanics

will be of interest in this manuscript.

These thermo-mechanical systems can be conveniently ordered according to the various time scales at which deformation may occur, or rather their inverse resulting in some equivalent average strain rate. Figure 1 is partly extracted from [60] and shows a simple and rough classification of some particular regimes of loading over a tenth of orders of magnitude of such average strain rate, which ranges from creep to ultra high strain rate. Each of these regimes can be associated available experimental techniques, which permit to test the mechanical response of materials at these strain rates. In regard to the above, some mechanical processes can also be affected to special sub-ranges of strain rate. A few of them will be of interest in the present work, whether they occur in quasi-static regime, at intermediate level (e.g. Friction Stir Welding), or at high or even very high strain rate (e.g. Hopkinson bars, electrohydraulic or electromagnetic pulse forming technologies).

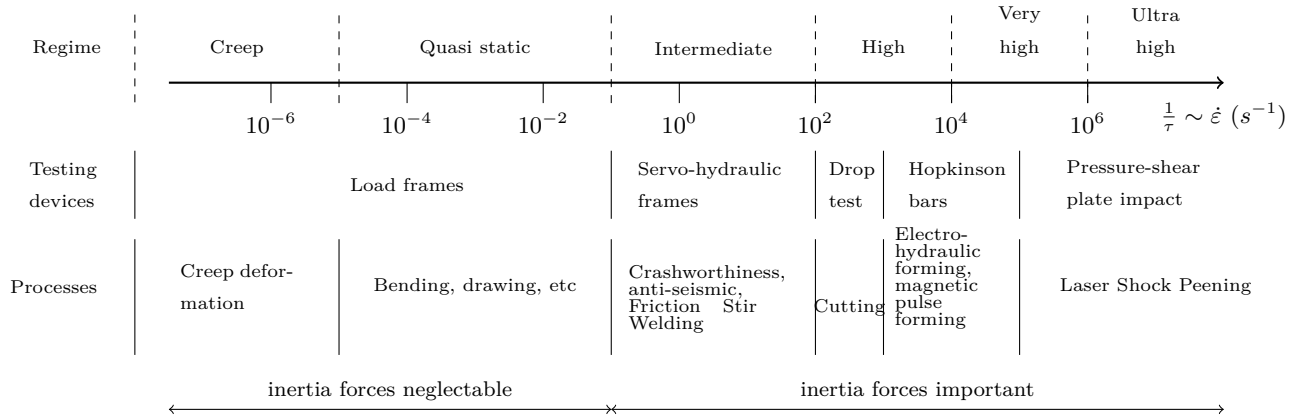

Figure 1: Strain rate regimes, and associated experimental techniques and processes.

An even more summary classification can also be established at first glance, tagging thermo-mechanical systems as being 'slow' or 'fast' ones. Slow thermo-mechanical systems will be considered as those for which mechanical inertia effects can be neglected. Usually, these systems involve quasi-static deformation process and are of diffusive nature, more precisely they include thermal (or mass) diffusion. Although the diffusion can be transient, the associated characteristic times are still very long, and compatible with those of the deformation process. Conversely, fast thermo-mechanical systems will be considered as those for which mechanical inertia effects cannot be neglected, and are of great importance. Depending on the time scale of phenomena involved in the envisaged applications and on their chosen description, diffusion and viscosities may be included in the modeling or not. For these applications implying impact loadings, adiabatic conditions are generally retained, and thermal diffusion can be neglected with respect to transient phenomena.

Such distinction between 'slow' and 'fast' systems may appear a bit sketchy at first glance, but it is also motivated by the strongly different mathematical nature of the respective modelings, and therefore of computational methods which will be involved. Indeed, the former involve parabolic or elliptic partial differential equations, whose solutions are smooth. For the latter, the presence of mechanical inertia effects implies the occurrence of new physical phenomena, and the choice of a method of time-stepping for the mechanics. Even more, when impacts occur on the structure, the modeling involve hyperbolic equations, whose solutions are of wave type, which can be continuous or not. In addition, since the deformation is fast, heat has no sufficient time to evacuate through thermal diffusion such that the assumption of adiabaticity becomes valid. Well-suited computational methods for these systems are therefore strongly different from those employed for slow processes.

0.3 A few contributions and approach followed

Obviously, the present works do not aim at embracing and treat all these regimes. Rather, a few contributions carried out over the years, treating some special topics here and there will be briefly presented, which can eventually be associated with some particular regime. Transverse to the above classified regimes, another grid of lecture of the present works can be provided through the introduction of a few topics associated with *particular*

methods of analysis, types of formulations or applications which can be listed here. They were the purpose of some studies that provided at their time of publication some novel contributions to the literature.

The first one is *the exploitation of the variational calculus for coupled problems*. Besides many interests which we will come back to later in Chapter 1, such framework allows to naturally make emerge consistent computational aspects from the modeling. For slow systems, such approach was applied for the coupling between diffusion processes and mechanics. This was the case for thermo-mechanically coupled problems exploiting variational h-adaption methods for both thermal and mechanical effects during the PhD thesis of Rohit Pethe, of for problems of transient diffusion of species, eventually coupled with electricity for application to Lithium-Ion batteries during the PhD thesis of Jorge de Anda Salazar. Such framework can also be exploited for fast thermo-mechanical systems, especially when coupled with conservative formulations in fast transient dynamics, then changing the temperature for the internal energy density as an input variable.

The second topic concerns the definition of efficient computational approaches for *multi-scale analysis of transient diffusion systems coupled quasi-static mechanics*, i.e. avoiding FE^2 approaches which are too much computationally intensive. Especially, this was the purpose of the PhD thesis of Abdullah Waseem, in which model order reduction of numerical homogenization was performed for linear problems within the special regime of relaxed separation of scales. Besides drastically reducing the computational cost, the main interest of such approach lies in the definition of some enriched continua at the macroscale, embedding only a limited number enrichment variables accounting for local transient effects. Such generalized formulations may also eventually be integrated within a variational framework.

A third one pertains to *take advantage of conservative formulations in computational fast transient solid dynamics*. Although much more popular in Computational Fluid Dynamics (CFD) than in Computational Structural Dynamics (CSD), yet these conservative formulations present a set of interests with respect to more conventional approaches (i.e. displacement-based Galerkin approaches) used in solid mechanics. Various existing numerical schemes developed at first in the context of CFD can be naturally adapted to fast transient solid dynamics problems (various finite volumes schemes, (space-)discontinuous Galerkin finite elements) providing non-oscillatory approximations, and mimicking at the discrete level mathematical properties of the continuous system. Especially, various aspects of the approximation of the exact solution can be investigated, like capturing nonlinear waves such as shocks, plastic waves which can be continous or discontinuous, or the entropy-positiveness of schemes. Another issue related to the above for fast transient problems is the numerical approximation of the kinematics of solid bodies undergoing large strains, especially in a Lagrangian context. This was the starting point for the development of a numerical scheme that would combine a non-oscillatory high order approximation of the solution to particle-based methods. Such work actually led to the Discontinuous Galerkin Material Point Method (DGMPM), which was the topic of the PhD theses of Adrien Renaud and of Alaa Lakiss.

A last one is associated with the study of *mechanical processes dedicated to the assembly or the disassembly of heterogeneous structures*. This part of my research appears as the most applied one as it is related to very practical engineering problems and technologies. However, on the one hand coupled thermo-mechanical phenomena are widespread in such mechanical processes which makes it a great playground, and on the other hand they also often serve for motivating the development of more fondamental works in thermo-mechanics. These processes appear as one instance among many others to make a direct connection between sciences and technologies, and to stay connected to scientific colleagues doing experiments, or even to participate. For example, I got interested during my PhD thesis in the process of Friction Stir Spot Welding, which consists in creating a spot weld between two superimposed sheets by penetration of a tool in rotation within the matter. On the one hand, a fully implicit monolithic thermo-mechanically coupled fluid/solid solver was developed in a commercial finite element code in an Arbitrary Lagrangian Eulerian context. On the other hand, dedicated experimental setups were developed. Another example pertains to high pulsed power technologies which consist of releasing a certain amount of (electrical) energy in a given medium in a very short time, and exploiting its effects. Both electromagnetic and electrohydraulic technologies were the purpose of some collaborations with Professor Guillaume Racineux, for which contributions were focused on the developments of theses processes for special geometrical configurations (i.e. rather experimental), and on the development of simple analytical solutions modeling some particular effects, although more refined numerical simulations are expected to come later and developed with the aforementioned methods of analysis.

0.4 Outline of the manuscript

For the sake of convenience and conciseness, the present manuscript is essentially organized around two chapters gathering works associated with slow and fast systems respectively. However, the above particular methods of analysis, types of formulations or applications will be found within the two chapters, and applied to the study of different kinds of systems.

A third and last chapter is dedicated to the description of some on-going works and outlooks of these first works. Again, this document has been written in order to be remain concise and give an ordered overview of my research works, hence only the main ideas are described, the details can be found within the papers and are not expanded here.

Chapter 1

Slow thermo-mechanical systems

1.1 Basics of variational calculus for transient heat transfer coupled mechanics

Variational principles have played a major role in mechanics (see e.g. [8]), and still continue to bring a sound framework which fosters strong advances in that domain. In short, one can say they consist in formulating a problem as the optimization of a scalar functional, as it is the case in elastostatics with the therorem of potential energy for instance. Although popular principles such as Hamilton's least action one only works for conservative systems, other principles were developed for dissipative systems, as it is the case for diffusion problems [118], limit analysis [132] or fracture mechanics [77] for instance. Variational approaches were found to provide many advantages with respect to the classical "vectorial's mechanics" obtained from Newton's laws of motion.

The first one is essentially *mathematic*. Since it relies on convex analysis and on the optimization of scalar functionals on manifolds, the study of the existence and uniqueness of solutions can be analyzed, especially for hyperelastic-based large strains problems for instance [24]. Its elegance also arises from being able to gather the complete dynamics of a system into a scalar functional, whose optimal point yields the governing equations.

The second kind of advantages are *physical ones*. First, the functional usually has a physical significance since it is often a quantity related to some energy or power, which are additive quantities. Next, it provides an interesting framework to build models for coupled problems. The modeler can directly work on the form of the functional, from which bulk and surface local equations naturally follow from stationarity conditions.

The third one is related to *computational aspects*. Indeed, from continuous principles, discrete incremental variational principles can be derived at different orders of approximation (though not always in a straightforward manner), for which the traditional solvers basically developed for optimization problems with or without constraints can be reused at profit. But many other advantages also appear at the discrete level. For instance, since the existence of a variational principle is linked to a certain symmetry in the problem at hand, it is inherited at the discrete level and translates as the symmetry of the Hessian matrix, hence leading to a reduction of the computational cost. It also provides a natural error indicator thanks to the minimum/maximum nature of the optimal point of the functional by comparison of its values for different meshes. For coupled problems, these discrete principles define a convenient framework for the design of partitioned, staggered algorithms from the monolithic system. Also, these algorithms can sometimes be reinterpreted as (bloc-)preconditioners applied to the monolithic system, eventually leading to reuse existing codes, then coupled in a convenient and consistent way.

For coupled thermo-mechanical problems, the variational formulations of the coupled thermo-elastic and thermo-visco-elastic problems have been extensively investigated (see e.g. [10, 11, 17, 15, 34]). But formulations for coupled thermo-mechanical problems involving non-linear dissipative behaviour, such as thermo-elasto-visco-plasticity have been more recently introduced in the work of Yang, Stainier and Ortiz [72] on the basis of a first isothermal version [56], then exploited [98, 92] and summarized in [111]. Such variational principle of course relies on the framework of *Generalized Standard Materials* [23], which allows to conveniently describe the constitutive model via the definition of a thermodynamic potential and a dissipation pseudo-potential,

which should satisfy some mathematical constraints to ensure the second principle of thermodynamics and the uniqueness of the solution of the problem. But besides this, this principle relied on the one hand on the introduction of a two-field thermal formulation (an external temperature T, appearing in the heat equation, and an internal temperature θ obtained through a state law), whose equality is enforced as an internal constraint in the constitutive model, and relaxed in state laws. On the other hand, a time dilatation of dissipative rate processes appearing in the dissipation pseudo-potential is considered via a change of time variable (called time rescaling by these authors), assumed to be a function of both equilibrium and current temperatures

$$t = f(T, \theta)t',$$

but here enforced to match at equilibrium, i.e. $f(T, T) = 1$. The integration factor $f(T, \theta)$ is then identified as $f = T/\theta$, so that to recover the requisite symmetry of the weak form. The obtained multi-field variational formulation also presents the interest of allowing a separate optimization with respect to local and global quantities, hence being consistent at the discrete level with standard finite element codes, separating the local time-discrete constitutive update performed pointwise at the integration points, from the solution of an incremental boundary value problem giving the unknown deformation mapping and external temperature on a mesh. Since most of the time, Helmholtz's free energy density W is a convex function of the displacement field $\mathbf{u}$, and concave with respect to the temperature T, the discrete solution fields are obtained from the saddle point of an incremental functional:

$$\{\mathbf{u}, T\}_{n+1} = \arg \inf_{\mathbf{u}_{n+1}} \sup_{T_{n+1}} I(\mathbf{u}_{n+1}, T_{n+1}).$$

The incremental functional $I(\mathbf{u}_{n+1}, T_{n+1})$ is sought in such a way that it approximates the integral of its continuous counterpart over the time increment $\Delta t = t_{n+1} - t_n$, and reads here as:

$$\begin{aligned} I(\mathbf{u}_{n+1}, T_{n+1}) = &\int_{\Omega_0} \left[\mathcal{W}_{n+1}(\mathbf{F}_{n+1}, T_{n+1}; \mathbf{F}_n, T_n, \mathbf{Z}_n) - \Delta t \left\langle \chi\left(-\frac{\boldsymbol{\nabla} T}{T}; \mathbf{F}(\tau), T(\tau), \mathbf{Z}(\tau) \right) \right\rangle \right] dV \\ &+ \int_{\Omega_0} \left[\Delta t\, \rho r_{n+1} \ln \frac{T_{n+1}}{T_n} - \rho \mathbf{b}_{n+1} \cdot \Delta \mathbf{u} \right] dV - \int_{\partial_t \Omega_0} \bar{\mathbf{t}}_{n+1} \cdot \Delta \mathbf{u} da - \int_{\partial_Q \Omega_0} \Delta t\, \bar{Q}_{n+1}\, \ln \frac{T_{n+1}}{T_n}\, da, \end{aligned} \tag{1.1}$$

where χ denotes the heat conduction potential, and $\mathcal{W}_{n+1}$ is obtained from a local optimization with respect to the set of internal variables $\mathbf{Z}_{n+1}$

$$\mathcal{W}_{n+1}(\mathbf{F}_{n+1}, T_{n+1}; \mathbf{F}_n, T_n, \mathbf{Z}_n) = \inf_{\mathbf{Z}_{n+1}} \mathscr{I}(\mathbf{F}_{n+1}, T_{n+1}, \mathbf{Z}_{n+1}; \mathbf{F}_n, T_n, \mathbf{Z}_n), \tag{1.2}$$

where the local incremental functional $\mathscr{I}_{n+1}$ is defined by

$$\begin{aligned} \mathscr{I}_{n+1}(\mathbf{F}_{n+1}, T_{n+1}, \mathbf{Z}_{n+1}; \mathbf{F}_n, T_n, \mathbf{Z}_n) = &W(\mathbf{F}_{n+1}, T_{n+1}, \mathbf{Z}_{n+1}) - W_n + \eta_n \Delta T \\ &+ \Delta t \left\langle \phi\left(\frac{T_{n+1}}{T_n} \frac{\Delta \mathbf{F}}{\Delta t}, \frac{T_{n+1}}{T_n} \frac{\Delta \mathbf{Z}}{\Delta t}; \mathbf{F}(\tau), T(\tau), \mathbf{Z}(\tau) \right) \right\rangle, \end{aligned} \tag{1.3}$$

provided brackets $\langle \bullet \rangle$ denote a consistent average value of the quantity $(\bullet)$ over the time increment [98], ϕ is the dissipation pseudo-potential and η the entropy density. The minimization (1.2) is also called *variational constitutive update*, which permits to solve the set of discrete constitutive equations through that of an optimization problem. Notice that the discrete (local) potential (1.3) yields a semi-implicit time integration scheme here, since the entropy density is evaluated at time t_n.

An extension of this work to non-associated evolutions equations, especially to non-linear kinematic hardening, and to any yield function being positively homogeneous of degree one was then proposed by Mosler and co-workers [93, 123, 119], following former works developed in the isothermal setting by these authors [89, 90, 100]. The potentially non-associative evolution equations are *a priori* enforced by employing a suitable parameterization of the flow rule and the evolution equations using pseudo-stresses, yielding eventually an unconstrained optimization problem. It is shown the consistency of such parameterization in the thermo-mechanical setting requires the initial yield stress to depend on the equilibrium temperature. Besides, the continuous variational problem is approximated by a fully-implicit time integration scheme [93].

Besides, being thermodynamically consistent, these approaches allow to correctly model and compute the non-constant partition of plastic work into heat and stored energy [61, 92, 93, 123], in contrast with empirical approaches inspired by the pioneering work of Taylor and Quinney [4], and followed in some other works [44].

1.2 Variational h-adaption for thermo-mechanical problems

As already mentioned, variational formulations can also be used to define variationally consistent h-adaption techniques for the optimization of the mesh size. Such approach was first proposed by Mosler and Ortiz for quasi-static isothermal dissipative mechanics problems in [73, 83], but then extended to other applications such as phase field approach to model fracture [148]. Such approach profits from the known convexity of the optimal point of the functional to drive the mesh adaption. More precisely, this is the comparison of the values of a functional computed on two different meshes which permits to drive the mesh adaption, leading to a sort of relative measure of the error. This is why it is rather called an error indicator, since it does not require any error estimates and associated (usually costly) reconstruction step of admissible fields. Also, it naturally works for non-linear problems without adding any additional complexities with respect to linear ones. However, finding a mesh which minimizes globally (if a minimum is considered) the value of the functional is a problem of combinatorial complexity, meaning that for each value of number of nodes, several meshes with different values of the functional are possible. Hence, an infinite number of choices of number of nodes are possible.

Practically speaking, a greedy approach is usually followed by means of an iterative procedure, and the mesh is divided into patches of elements taking advantage of the additive property of the functional (which is generally an energy-like quantity). During the iterative procedure, each patch may be refined or unrefined given a local adaption technique, and is the purpose of a local solution and evaluation of the functional, while fixing the value of the primal field on the patch boundary. The relative improvement (or not) of the functional on each patch leads to that the refined (or unrefined) patch is kept (or not) at the current iteration. Once all patches have been updated, a global solution is computed on the updated mesh, and the algorithm can go for the next iteration. The local treatment of mesh adaption on patches also allows to avoid complex remapping procedures of internal

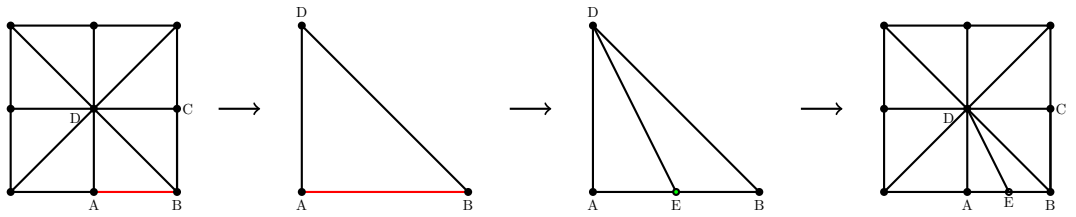

(a) The identified boundary edge AB leads to that the patch consisting of the single element DAB is bisected.

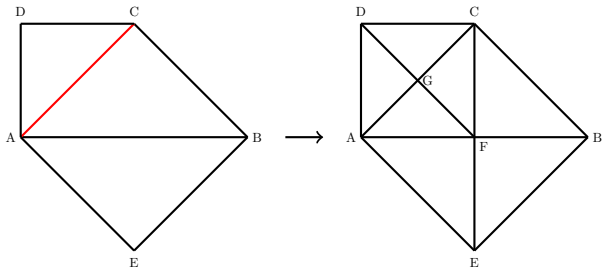

(b) The edge identified is AC, shared by triangles ACD and ACB. The segment AC is the longest edge for the triangle ACD but not for the triangle ACB. Edge AB is the longest edge of both triangles ACB and AEB, and hence is the terminal longest edge in LEPP so that it should first be bisected. Then the edge AC is bisected which is now the terminal longest edge in LEPP.

Figure 1.1: Various local refinement techniques: (a) single edge bisection, (b) Longest Edge Propagation Path (LEPP). Extracted from [154].

variables, which are generally costly and numerically diffusive. In practice, nearest-neighbor interpolations is used assuming a constant distribution of internal variables over elementary cells consisting of the intersection between Voronoï cells and triangular elements.

Patches are usually refined either using a single edge bisection technique [73], or Rivara's Longest Edge Propagation Path (LEPP) algorithm [54, 53], as shown in Figure 1.1. The former generally yields anisotropic meshes, and elongated elements, but which are consistent with the physics approximated on the mesh since the geometry of these elements is driven by the variational principle. The latter enforces a constraint on the element aspect ratio, yielding a constrained optimization problem. This is why the latter generally leads to higher converged values of the functional (for a minimal point) than those obtained with the single edge bisection technique.

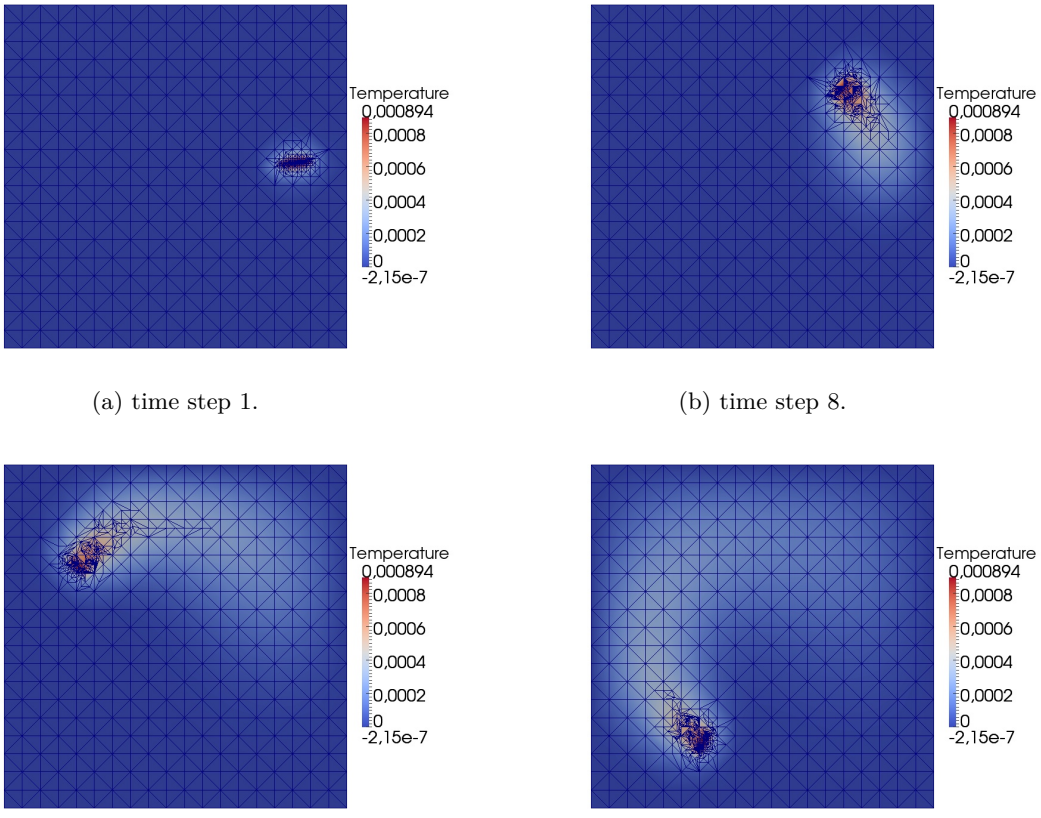

(a) time step 1.

(b) time step 8.

(c) time step 24.

(d) time step 40.

Figure 1.2: Temperature field on adapted meshes at different times. Extracted from [150].

The purpose of the PhD thesis of Rohit Pethe, which I co-supervised with Laurent Stainier, was to extend such approach to coupled thermo-mechanical problems taking advantage of the variational formulation introduced in [72], which couples transient thermal heat transfer to quasi-static dissipative mechanics. On the one hand, the transientness of phenomena now implies to correctly handle both mesh refinement and coarsening at each time step. Figure 1.2 illustrates this, and shows the temperature field on the adapted meshes computed at different times for a simple purely transient thermal test case consisting of a sharp heat source rotating about the center of a square computational domain. The mesh coarsening upstream from the heat source appears as efficient as the mesh refinement where the heat source is located. Still regarding purely transient heat transfer problems, one interesting result demonstrated in [150] showed that half of the square of the H^1 norm of the

interpolation error equals the difference in the incremental variational potential, namely

$$\frac{1}{2}\|\bar{\theta} - \bar{\theta}_h\|_1^2 = I(\bar{\theta}) - I(\bar{\theta}_h),$$

where $\bar{\theta}$ denotes some dimensionless temperature and $\bar{\theta}_h$ its approximation, hence making a direct connection between variational approaches and gradient based error indicators. On the other hand, the thermo-mechanical coupling is treated via a staggered algorithm and uses different meshes for the two different fields. The sequential adaption of different meshes allows to capture different scales and spatial resolutions of the different fields. However, handling both temperature and displacement fields in a staggered way on different meshes required some adaption of the previous works. Especially, the solution of each physics can be ordered differently within a time step according to the strength of the coupling, and various split (isothermal or adiabatic [39]) can be considered. Algorithm 1.2.1 summarizes the strategy followed in the case where the mechanical problem is solved before the thermal one during a given time step.

Algorithm 1.2.1 (Staggered computation and adaption of meshes)
Provided the solutions $(\mathbf{u}_n, T_n, \mathbf{Z}_n)$ *defined on their respective meshes at time* t_n*,*

1. *Solve the mechanical problem*
   while *convergence is not obtained, iterate on* k *such that*
   - *(i) Adapt the mechanical mesh on each patch.*
   - *(ii) Find* $\mathbf{u}_{n+1}^{(k)}$ *minimizing* (1.1)*.*
   - *(iii) Update* $\mathbf{Z}_{n+1}^{(k)}$ *at each Gauss point of the mechanical mesh by minimizing the local functional* $\mathscr{I}(\mathbf{F}_{n+1}^{(k)}, T_n, \mathbf{Z}_{n+1}^{(k)}; \mathbf{F}_n, \mathbf{Z}_n)$ (1.3)
2. *Solve the thermal problem*
   while *convergence is not obtained, iterate on* k *such that*
   - *(i) Adapt the thermal mesh on each patch.*
   - *(ii) Find* $T_{n+1}^{(k)}$ *by maximizing* (1.1)*.*
   - *(iii) Update* $\mathbf{Z}_{n+1}^{(k)}$ *at each Gauss point of the thermal mesh by minimizing the local functional* $\mathscr{I}(\mathbf{F}_{n+1}, T_{n+1}^{(k)}, \mathbf{Z}_{n+1}^{(k)}; \mathbf{F}_n, T_n, \mathbf{Z}_n)$ (1.3)

Such staggered approach combined with two meshes requires to transfer some informations from one mesh to another during one time step. For nodal fields, this transfer consists of a simple interpolation of fields to the Gauss points of the other mesh. For variables defined at integration points, the process consists in finding the closest integration point in the other mesh and the values are inherited. These developments were implemented in the home-made library ZorgLib [168] written in C++.

Figure 1.3 shows an illustration of a coupled thermo-mechanical simulation of shear banding occurring in a hat shaped specimen (here made of an $\alpha-$titanium). Shear banding is triggered by thermal softening, modelled here with the constitutive model validated in [92]. Optimal thermal and mechanical meshes are obtained via Rivara's LEPP mesh adaption technique, an isothermal split, and P1 finite elements. Those two meshes look quite different, the mechanical one being much more refined due to stronger gradients.

Another illustration is shown in Figure 1.4 associated with a simplified linear friction welding test case. This process allows to weld two parts put in contact with a given pressure, then rubbed against each other. The numerical simulation is here carried out with simplified equivalent boundary conditions (prescribed heat flux and tractions). Figures 1.4a and 1.4b show the computed effective stress and temperature fields on their respective adapted (deformed and undeformed) meshes.

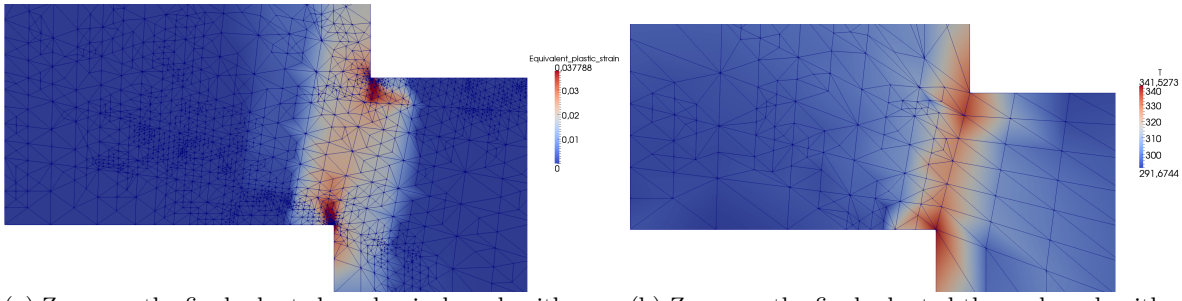

(a) Zoom on the final adapted mechanical mesh with map of the equivalent plastic strain.

(b) Zoom on the final adapted thermal mesh with map of the temperature.

Figure 1.3: Shear banding in a hat shaped specimen. Extracted from [154].

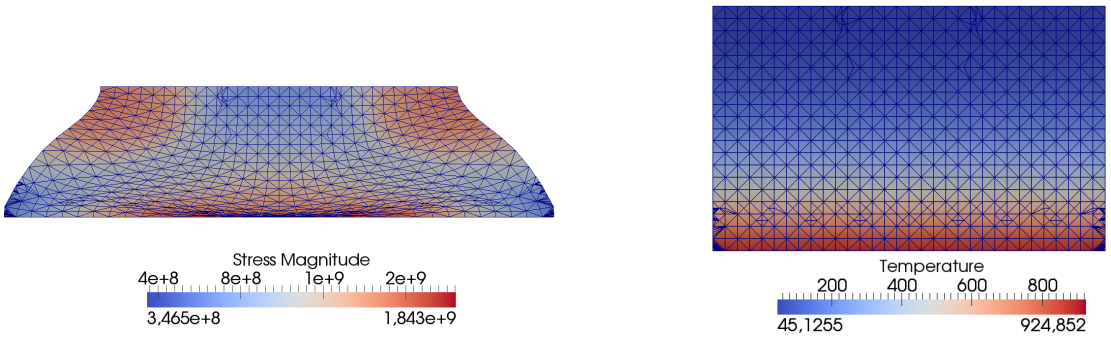

(a) Magnitude of the stress field shown on the deformed mechanical mesh at the final time step.

(b) Temperature field shown on the undeformed thermal mesh at the final time step.

Figure 1.4: Simplified linear friction welding test case. Extracted from [154].

1.3 Variational formulation of transient diffusion problems

Thanks to an existing strong analogy between heat and species transfer known for a while [1], developments already performed in thermo-mechanics (and especially variational principles) may be adapted to the coupling between transient diffusion of species and quasi-static mechanics.

Such analogy is of primal importance because the coupling between diffusion of species and mechanics is involved in many engineering applications. To only list a few of them, one can for instance cite problems linked to ion transport, like lithium-ion electrical batteries which are now everywhere in our society. The cyclic process of lithiation and delithiation occurring within electrodes during the charge and discharge steps is due to the diffusion of lithium-ions within active particles making them swelling and hence generating stresses within the medium, which in turn affects the flux of species. This cyclic loading leads to cracks and eventually to a loss of contact with the matrix, which gradually results in a capacity loss and a failure of the battery. Another example pertains to the diffusion of water in biological tissues. In the context of tissue reconstruction of intervertebral discs, some hydrogels can be used as replacement material for degraded *Nucleus Pulposus* (see e.g. [101, 114]). These hydrogels are formed of a cross-linked polymer chains network within which small solvent molecules can diffuse without being dissolved. This generates large volume changes of the gel, as well as elastic swelling deformations and associated stresses.

It is a common practice when using Fick's laws [1] to solve for the concentration c of a given species and, if needed, compute the chemical potential μ afterwards through a constitutive law like mass action laws. Such procedure appears as a post-process relation, which describes a system where the chemical potential does not affect its behavior, although the chemical potential may play a major role and especially that of driving force for transport in irreversible processes. Especially, this variable may become essential if we are interested in the solution of coupled problems, like diffusion coupled mechanics for instance, or if we want to derive a variational principle for transient diffusion, eventually embedding a coupling with another physics, from which efficient computational approaches may follow. It is easy to see that the weak forms of the heat equation or of the balance of species expressed as a function of the concentration do not derive from the stationarity of any potential. Such procedure can only eventually be made in the discrete setting once a time-stepping scheme has been used. As already shown in [72, Section 3.1], a variational principle of the transient heat transfer problem involves (at least) two fields, hence by analogy the transient diffusion of species also requires a multi-field modeling. But, even if we only consider diffusion (and therefore a uniphysics system), the interesting point is that such multi-field modeling opens the path to explore multiphysic problems, which also involves several fields.

In that framework, the purpose of the PhD thesis of Jorge de Anda Salazar was to propose some developments regarding variational principles for coupled problems, and especially those embedding diffusion processes, but also to push the effort forward by studying various algorithmic strategies which could naturally follow from these continuous formulations. His PhD thesis was the purpose of a collaboration between Centrale Nantes (with advisors Laurent Stainier and I) and the Technical University of Munich in Germany within the research group of Wolfgang Wall, and took place within the context of the EMJD-SEED (Simulation in Engineering and Entrepreneurship Development) funding program, financed by the European Commission. His work focuses on a phenomenological approach at the macro-level that avoids the complexities of advanced averaging theories. Multi-scale approach of such problem was rather addressed in the PhD thesis of Abdullah Waseem, whose summary is performed in Section 1.4. One important work regarding the derivation of variational principles for diffusion problems was made by Miehe et *al.* [118], who proposed a dedicated variational framework for the coupling between large strain hyperelasticity and Cahn-Hilliard-type diffusion of species. Incremental principles are also derived and exploited up to the finite element implementation, which takes advantage of the inherent symmetry of operators obtained from the variational structure of the system. However, it is interesting to observe that Miehe et *al.* [118] derived a multi-field variational principle for diffusion coupled mechanics following an *integration process*. More precisely, the combination of the definition of the variational derivative[1] and balance equations combined with constitutive ones allows him to identify the first variations of his potential (the Euler-Lagrange equations), and hence to obtain it by *integration*, resorting to a so-called *generalized Legendre transform*. If we momentarily set aside both mechanical and chemical micro-forces contributions appearing in his derivations, the latter being associated with Cahn-Hilliard-type diffusion of species, he obtains a two-field variational principle to describe standard diffusion, involving both the chemical potential and the concentration rate. Observe also that such principle is completely analog to that derived for heat transfer in [72, Section 3.1], provided the entropy density is the analog of the concentration, and the temperature is that of the chemical potential.

1.3.1 An approach based on Onsager's energy rate

The approach followed in the PhD thesis of Jorge de Anda Salazar is quite different, although it also allows to recover among others the same two-field variational principle. The starting point comes with the introduction of Onsager's energy rate [5]:

$$\Pi_0[\dot{c}, \mathbf{j}] := \int_\tau \left[\int_\Omega \left(\dot{E}(c) + \chi^*(\mathbf{j}, c) \right) dV + \int_{\partial_\mu \Omega} \bar{\mu} (\mathbf{j} \cdot \mathbf{n}) da \right] dt \tag{1.4}$$

where E and χ^* denote the internal energy density and the dual dissipation pseudo-potential, $\mathbf{j}$ the flux of species, $\mathbf{n}$ the outward unit normal and $\bar{\mu}$ a known value of the chemical potential defined at the Dirichlet boundary $\partial_\mu \Omega$. Due to the dissipation pseudo-potential, the integral Π_0 is a path-dependent quantity which

[1] The variational derivative is defined as $\delta_{\mathbf{y}} f(\mathbf{y}, \boldsymbol{\nabla}\mathbf{y}) = \partial_{\mathbf{y}} f(\mathbf{y}, \boldsymbol{\nabla}\mathbf{y}) - \mathrm{Div}[\partial_{\boldsymbol{\nabla}\mathbf{y}} f(\mathbf{y}, \boldsymbol{\nabla}\mathbf{y})]$.

depends on the history of fields $c(\mathbf{x},t)$ and $\mathbf{j}(\mathbf{x},t)$. The evolution of the system can be obtained by optimizing Onsager's energy rate (1.4), provided this optimum satisfies the balance of species and associated Neumann boundary condition. This leads to the following constrained optimization problem

$$\{\dot{c},\mathbf{j}\} = \arg\inf_{\dot{c},\mathbf{j}} \Pi_0 \qquad \text{subject to} \qquad \begin{cases} \dot{c} + \nabla\cdot\mathbf{j} - r = 0 & \forall\,\mathbf{x}\in\Omega \\ \bar{j} - \mathbf{j}\cdot\mathbf{n} = 0 & \forall\,\mathbf{x}\in\partial_j\Omega \end{cases} \tag{1.5}$$

where constraints are enforced through Lagrange multipliers, from which a set of variational principles are derived. Without going into details which can be found in [163], such approach presents several interests. First, it allows to identify what quantities are hidden behind Lagrange multipliers (here the opposite of the chemical potential). Second, it allows to show that the flux of species $\mathbf{j}$ is conjugate to the opposite of the chemical potential gradient, i.e. $-\boldsymbol{\nabla}\mu \equiv \mathbf{g}$. Third, the conjugate function χ^* is identified as the dissipation pseudo-potential needed to enforce the second principle of thermodynamics in the model. The latter highly contrasts with the explicit dependence defined by Fick's first law $\mathbf{j}(c)$. A 3-field variational formulation whose solution fields are $\{\mathbf{j},\dot{c},\mu\}$

$$\{\mathbf{j},\dot{c},\mu\} = \arg\inf_{\dot{c},\,\mathbf{j}} \sup_{\mu} \Pi_3[\mathbf{j},\dot{c},\mu]$$

naturally follows from the solution of Problem (1.5), whose Euler-Lagrange equations allows to recover balance equations and conjugacy relationships through both the internal energy density E and dual dissipation pseudo-potential χ^*. This 3-field variational principle clearly shows that (at least) three main ingredients are required to derive a variational principle for diffusion-type systems: *conjugate variables*, *existence of energy-like potentials* and *system's constraints*. A reduction of the number of independent fields can then be operated by introducing the primal dissipation pseudo-potential through its Legendre transform

$$\chi(\mathbf{g},c) = \sup_{\mathbf{j}} \left\{ \mathbf{g}\cdot\mathbf{j} - \chi^*(\mathbf{j},c) \right\}$$

yielding the reduced optimization problem

$$\{\dot{c},\mu\} = \arg\inf_{\dot{c}} \sup_{\mu} \Pi_2[\dot{c},\mu],$$

which is identical to that found by Miehe et *al.* [118]. However, operating such reduction leads to loose some informations, especially the relationship between the Lagrange multipliers and the chemical potential, and the conjugacy between the flux of species and the opposite of the chemical potential gradient. Especially, the latter should be *defined and supplemented* to the Euler-Lagrange equations to provide the same strong form, and this is also what was done in [118]. However, the 2-field formulation still appears to provide the best compromise between complexity and generality, especially in the discrete setting since it allows for treating transient diffusion problems with a minimal number of independent fields that are scalar quantities. In contrast, the 3-field formulation would increase the computational cost, with numerical advantages that remain to be made clear. A further reduction leading to a 1-field variational formulation can even be performed by introducing the Legendre transform of the internal energy density. However, this one is shown to be only compatible with steady-state diffusion processes, and is thus of less interest. Notice also that such procedure based on Onsager's energy rate can also be applied to gradient-extended diffusion theories, and especially that of Cahn-Hilliard, though not published yet at the time being. One 4-field variational formulation $\{\dot{c},\mathbf{j},\mathbf{k},\mu\}$ can be derived, where $\mathbf{k}$ here stands for the micro-force traction vector, two 3-field formulations $\{\dot{c},\mathbf{k},\mu\}$ and $\{\dot{c},\mathbf{j},\mu\}$ respectively, introducing Legendre transforms of the dissipation pseudo-potential with respect to different fields, and then several 2-field ones, showing that much work remains to be developed in that domain.

1.3.2 Solution strategies in the discrete setting

From these developments in the continuous setting, various solution strategies of the diffusion problem were studied in the PhD thesis of Jorge de Anda Salazar. Generally, computational aspects derived from variational approaches follow an incremental format, especially various incremental functionals yielding fully or semi-implicit time discretizations may be introduced [163], which approximate the continuous time integral over a time step. Such approach does not proceed in applying a given time-stepping scheme to a set of governing

equations of a system, but rather in proposing a discrete incremental functional that will satisfy the consistency conditions. The latters ensure that the continuous expression of the functional is retrieved by the discrete one as the time step goes to zero, and that discrete Euler-Lagrange equations will also converge towards their continuous counterparts. Focusing on the 2-field variational formulation of the diffusion problem, a nodal finite element approximation was performed for the chemical potential while the concentration was discretized at integration points since its gradient is not involved in governing equations of the system. A Newton-type approach can be followed for the numerical solution. The residual is obtained from the first discrete variation, while the Hessian (symmetric) matrix is obtained from the second one. Such strategy is called monolithic since the two fields are solved simultaneously. Figure 1.5 shows an illustration of a one-dimensional flow of species within an insulated cavity made of a composite medium that consists of a few inclusions within a matrix.

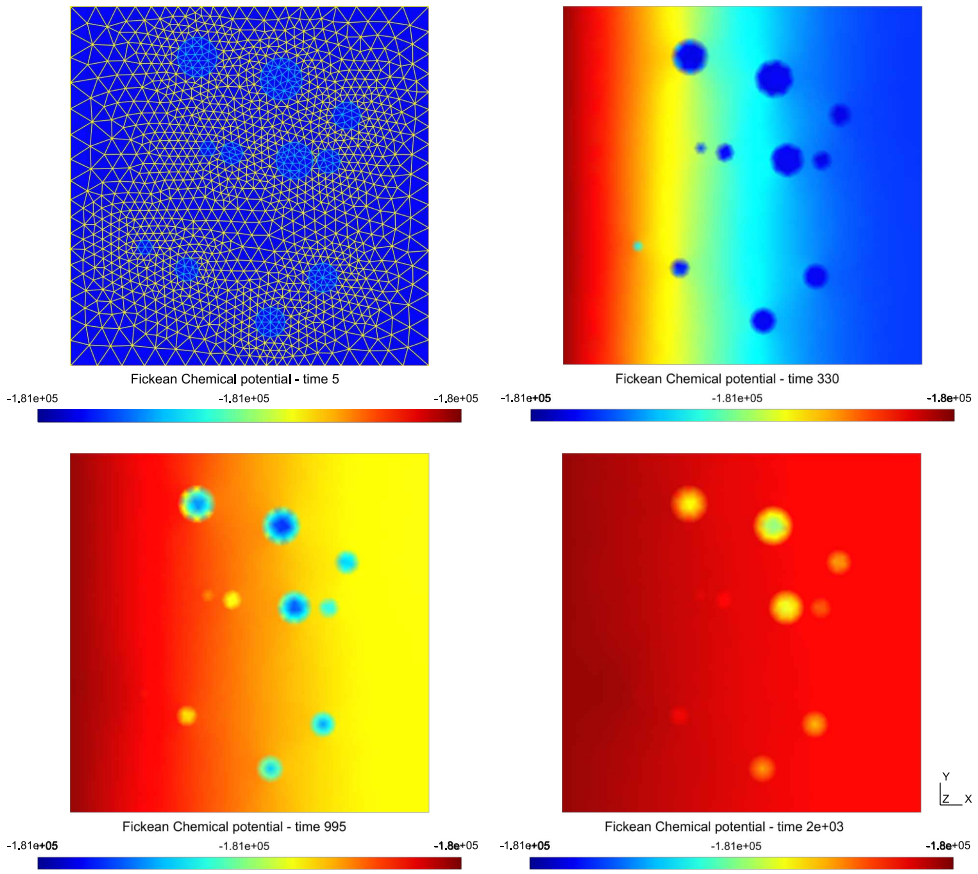

Figure 1.5: One-dimensional flow of species within an insulated cavity made of a composite medium. Extracted from [163].

However, different numerical strategies can be followed to solve the monolithic system. Especially, various partitioned schemes can be set up, thus introducing a split of the system into several blocks associated with fields. These are sometimes called mild or loose algorithmic coupling algorithms, yet used for solving strongly coupled systems, and aim at making the solution of the coupled system easier through that of smaller blocks of equations. Blocks are then solved through successive stages in an *asynchronous* manner, and may be linked to each other through some *hierarchy* during the iterative process, especially for nested approaches. Regarding the 2-field variational formulation of the diffusion problem, two different splits can be introduced. The latters are defined by introducing some explicit dependencies between the two fields during the first stage of these split algorithms, namely $c(\mu)$ and $\mu(c)$, respectively giving the $c-$ splitting and $\mu-$splitting

$$\underline{c-\text{splitting}} \qquad\qquad \underline{\mu-\text{splitting}}$$
$$\hat{\mu} = \arg\sup_{\mu} \Pi[\mu, c(\mu)] \qquad\qquad \hat{c} = \arg\inf_{c} \Pi[c, \mu(c)]$$
$$\hat{c} = \arg\inf_{c} \Pi[c; \hat{\mu}] \qquad\qquad \hat{\mu} = \arg\sup_{\mu} \Pi[\mu; \hat{c}]$$

where the semi-colon denotes a parametric dependence of the functional to the first optimized field during the second stage. Such explicit dependence brings a new term in the variation computed during the first stage, i.e. $\delta_c\Pi\frac{\partial c}{\partial \mu}$ for the $c-$ splitting for instance, which is the starting point of various solution strategies. The first solution strategy consists in considering that this term does not vanish, which implies that the concentration c actually changes (i.e. $\delta_c\Pi[\mu, c(\mu)] \neq 0$) during the first stage defined by $\delta_\mu\Pi[\mu, c(\mu)] = 0$, though not optimal yet. The second stage thus serve as a corrector for the concentration, while the chemical potential μ remains unchanged. Such approach is consistent with a *staggered strategy*, which basically consists of a succession of solutions of iterative-blocks with no feedback, keeping fixed the degrees of freedom associated with one field while solving for the other. However, since the residual of this first stage is changed with respect to that obtained with a Newton method, this leads to consider a slight modification of the system solved. More precisely, one can show it amounts to add some artificial concentration (for the $c-$ splitting) within the equivalent discrete strong equations. A second strategy amounts to consider that the additional term vanishes, which necessarily implies that the concentration does not vary during the first stage $\delta_c\Pi[\mu, c(\mu)] = 0$. Therefore, for each variation applied on μ, the concentration c must at least be an approximated optimal solution. In essence, for each iteration performed on μ, an approximate solution of c should be computed iteratively. This leads to follow a *nested strategy* involving nested loops on both c and μ, which consists in iterating on the lowest hierarchy block (actually c for the $c-$splitting) at a given iteration of the highest one (i.e. μ).

One interesting feature of the above partitioned strategies is that they directly result in *physically-based block-preconditionings*. More precisely, the staggered strategy results in a multiplicative preconditioner, where both the residual and the matrix are changed with respect to the monolithic system of equations, while the nested strategy can be identified as an additive preconditioner (only the matrix is changed, not the residual) provided a null space condition is satisfied. In other words, while it is not a trivial task to propose efficient preconditioners on a purely numerical basis for coupled problems to speed up the solution process, variational approaches provide an interesting framework for the development of *consistent physically-based preconditioners* for coupled systems through the definition of partitioned numerical strategies. This is achieved via the introduction of explicit dependencies between fields the functional depends on, which allows to make a connection between variational approaches and linear algebra via row (block) operations.

1.3.3 Extension to the electro-chemical coupling

The work performed by Jorge de Anda Salazar in his PhD thesis regarding multi-field variational principles and associated algorithmic solution strategies established for diffusion of species can be extended to any type of diffusive process. Especially, an extension to electro-chemical processes was investigated which couples diffusion of species to electricity, with application to lithium-ion battery cell. The balance of species is now supplemented with the balance of electric charge. The coupled system then yields a 4-field variational principle [143] written on fields $\{(\dot{\rho}, \phi), (\dot{c}_k, \mu_k)\}$, where ρ stands for the electric charge density, ϕ is the electric potential, and $(\dot{c}_k, \mu_k)$ the concentration rate and the chemical potential of the kth species. A reduced 3-field formulation $\{\mu, \dot{c}, \phi\}$ can eventually be obtained by resorting to the so-called electro-neutrality condition assumed to be valid within the electrolyte (i.e. $\boldsymbol{\nabla} \cdot \mathbf{i} = 0$, where $\mathbf{i}$ is the current density). From several available and known constitutive equations relating the flux of species, the current density, the electric potential and chemical quantities[2], a generic form of dissipation pseudo-potential yielding linear relationships between thermodynamic fluxes and forces was identified, especially being consistent with Onsager's symmetry conditions [3]. An extension of the aforementioned electro-chemical coupled system can be obtained if we consider a domain consisting of both electrode and electrolyte. These are joined by an interface which is usually the purpose of a charge transfer kinetics, governed by an interface equation such as the widely used Butler-Volmer current density model [104, 135]. Considering such domain provides an additional electro-chemical coupling at the level of the electrode-electrolyte interface, in addition to that already occurring within the bulk of the electrolyte. The Butler-Volmer

[2] especially those of Nernst-Planck, Stefan-Maxwell and Ion transport models.

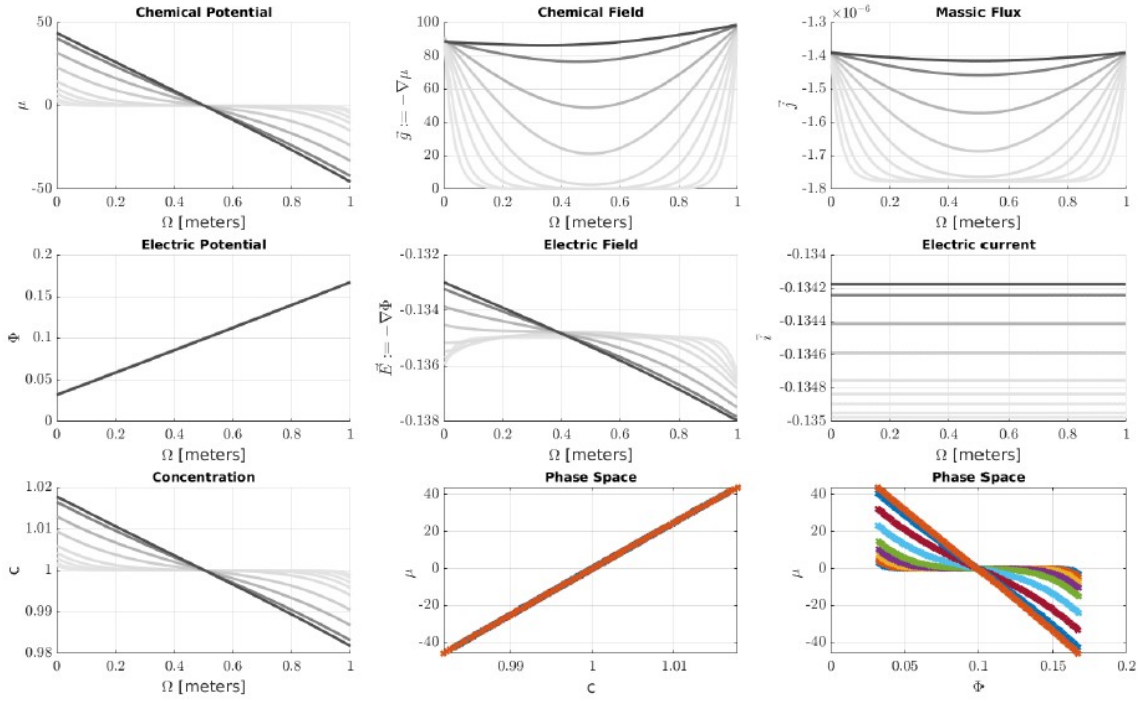

Figure 1.6: Numerical simulation on a one-dimensional mesh of the electrode-electrolyte composite system, with electro-chemical bulk coupling and Butler-Volmer interface equation.

equation can be embedded within the variational formulation through the definition of an interface functional $\Pi_{\Gamma_{BV}}$. The functional describing the electro-chemical response of the lithium-ion battery now consists of the sum of electrolyte (el), electrode (ed) and interface (Γ_{BV}) contributions

$$\{(\dot{c}_{el}, \mu_{el}, \phi_{el}), (\dot{c}_{ed}, \mu_{ed}, \phi_{ed})\} = \arg \inf_{(\mu_{el},\phi_{el},\mu_{ed},\phi_{ed})} \sup_{(\dot{c}_{el},\dot{c}_{ed})} \Pi[\dot{c}_k, \mu_k, \phi]$$
$$\text{with } \Pi[\dot{c}_k, \mu_k, \phi] = \Pi_{el}[\dot{c}_{el}, \mu_{el}, \phi_{el}] + \Pi_{ed}[\dot{c}_{ed}, \mu_{ed}, \phi_{ed}] + \Pi_{\Gamma_{BV}}[\dot{c}_{el}, \mu_{el}, \phi_{el}, \dot{c}_{ed}, \mu_{ed}, \phi_{ed}]$$

where eventually a decoupling between chemical $(\dot{c}_{ed}, \mu_{ed})$ and electrical ϕ_{ed} quantities can be operated within the electrode. Notice also that partitioned schemes can also be derived for the coupled electro-chemical system. Figure 1.6 shows an illustration of a such coupling through a simple numerical simulation performed on a one-dimensional mesh of the response of an electrode-electrolyte composite domain when submitted to initial gradients of chemical and electric potentials. Several profiles of fields are superposed on the graphs and show their time evolutions.

1.4 Multi-scale transient diffusion and coupled mechanics problems

For materials with a complex heterogeneous microstructure, some well-known diffusion field theories such as Fick's one may not be sufficient to describe the macroscopic diffusion response. Following a phenomenological approach as depicted in the previous section consisting in proposing mathematical forms of potentials, then calibrating them either on numerical or experimental data, is not always an easy task. This is especially the case when the material properties of the various constituents of the microstructure are very different. To this end, the identification of macroscopic continuum theories through multi-scale approaches has been the purpose of a number of methods of analysis to describe diffusive transport in heterogeneous media. These approaches usually require the solution of a boundary value problem defined on a Representative Volume Element (RVE) of

the microstructure in order to identify effective parameters to be used at the macroscale. However, most of these approaches in homogenization assume a quasi-static regime at the microscale, meaning that a net decoupling is assumed to hold between the loading characteristic time and the diffusion characteristic times of the various constituents of the microstructure. However, such a full separation of scales is sometimes not completely achieved for some materials under particular loading conditions. This is especially the case when there is a high contrast between the diffusivities of the phases, which may lead to that the diffusion through the slow phase induces a memory effect at the macroscopic scale. Microscopic transient effects may be particularly relevant for problems of diffusion of species, as compared to heat conduction problems, as the diffusion coefficients between the phases can vary by several orders of magnitude. For instance, the inclusion/matrix ratio of diffusion properties within an electrode of a lithium-ion battery can be of the order of 10^5 [144]. In these conditions, and according to the loading characteristic time, a homogenenized modeling in quasi-static regime may not give the expected accuracy of the macroscopic response if transient effects at not accounted for at the microscale.

Analytical or semi-analytical approaches have been designed for the homogenization of transient heat transfer problems [27, 29]. Especially, it has been showed how local transient effets within the slower phase translates into memory effects at the macroscale [99]. Recent works also proposed semi-analytical approaches to get estimates of the effective transient diffusion response of slow inclusions of arbitrary geometries [133, 144]. On another side, computational homogenization approaches have become much popular upscaling techniques, from which the effective behaviour is computed numerically by solving a boundary value problem on a Representative Volume Element of the microstructure at each integration point of a macroscale analysis [86]. The main interest lies in that it can handle non-linear constitutive models and general microstructures, but at the price of a dramatically high computational cost associated with solving large-scale boundary value problems, as the method does not provide expressions of the effective behaviour in closed-form. Recent works introduced Computational Transient Homogenization (CTH) techniques, either for linear elastodynamics [109], or for transient heat transfer problems [88, 131], hence all phases can be accounted for in the transient homogenization, and not only the slower one as it is the case with semi-analytical methods. However, these transient computational techniques turn out to be more costly than quasi-static ones, since at each time step and for each Gauss point of the macroscopic mesh, a microscopic finite element solution is performed on an elementary cell over the current time step, which permits to get by averaging the macroscopic flux and internal energy for heat transfer for instance. Furthermore, depending on the homogenization level, CTH can become even more costly than a direct numerical solution performed on the microstructured body. So CTH does not completely makes the problem of the computational cost go away in transient homogenization.

1.4.1 Model order reduction based on mode synthesis for computational homogenization of transient diffusion problems

In that context, the purpose of the PhD thesis of Abdullah Waseem was to propose efficient numerical methods in order to simulate the transient diffusion of species in heterogeneous materials *with much less computational effort* than with computational transient homogenization or with direct numerical simulation. His PhD thesis was the purpose of a collaboration between Centrale Nantes (with advisors Laurent Stainier and I) and the Eindhoven University of Technology in the Netherlands, with advisors Varvara Kouznetsova and Marc Geers. This PhD thesis also took place within the context of the EMJD-SEED (Simulation in Engineering and Entrepreneurship Development) funding program, financed by the European Commission.

For transient multi-scale analysis, the downscaling and upscaling procedures show some differences with respect to quasi-static ones. A classical first order Taylor's approximation of the primal field (e.g. the chemical potential μ for the diffusion of species, or the temperature difference θ for heat transfer problems) is usually performed for the downscaling, but is here added some fluctuations $\tilde{\mu}$ to account for the local transient effects

$$\mu(\bar{\mathbf{x}}, \mathbf{x}, t) = \bar{\mu}(\bar{\mathbf{x}}, t) + \bar{\boldsymbol{\nabla}}\bar{\mu} \cdot (\mathbf{x} - \bar{\mathbf{x}}) + \tilde{\mu}(\bar{\mathbf{x}}, \mathbf{x}, t),$$

where quantities with a bar on top refer to macroscopic ones. The average of these fluctuations and of their gradient over the elementeray cell should vanish (i.e. $\langle\tilde{\mu}\rangle = 0$ and $\langle\boldsymbol{\nabla}\tilde{\mu}\rangle = \mathbf{0}$), which is a consequence of that macroscopic quantities and their gradient are enforced to equal the average of their microscopic counterparts. The upscaling is performed by equating the virtual power (per unit volume) at a given macroscopic point $\bar{\mathbf{x}}$ to the volume average of the virtual power at the microscale, including transient contributions. This weak equality

yields generalized Hill-Mandel conditions, as shown in [131, 160] in the context of heat transfer. In the context of the diffusion of species, these conditions read

$$\bar{\mathbf{j}} = \langle \mathbf{j} - \dot{c}(\mathbf{x} - \bar{\mathbf{x}}) \rangle = \frac{1}{V} \int_{\partial\Omega} j_n (\mathbf{x} - \bar{\mathbf{x}}) da \tag{1.6}$$

$$\dot{\bar{c}} = \langle \dot{c} \rangle = -\frac{1}{V} \int_{\partial\Omega} j_n da \tag{1.7}$$

giving the averaged, macroscopic flux of species $\bar{\mathbf{j}}$ and concentration rate $\dot{\bar{c}}$. Observe that these quantities can be computed by only knowing the normal outward flux j_n at the boundary of the microscopic domain, whose computation is therefore the purpose of a subsequent model order reduction technique.

The computational approach followed in the work of A. Waseem was based on a model order reduction technique already experienced in the context of linear elastodynamics [128], and here extended to transient diffusion problems. The methodology followed relied on two main assumptions. The *first one* is the introduction of a so-called *regime of relaxed separation of scales*. Indeed, such regime appears as some intermediate one since it considers that local transient effects may occur within the inclusion, but not within the matrix. Therefore, this regime is characterized by some specific material properties, a fast matrix within which the steady state is reached almost instantaneously, and slow inclusions where diffusion takes time to proceed. Such regime is defined as

$$T \sim t_i >> t_m$$

where the characteristic times (T, t_i, t_m) are associated with the loading and diffusion within the inclusion and the matrix respectively. The *second assumption* this work relies on considers only *a linear material response* of the constituents of the microstructure. Such linearity can then be exploited separating the Initial Boundary Value Problem (IBVP) defined at the microscale into steady state and transient ones (see e.g. [6]). This split is valid as long as surface conditions of the IBVP are time-independent. This is why it is only compatible with the regime of relaxed separation of scales, within which transient effects are not expected to occur within the matrix, which also occupies the boundary of the elementary cell. Such approach is also found in sub-structuring techniques like that of Craig-Bampton [20]. Sub-structuring involves the division of a whole system into smaller sub-structures with connected boundaries, where the latters should not experience any transient effects that would provide a stiffer approximation [128]. In the context of computational homogenization, each microscopic domain attached to a macroscopic material point is assumed to be a substructure attached to the macroscopic domain.

An elementary cell consisting of inclusions embedded within a matrix is first discretized with finite elements. Once the mesh nodes have been divided into tied and retained ones, the discrete solution is decomposed into the sum of microscopic steady-state and transient contributions. The steady-state contribution is obtained by performing a static condensation or Guyan reduction, expressing the response of free nodes as a direct function of prescribed ones. The description of the transient contribution profits from that any parabolic system has natural solutions decaying exponentially in time, which yields some eigenvalue-like problem, well-known in thermal analysis for instance [105]. The associated eigenvalues $\alpha^{(k)}$ are then interpreted as the inverse of characteristic times (i.e. $\tau^{(k)} = 2\pi/\alpha^{(k)}$). The transient contribution to the solution field is thus expressed as a linear combination of eigenvectors $\mathbf{\Phi}^{(k)}$ through variables $\eta^{(k)}$, the latter being solution of a system of uncoupled Ordinary Differential Equations (ODE). At this stage, no reduction of the number of degrees of freedom has been performed, only the format of description of the solution has been changed. But by selecting only a limited number of eigenvectors, especially associated with the most influent decay times, a drastic reduction of the amount of degrees of freedom can be operated, and hence of the computational cost. Such approach amounts to make a mode synthesis for diffusion type problems, as the one performed by Craig-Bampton for linear elastodynamics [20]. It means that only a few enrichment variables $\eta^{(k)}$ now allow to account to transient effects at the microscale. Figure 1.7 shows an illustration of modes extracted from such decomposition for an elementary cell consisting of a circular inclusion centered in a square matrix. The mode synthesis carried out thus amounts to replace a numerical model fully discretized with finite elements at the microscale with thousands of coupled degrees of freedom, by a reduced one consisting of only a few degrees of freedom (~ 6), solution of a set of decoupled ODEs with a forcing right hand side once the superposition of both steady-state and transient contributions has been performed. Given the time evolution of a macroscopic loading, these ODEs can be solved with any discrete time-stepping method. Since the normal reaction flux j_n can be explicitly expressed

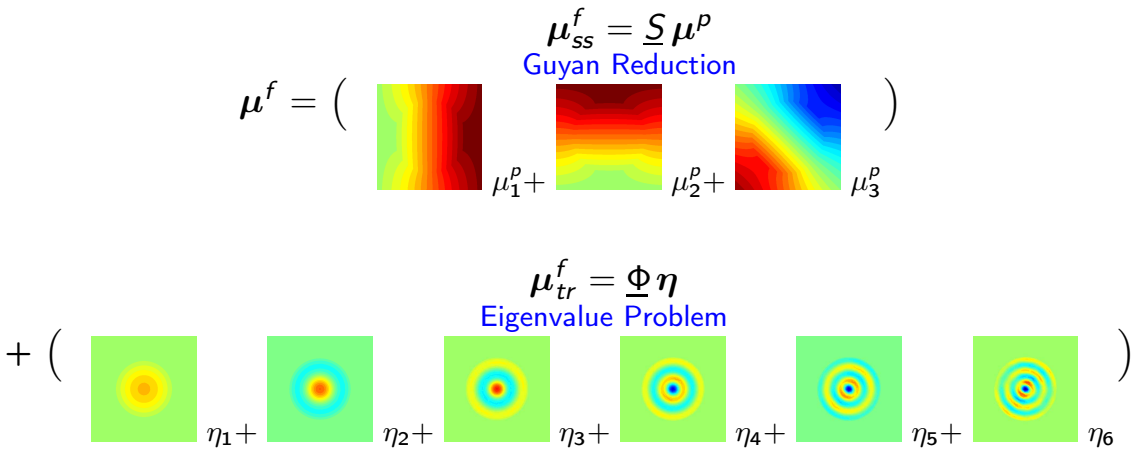

Figure 1.7: Solution decomposition into steady-state and transient contributions. Only a few transient modes are sufficient to provide a sufficiently accurate approximation of the solution.

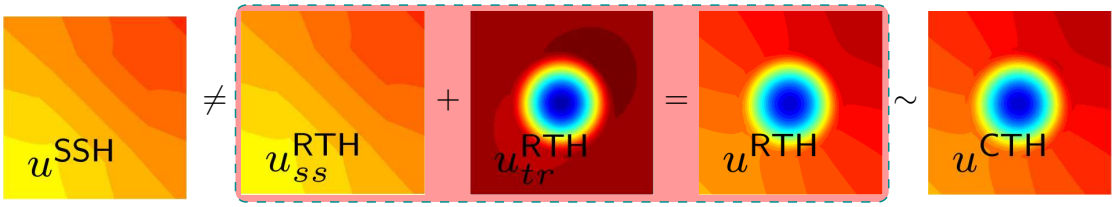

Figure 1.8: Maps of the dimensionless chemical potential computed on an elementary cell consisting of a circular inclusion centered in a square matrix, submitted to a macroscopic harmonic loading. Three cases are considered: (i) steady-state (SSH), (ii) transient fully-resolved with finite elements (CTH), and (iii) transient with the reduced model (RTH).

as a function of these enrichment variables, and of macroscopic quantities, the upscaling conditions (1.6) and (1.10) allow to get the expressions of the macroscopic mass flux and concentration rate in a closed-form.

Figure 1.8 shows maps of the dimensionless microscopic chemical potential, computed with the different approaches on a simple elementary cell consisting of circular inclusion centered in a square matrix. This cell is submitted to harmonic loading, both on the chemical potential and its gradient. Clearly, the transient solution is much different from the quasi-static one, while the reduced model (RTH) permits to get a very close solution to a fully-discrete finite element approach at a much lower computational cost. Figure 1.9 shows the time evolutions of the macroscopic quantities, from which it can be seen that transient homogenization has a significant influence on the capacitance of the system, much more than on the flux of species.

1.4.2 Two-scale analysis of transient diffusion problems through a homogenized enriched continuum

One great interest of the proposed approach is that an enriched continuum formulation has been substituted to a more classical homogenized medium through model reduction. Such formulation consists of the balance of species, constitutive equations for the macroscopic mass flux and the concentration rate, and a set of decoupled

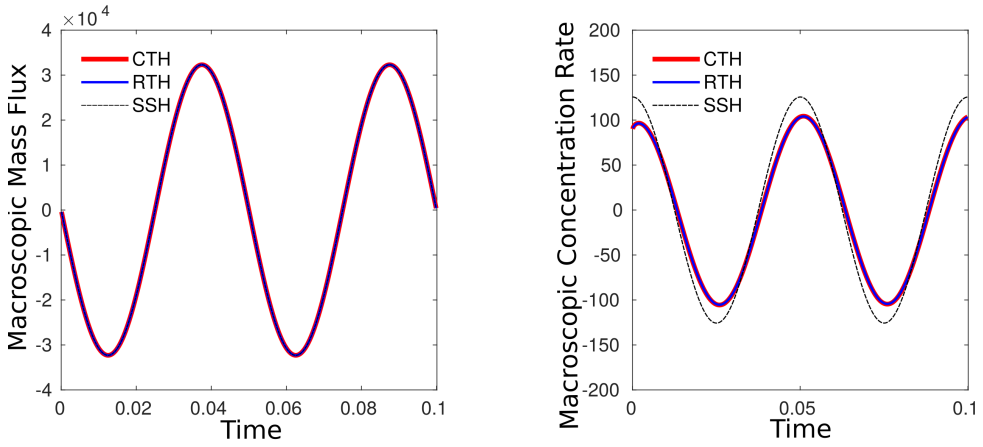

Figure 1.9: Dimensionless time evolutions of the macroscopic flux of species and concentration rate, computed from (i) steady-state (SSH), (ii) transient fully-resolved with finite elements (CTH), and (iii) transient with the reduced model (RTH) solutions.

ODEs written on the enrichment variables which drive their time evolutions:

$$\dot{\bar{c}} = -\bar{\boldsymbol{\nabla}} \cdot \bar{\mathbf{j}} \tag{1.8}$$

$$-\bar{\mathbf{j}} = \mathbf{a}^T \dot{\boldsymbol{\eta}} + \mathbf{B} \cdot \bar{\boldsymbol{\nabla}} \bar{\mu} + \mathbf{c} \dot{\bar{\mu}} + \mathbf{C} \cdot \bar{\boldsymbol{\nabla}} \dot{\bar{\mu}} \tag{1.9}$$

$$\dot{\bar{c}} = \mathbf{a}^T \dot{\boldsymbol{\eta}} + \mathbf{e} \cdot \bar{\boldsymbol{\nabla}} \bar{\mu} + f \dot{\bar{\mu}} + \mathbf{f} \cdot \bar{\boldsymbol{\nabla}} \dot{\bar{\mu}} \tag{1.10}$$

$$\dot{\boldsymbol{\eta}} = -\boldsymbol{\alpha} \boldsymbol{\eta} - V(\mathbf{d}^T \dot{\bar{\mu}} + \mathbf{a}^T \cdot \bar{\boldsymbol{\nabla}} \dot{\bar{\mu}}) \tag{1.11}$$

Mode synthesis in a computational framework has thus allowed to overcome two drawbacks of computational homogenization. On the one hand, it has permitted to drastically reduce the computational cost, thus making such approach affordable. On the other hand, it has provided a closed-form modeling of the effective behaviour, through the form of an enriched continuum embedding only a few well chosen enrichment variables, solution of ODEs. Such formulation is then compatible with a two-stage solution procedure. First, an *offline stage* will amount to pre-compute the coefficients $(\mathbf{a}, \mathbf{B}, \mathbf{c}, \mathbf{C}, \ldots)$ appearing in the enriched formulation (1.8)-(1.11). Those coefficients depends on both static and transient modes retained in the approximation of the microscopic fields, which in turn depend on finite element matrices associated with the mesh of the elementary cell. Second, an *online stage* during which both the enrichment variables $\boldsymbol{\eta}$ and the primal field of the diffusion problem (actually the chemical potential μ) are solved together on the macroscopic mesh.

Two solution methods using finite elements have been proposed [171] to handle both the enrichment variables and the chemical potential on the macroscopic mesh. The first one is a multi-field finite element implementation, associated with a multi-field weak form of Equations (1.8) and (1.11). A nodal finite element approximation is then performed on the macroscopic mesh for both types of fields. Once discretized in space by finite elements, and in time by an Euler Backward finite difference time scheme, a coupled system of equations is obtained, solved on the nodal values of the macroscopic chemical potential and those of the enrichment variables. One drawback of this approach lies in the number of equations this system consists of. If M is the number of nodes of the mesh, the number of unknowns are $M(1 + N_q)$ where N_q is the number of enrichment variables, generally of the order of 6. In addition, the matrix is not symmetric, which requires an LU factorization which is more costly. The latter is a direct consequence to that the present multi-field weak form has not been derived from any variational principle. However, recasting the present enriched continuum formulation (1.8)-(1.11) within a variational framework is clearly a very interesting issue to address in the future, as it would permit to recover a symmetric matrix and hence decrease the computational cost. A second solution method proposes to treat the enrichement variables as internal ones. If we assume these enrichment variables as discretized with piecewise constant shape functions, they can be condensed to eliminate them from the previous multi-field discrete system. Such approach is now compatible with a single-field weak form of the balance of species (1.8),

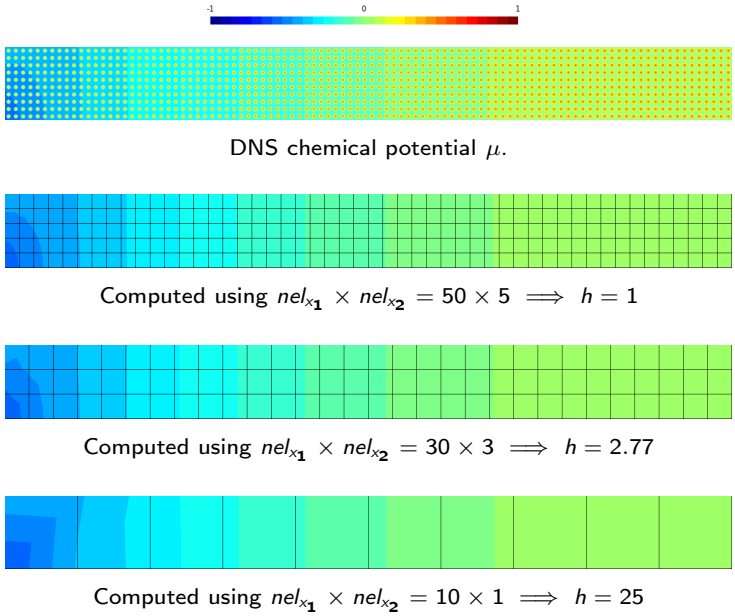

Figure 1.10: Maps of the dimensionless chemical potential computed on several macroscopic meshes of a rectangular computational domain. Comparison is performed with a DNS simulation.

within which the macroscopic constitutive equations (1.9)-(1.10) are introduced. This is supplemented with a time discretization of ODEs (1.11). A basic backward Euler scheme can eventually be chosen, which is first order accurate, or better a second order accurate exponential-based time integrator, as already used in the context of viscoelasticity for instance [71]. A linear system of only M equations written on nodal values of the macroscopic chemical potential is obtained. This system profits from a symmetric matrix now, and its solution is alternated with the integration of the enrichment variables at integration points at each time step. However, the only drawback of this approach lies in that the right hand side needs to assemble the contribution of the previous time step due to the elimination, which has appeared to be time consuming.

Figure 1.10 shows some numerical illustrations of maps of the dimensionless chemical potential computed on several macroscopic meshes of a rectangular computational domain. Several homogenization levels[3] are thus achieved, and a good agreement is shown between the homogenized solution and that obtained from a Direct Numerical Simulation (DNS). Figure 1.11 shows a plot of the relative error of the macroscopic concentration rate as a function of the homogenization level. Clearly, a very good accuracy of homogenized solutions is achieved with respect to the CTH one. At last, Figure 1.12 shows the associated CPU time. The two homogenized numerical solutions (computed with the two finite element implementations) lie at two orders of magnitude below that of CTH, which is a severe reduction of the computational cost. The internal-variable finite element implementation appears slightly more costly than the multi-field one. Most of its cost is due to the element-level calculations and the assembly of the internal flux vector appearing at the right hand side of the system of linear equations. Figure 1.12 also shows that the CTH solution can even get more costly than the DNS for homogenization levels close to unity.

1.4.3 Extension to the coupling between transient diffusion and mechanics

During his PhD thesis, Abdullah Waseem also extended the model order reduction based on mode synthesis for computational homogenization to the *coupling between transient diffusion and mechanics* [161]. The mechanics

[3]The homogenization level is defined as the ratio of the number of unit cells within the geometrical domain to the number of integration points the macroscopic mesh consists of.

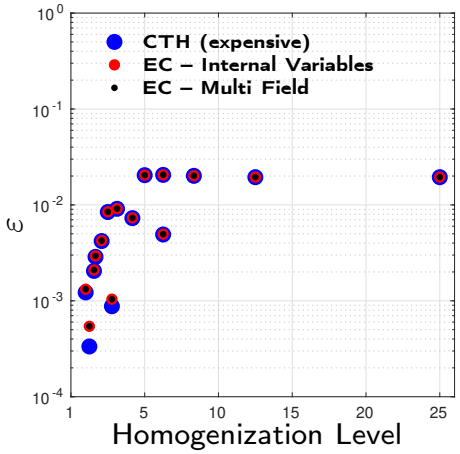

Figure 1.11: Relative error of the macroscopic concentration rate $\varepsilon = \frac{\|\dot{\bar{c}} - \langle \dot{c} \rangle\|}{\|\langle \dot{c} \rangle\|}$ as a function of the homogenization level, computed for the different solution approaches.

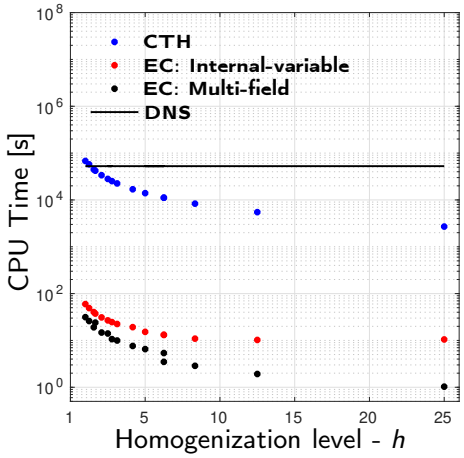

Figure 1.12: CPU time plotted as a function of the homogenization level, computed for the different solution approaches.

is here considered as quasi-static, providing the following decoupling of characteristic times

$$T \sim t_i >> t_m \sim t_{mech}$$

where $t_{mech} = \boldsymbol{\varepsilon} : \dot{\boldsymbol{\varepsilon}}$ denotes the characteristic time associated with the deformation process. The key ingredient this extension relies on pertains to the modeling of the coupling between the diffusion and mechanical processes, and in particular the associated choice of the energy density function or potential. Both Helmholtz's free energy density $\psi(c, \boldsymbol{\varepsilon})$ or its dual potential $\psi^*(\mu, \boldsymbol{\varepsilon})$ obtained by a Legendre transform are available possibilities

$$\begin{aligned} \psi(c, \boldsymbol{\varepsilon}) &\rightarrow (c, \boldsymbol{\varepsilon}) \text{ formulation} \\ \psi^*(\mu, \boldsymbol{\varepsilon}) &\rightarrow (\mu, \boldsymbol{\varepsilon}) \text{ formulation} \end{aligned}$$

leading to the definition of different primal unknown to describe the diffusion in addition to the strain $\boldsymbol{\varepsilon}$. However, a quick look to the coupled systems of equations derived in both cases

$(c, \boldsymbol{\varepsilon})$ formulation

$$\begin{aligned} &\boldsymbol{\nabla} \cdot [\boldsymbol{M} \cdot \boldsymbol{\nabla}(\Lambda(c - c_0) + \boldsymbol{S} : \boldsymbol{\varepsilon})] = \dot{c} \\ &\boldsymbol{\nabla} \cdot [\mathbb{C} : \boldsymbol{\varepsilon} + \boldsymbol{S}(c - c_0)] = \boldsymbol{0} \end{aligned}$$

$(\mu, \boldsymbol{\varepsilon})$ formulation

$$\begin{aligned} &\boldsymbol{\nabla} \cdot (\boldsymbol{M} \cdot \boldsymbol{\nabla}\mu) + \frac{\boldsymbol{S} : \dot{\boldsymbol{\varepsilon}}}{\Lambda} = \frac{\dot{\mu}}{\Lambda} \\ &\boldsymbol{\nabla} \cdot \left[\left(\mathbb{C} - \frac{\boldsymbol{S} \otimes \boldsymbol{S}}{\Lambda} \right) : \boldsymbol{\varepsilon} + \frac{\mu \boldsymbol{S}}{\Lambda} \right] = \boldsymbol{0} \end{aligned}$$

shows that the divergence of the gradient of the strain $\boldsymbol{\varepsilon}$ appears in the balance of species associated with the $(c, \boldsymbol{\varepsilon})$ formulation, which after integration by part in a weak formulation would require a $\mathcal{C}^1$ continuity of the finite element approximation of the displacement field. Such approximation is not standard and therefore not convenient. Rather, the strain rate directly appears in the balance of species associated with the $(\mu, \boldsymbol{\varepsilon})$ formulation, then only requiring standard $\mathcal{C}^0$ continuity of the finite element approximation of the displacement field. In essence, the $(\mu, \boldsymbol{\varepsilon})$ formulation resembles much to the classical Fourier-based linear thermoelasticity, where the balance of species is here the analog of the heat equation, the chemical potential is the analog of the temperature increase, and the concentration is the analog of the entropy density. The strain rate also appears in the heat equation, but with a minus sign to make the temperature decrease as the volume increases. Consistently with the discussion carried out in Section 1.3 around variational principles for transient diffusion problems, the chemical potential plays the role of a driving force which is better suited than the concentration to describe the coupling with other physics, and especially here mechanics.

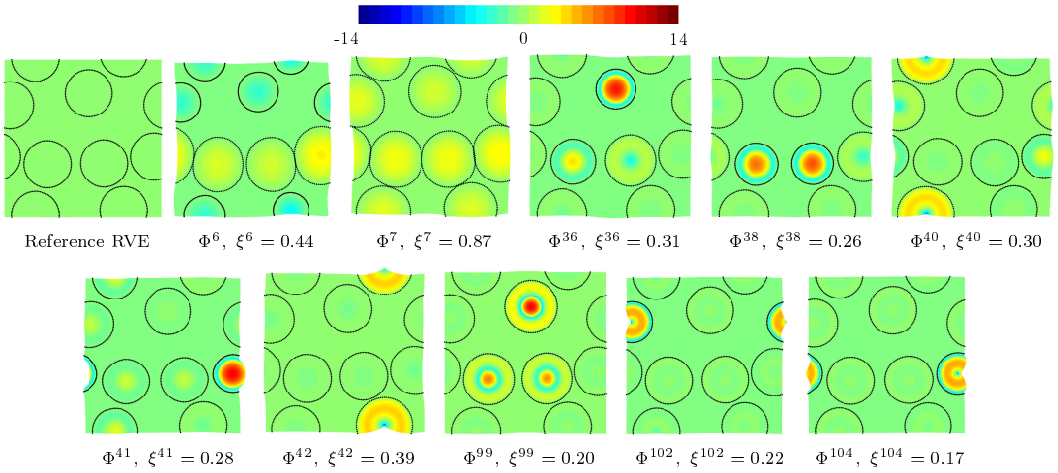

Figure 1.13: Transient modes selected, showing the maps of the dimensionless chemical potential plotted on the deformed geometry (scaled with a factor five). Extracted from [161].

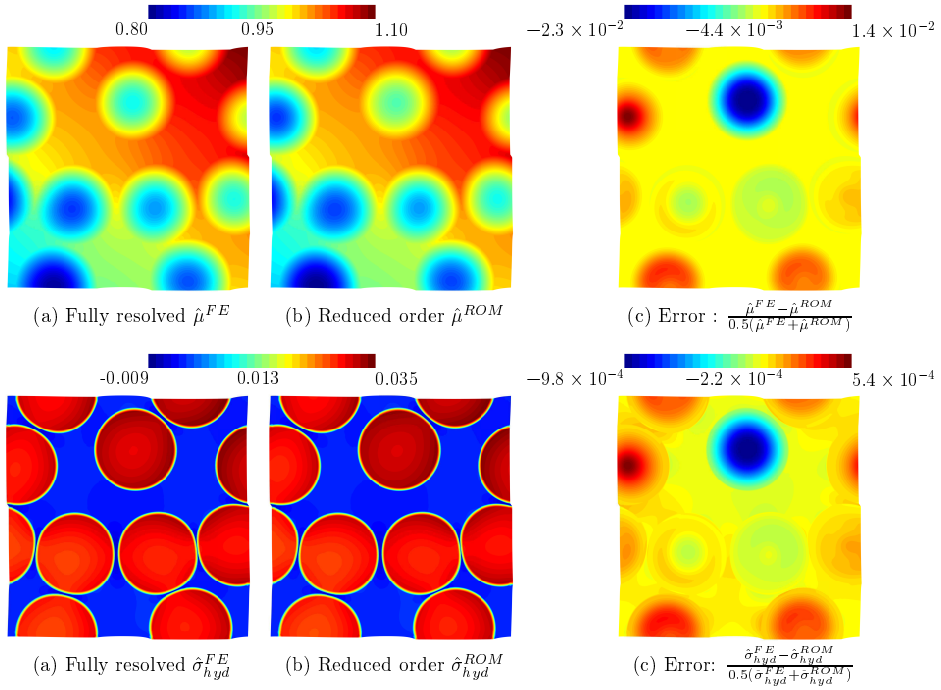

Figure 1.14: Maps of the dimensionless chemical potential (top row) and hydrostatic stress (bottom row), computed with both fully resolved and reduced order model, as well as error maps of both fields. Extracted from [161].

Following the same path than for pure diffusion, a first order homogenization is performed on both the chemical potential and the displacement fields, including fluctuations associated with transient effects at the microscale. Upscaling conditions are also derived for both physics, equating virtual powers at both micro and

macroscales, which were already derived by Kaessmair and Steinmann [139] who made a conventional transient homogenization in chemo-mechanics. Next, the model reduction process essentially follows the same lines than those already explained for pure diffusion, and can be found in [161]. One interesting point though can be observed on the transient contributions of the displacement fields, which is deduced up to a pre-multiplying finite element matrix from that of the chemical potential, the latter being defined via the chosen transient modes. An enriched continuum is also obtained, gathering macroscopic balance and constitutive equations for both diffusion and mechanical component, supplemented with a small set of uncoupled ODE written on enrichment variables, whose right hand side now consists of both chemical and mechanical contributions.

As an illustrative example, an elementary cell consisting of few non-ordered inclusion is considered, and submitted to an *a priori* known harmonic macroscopic loading on the chemical potential and its gradient. Such cell may eventually represent a cathode-electrolyte system of a lithium-Ion battery with active particles. The offline stage first consists in pre-computing coefficients of the enriched continuum, and especially a few transient modes as shown in Figure 1.13, which are selected according to a scalar quantity weighting coefficients of the forcing term of ODEs which the enrichment variables are solution. Next, the set of uncoupled ODE is integrated in time given a macroscopic loading, from which the microscopic fields can be reconstructed. Figure 1.14 shows maps of both the dimensionless chemical potential (top row) and hydrostatic stress (bottom row) are shown at a given time, and computed with both fully resolved and reduced order model. A very good agreement can be observed, especially as shown by the associated error maps.

1.4.4 One route among others for non-linear problems

The model order reduction presented so far in Section 1.4, applied to computational homogenization during the PhD of A. Waseem, relied among other things on the *linear material response* of the constituents of the microstructure. The exploitation of this linearity has allowed to perform an additive split of the solution between steady-state and transient contributions. However, such split does not hold anymore if a *non-linear material response* is considered for the different phases, and another strategy should be followed. Besides, one difficulty associated with the non-linear case is that the effective macroscopic response is not always amenable to a closed-form.

One interesting idea output from the model order reduction based on mode synthesis in the linear case is the efficiency of the obtained computing method if we pre-compute and store once for all some intrinsic feature of the system. This took the form of static and transient modes, then of various coefficients of the enriched continuum. But these quantities could be use and reuse at profit during the computation at the macroscale. This is what was lacking to traditional computational homogenization techniques, in which the solutions of a microscale problem are not reused in any way. One way to extend the model order reduction framework to non-linear problems, while recycling the microscopic solutions is to follow an approach using data sets. Following the one introduced by Kirchdoerfer and Ortiz [126], it consists in replacing the constitutive equations, translating into mathematics the constitutive response of a material, by a data set gathering a discrete collection of material responses. The latter are assumed to be known data, either from experiments or from numerical simulations. When no closed-form modeling of the effective macroscopic response is available, one interest in using data sets lies in that one solution of a microscale problem can be reused at a different time step, or at another location of the computational domain. The associated computational cost stems only from the data search operation.

However, the cornerstone of such approach lies in the design of the data set. Especially, if this approach is expected to be competitive with respect to Computational Transient Homogenization, the step of data search should be much cheaper than the computation of a finite element solution at the microscale. One crucial question raised thus concerns the quantities that should be stored within the data set, especially if the constitutive response depends on the history. One solution would be to store all time steps of all fields of the microscopic solution obtained from one loading path, and redo the same for all possible loading paths. But this would yield a huge data set, and searching within it would be quite costly, hence decreasing the efficiency of this approach. Another solution is to introduce a set of history variable, which avoids to search within a too large data set. Here comes the interest of using a model order reduction technique, eventually leading to an enriched continuum, allowing the natural emergence of a finite set of enrichment variables. On the one hand, using such reduced model allows to make the construction of the data set computationally reasonable, by generating efficiently the effective macroscopic responses of the microscopic system. Eventually, adaptative methods can be designed to enrich the data base on-the-fly during the online stage. On the other hand, a data

set of moderate size, containing just a few history variable emerging from the reduced model, permits a fast step of data search.

These ideas have allowed to design a procedure called *data-driven reduced homogenization* [172], which consists of three steps. The *first one* consists of the construction of a reduced model of the microscale system, which allows to make emerge just a few enrichment variables and obtain the effective macroscopic response at a low computational cost. The *second step* is associated with the data generation, which involves the solution of many microscale problems for given loading paths. This step is crucial because the data set should be sufficiently rich in order to be able to provide an accurate effective macroscopic response to the solver at the macroscale. It raises the question of the set of loading paths that should considered. In a sense, the data set actually 'learns' the subspace of the effective macroscopic non-linear response (provided by the reduced model) which is required by the macroscopic solver in order to provide a compatible and equilibrated macroscopic solution. The *third step* is the data search, which will be efficient if and only if few enrichment variables allow to account for history or transient effects at the microscale.

Although designed for *a priori* non-linear problems, such approach was at first applied to linear transient diffusion problems, for which a reduced model was developed. Therefore for such problem, the data set consists of all quantities involved in its description, plus their rate

$$\mathcal{D} = \{\mathbf{z}^* = (\mu^*, \dot{\mu}^*, \mathbf{g}^*, \dot{\mathbf{g}}^*; c^*, \dot{c}^*, \mathbf{j}^*; \boldsymbol{\eta}^*, \dot{\boldsymbol{\eta}}^*\},$$

except the rate of the flux of species, and recall that $\mathbf{g} \equiv -\boldsymbol{\nabla}\mu$. Next, a distance $d(\mathbf{z}, \mathbf{z}^*) = |\mathbf{z} - \mathbf{z}^*|$ should be defined between a state satisfying the set of compatibility, balance and boundary equations, and a state lying in the data set. Usually, an L^2 norm is chosen

$$|\mathbf{z}| = \left[\frac{1}{2}\left(\mathcal{C}_1\mu^2 + \mathcal{C}_2\dot{\mu}^2 + \mathcal{C}_3\mathbf{g}^2 + \mathcal{C}_4\dot{\mathbf{g}}^2 + \mathcal{C}_4\boldsymbol{\eta}^2 + \mathcal{C}_6\dot{\boldsymbol{\eta}}^2 + \mathcal{C}_7c^2 + \mathcal{C}_8\dot{c}^2 + \mathcal{C}_9\mathbf{j}^2\right)\right]^{\frac{1}{2}}$$

and a set of coefficients $\mathcal{C}_\alpha$ are introduced to weight the contribution of each quantity. These coefficients are here to define a dimensionally-consistent distance. Normally they are tuned according to the importance of each term, but of course no unique definition of the distance and of these weighting coefficients exist. Indeed, by applying approaches based on data sets, we are led to apply the law of large numbers, which says here that in the limit of an infinitely rich data set, the definition of the distance function and the tuning of weighting coefficients have no influence on the solution found.

The initial boundary value problem is then formulated as the following optimization problem

$$\inf_{\mathbf{z}\in\mathcal{E}_{n+1}} \inf_{\mathbf{z}^*\in\mathcal{D}} d(\mathbf{z}, \mathbf{z}^*)$$

This double minimization problem is a combination of continuous and discrete optimization problems, and it has a combinatorial complexity. Usually, a two-stage staggered solution scheme is adopted, which consists, at some iteration k of a given time step, to first compute an equilibrated state from a known point of the data set, and then to search in the data set the closest point to the new equilibrated point obtained, namely

(i) $\mathbf{z}_{n+1}^{k+1} = P_{\mathcal{E}_{n+1}}(\mathbf{z}_{n+1}^*)^k$

(ii) $(\mathbf{z}_{n+1}^*)^{k+1} = P_{\mathcal{D}}\mathbf{z}_{n+1}^{k+1}$,

where $P_{\mathcal{E}_{n+1}}$ and $P_{\mathcal{D}}$ denote the projectors to spaces $\mathcal{E}_{n+1}$ and $\mathcal{D}$ respectively. This process continues up to convergence. Notice that the projector of the first step is obtained by writing a Lagrangian functional consisting of the distance augmented by the discrete residual of the balance of species enforced to vanish through some Lagrange multiplier:

$$\delta\mathcal{L}_{n+1} = 0, \text{ with } \mathcal{L}_{n+1} = d(\mathbf{z}_{n+1}, \mathbf{z}_{n+1}^*) + \lambda_{n+1}\mathcal{R}(\mathbf{z}_{n+1}).$$

The obtained discrete Euler-Lagrange equations, and their combination lead to that two linear systems of equations should be solved to get the solution. The first one is written on the chemical potential, the other on the Lagrange multiplier.

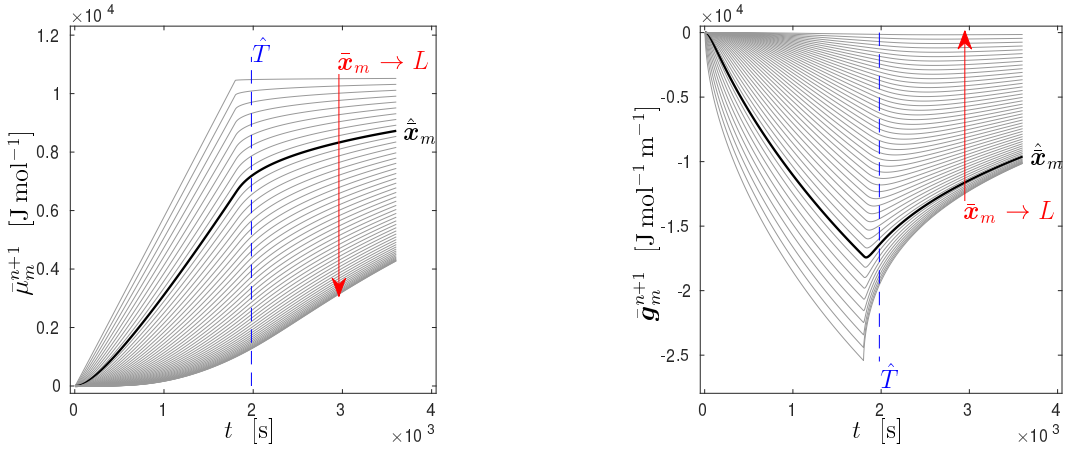

Figure 1.15: Input data applied to the reduced model, obtained by the post-processing of the solution of the enriched continuum at each integration point of a one-dimensional macroscopic mesh, when submitted to a ramp loading.

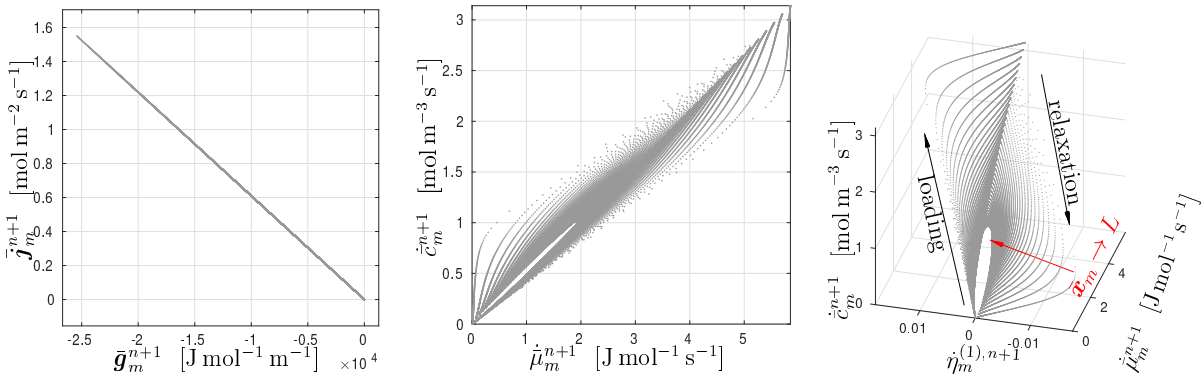

Figure 1.16: Macroscopic quantities output from the reduced model, stored within the data set together with input data.

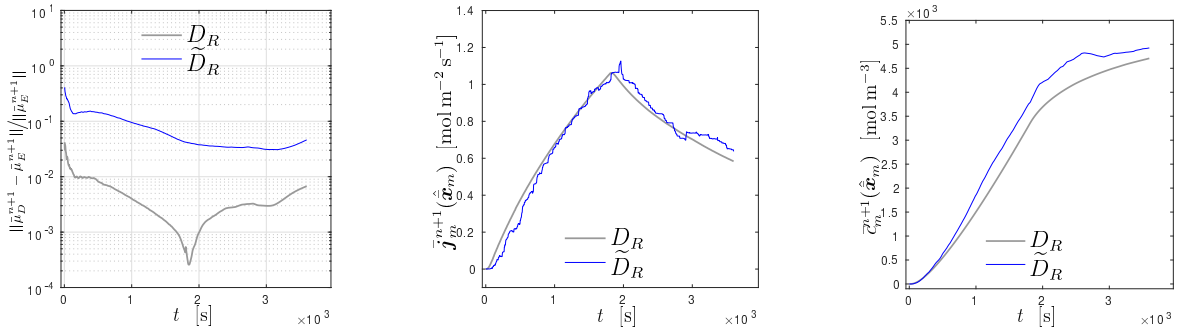

Figure 1.17: Time evolutions of the relative error of the chemical potential and of macroscopic quantities, computed with noisy and noiseless data sets.

As an illustration for validation purpose of the data-driven solver, Figure 1.15 shows the loading conditions $(\mu, \mathbf{g})(t)$ which are applied to the reduced model in order to generate the data base. These input data are here obtained by the post-processing of the solution of the enriched continuum at each integration point of a one-dimensional macroscopic mesh, when submitted to a ramp loading. Once applied to the reduced model, Figure 1.16 shows the response of the reduced model through the macroscopic output data, which together with input data, allow to fill the data set. No prominent history effect appears in the relation between the flux of species and $\mathbf{g}$. But a non-Fickian behaviour appears on the capacitance part. Especially, since only one enrichment variable was here found sufficient to describe transient microscopic effects, the 3D graph clearly shows the different loading and relaxation paths, which can be departed thanks to the enrichment variable.

When the data set is filled with the reference solution (obtained from the enriched continuum), the data-driven solver permits to recover it on the macroscopic mesh with a quite good accuracy. It can be viewed as a sort of consistency test, checking the numerical error carried out by the two-stage staggered solution scheme, which has been fed with the perfect data set. However, when the reference solution is not known, the data set should be filled with data obtained from carefully designed loading paths. Even more than that, the data can be noisy if they are obtained from experiments. Figure 1.17 shows a comparison of the time evolutions of macroscopic quantities when computed with a noiseless data set D_R and a noisy one $\tilde{D}_R$, obtained by adding some white Gaussian noise. Although measured, their evolutions is clearly sensitive to the addition of such noise, as also seen on the time evolution of the relative error of the chemical potential.

In this work, a first attempt to define a framework for reduced numerical homogenization to treat non-linear problems was made by combining an approach based on data sets and an *a priori* known reduced model of the microscale system. Although it was only applied to transient linear problems to profit from the previously developed solver, the application of such framework to true non-linear problems requires to address the question of the definition of a well-suited reduced basis in such case. A discussion of this outlook is addressed in Section 3.2.

Chapter 2

Fast thermo-mechanical systems

2.1 Exploiting velocity effects

Among the current major societal challenges is, among other things, the reduction of energy and resources employed everyday. This is especially the case of the production processes, or of the transports, for which such reduction would also lead to a reduction of costs and of process emissions. One approach followed so far by the manufacturing industries is to make a lightweight design of their products, that is either increasing the use of lightweight materials in structures or using lighter hybrid components. For instance, steel tends to be replaced when possible by lighter materials, such as aluminium alloys or fiber-reinforced composites (FRC). Or, when possible, hybrid structures metal/composite may advantageously replace full-steel structures, as for instance for ballistic protection purpose in light vehicules. However, to widen their use some major technical issues are faced. *Firstly*, assembling dissimilar materials/structures becomes then widespread in every industrial product, but it is also a major issue due to the dissimilarities in physical, thermal and chemical properties. Avoiding additional fixing components (for mechanical joining technologies), difficulties due to material melting and heating into the joined parts for Resistance Spot Welding (RSW) or more generally fusion based thermal technologies, or the formation of brittle InterMetallic Compounds (IMCs), constitute the major challenges to make successful these assemblies. Hence, solid state thermo-mechanical processes such as Friction Stir Welding have become popular though it still poses problems for dissimilar structures. *Secondly*, these materials are often associated with limited processing properties (e.g. machinability or formability). This is why forming and machining technologies reach their limits in terms of feasibility (ductile failure, chip geometry, tolerances) and profitability. It thus needs considerable effort involved in process, tools and machines to become efficient in manufacturing complex components. *Thirdly*, from the industrial viewpoint any joining process should respond to at least four criteria: (1) mass production (high performance, high productivity and relatively low cost); (2) ability to not disturb the organisation of assembly lines (automation), (3) ability to not disturb the design (spot welding); and (4) versatility to justify its material and human investment (acquiring of technical and scientific skills for industrial control of the technology). The same process must thus be able to produce the Al to Al, Al to galvanized steel and Al assemblies or galvanized steel to FRC.

Exploiting velocity effects has been shown to offer many opportunities [96] for different processing aspects in areas such as manufacturing, dynamics of structures, or assembling lightweight dissimilar materials. For instance, an improvement of the processing limits is observed on forming limit curves obtained in dynamics for aluminum [46] or even steel [69] thin sheets, when compared to quasi-static situations. A reduction of the 'structural' elastic springback of parts is also observed in that context, as well as a decrease of wrinkling. Dynamic bonding (or welding) is also made possible for materials known to be difficult to weld (especially aluminium alloys) with more classical technologies (and especially fusion-based welding processes), hence addressing industrial issues related to dissimilar assemblies. These velocity effects can be triggered after the generation of a short pulse or impact on a structure, or via a dynamic cyclic loading, deforming the medium and propagating different kinds of waves within it according to the magnitude of the applied pressure. On the one hand, materials submitted to high strain rates are known to exhibit a quite different constitutive response than in quasi-statics. For instance, an increasing flow stress is observed as a function of the strain rate [35, 76] for various metallic

alloys, of when strongly stirred it can behave as a pasty fluid. On the other hand, an impact on a structure will generate waves propagating in the medium a quite different mechanical field than the one that would be obtained in quasi-statics. An easy and academic example of this can be shown on an elastic sphere under inner pressure. Indeed, its well-known solution in quasi-static yields radial and hoop stress components of different signs and varying as $1/r^3$, while in dynamic these components share the same sign and vary as $1/r$ [75]. These dynamic effects thus permit to play differently with the geometry of a structure in order to achieve a given objective. Both items contribute to what are generally called 'velocity effects', whose benefits can among others be observed on the forming limit curves of metallic alloys.

These velocity effects can be implemented via various technologies. The use of Laser, high pulsed power technologies, or explosives represent a non-exhaustive list of means allowing to generate dynamic loadings, whose effects can then be exploited to fulfill a dedicated objective. Notice also that some of these technologies can either be used for material processing or for dynamic testing purposes, as shown in Figure 1. In the latter case, the objective is rather to identify some strain-rate dependent constitutive response.

In that context, my research works in this area have focused on several points. First, some interest has been devoted to the study, the numerical simulation and eventually the development of some dynamic assembly or forming processes. Associated contributions are summarized in Section 2.2. Especially, I got interested during my PhD thesis by a variant of the Friction Stir Welding process, whose contributions are described in Section 2.2.1. Next, I was introduced to high pulsed power technologies working with Professor Guillaume Racineux, which were the purpose of some contributions summarized in Section 2.2.2. Second, I was also interested in experimental material dynamic testing techniques, since a good knowledge of the thermo-mechanical response of the material is required on a wide range of strain rate to accurately predict the strength of structures or to master the feasibility of forming processes. Some works related to an experimental system designed to obtain the material constitutive response at very high strain rate is summarized in Section 2.3. Third, research works were also devoted to the modeling and computational aspects of fast transient thermo-mechanical processes, which occur after impacts on structures, as for instance during high speed forming processes. These contributions are summarized in Section 2.4.

2.2 Material processing at high strain rates

2.2.1 Friction Stir Spot Welding (FSSW)

Friction Stir Spot Welding is a solid state welding process, derived from Friction Stir Welding, and introduced in the 2000s by the car manufacturer Mazda [63]. It consists in creating a spot weld between two superimposed sheets by penetration of a rotating tool, composed of a pin and a shoulder, into the material. A sketch of the principle is shown in Figure 2.1. The heating generated by friction as well as the motion of the material driven in the vicinity of the tool allow a mixture ensuring the solidarity of the parts to be joined after cooling. This process of welding in the solid state and without filler metal is particularly interesting for carrying out the assembly of non-ferrous metals such as aluminum or copper alloys, reputed to be poorly weldable with conventional processes. Such process was aimed in the 2000s at being competitive with respect to the widespread process of resistance spot welding, to perform spot welds in the automotive industry, due to its high productivity and relatively low required input of energy.

2.2.1.1 Modeling fluid/solid coupling for high temperature assembly processes

As the rotating tool penetrates the upper sheet, the stirred and hence softened material below the tool becomes mushy. From the modeling viewpoint, Lagrangian approaches hardly simulate such problem due to the high level of deformation involved, generating mesh entanglement, requiring remeshing, costly and diffusive remapping steps of internal variables, and do not profit from the evanescent memory of the stirred matter. On another side, Eulerian approaches require dedicated techniques to track the boundaries. In that context, the purpose of my PhD thesis was to develop a numerical framework dedicated to the numerical simulation of welding processes in which a subdomain undergoing both a high level of deformation and high strain rates coexists with another one following a more classical solid behaviour. Friction Stir Spot Welding was thus representing a first step before arc welding processes. This PhD took place between University Pierre et Marie Curie in Paris, the Ecole

Nationale d'Ingénieurs de Saint-Étienne (ENISE), and the company ESI Group (located in the center of Lyon), under the supervision of professors Jean-Baptiste Leblond and Jean-Michel Bergheau.

In these works, an Arbitrary-Lagrangian-Eulerian (ALE) approach allows to decouple the motion of the matter from that of the mesh only in the stirred area, so that several rotations of the tool can be more easily simulated while following the boundaries of the welded sheets. A more classical updated Lagrangian description [58] is followed in the solid area. In addition to the different description of the kinematics in the two subdomains, different constitutive modelings were considered. Indeed, the mushy state of the matter in the stirred area invite to consider an incompressible viscous fluid constitutive response. Usually, a Norton-Hoff flow rule is considered for such constitutive response. The solid subdomain is described with a constitutive response depending on the history of the loading path. Here, a formalism based on a hypoelastic-plastic constitutive response [58] is followed. This type of approach based on a fluid/solid coupling provides a correct local description of the mechanical constitutive response while relying on relevant kinematic descriptions of the two subdomains of the structure [94]. More generally, the purpose of the proposed approach was to unify usual numerical modelings of welding processes, which historically focused either on the modeling of the process itself (the molten pool in the case of fusion welding processes) or on the induced consequences, i.e. residual stresses and distortions.

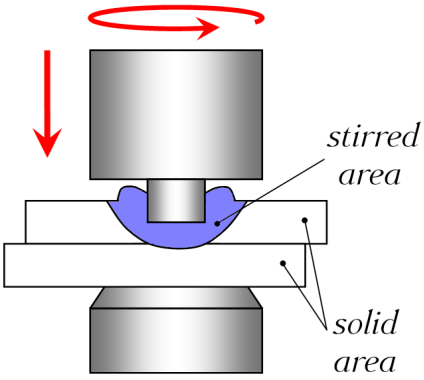

Figure 2.1: Sketch of the principle of Friction Stir Spot Welding, with both stirred and solid areas.

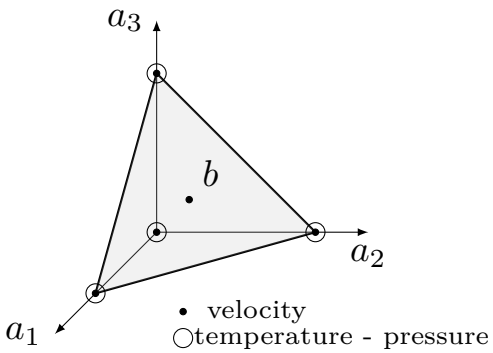

Figure 2.2: Mixed P1+/P1 (or MINI-)finite element, applied with a monolithic thermo-mechanical coupling.

The P1+/P1 finite element, also called MINI-element [31], was used for the spatial discretization. The approximation P1+ is related to that of the velocity field, enriched with degrees of freedom linked to an additional internal node located at the barycenter of the element (see Figure 2.2), which is associated a bubble function. This element is compatible with multi-field formulations, and usually allows to enforce an internal constraint related to the total or partial incompressibility of the medium. In this work, this enriched tetrahedral finite element ensures here the continuity of temperature, pressure and velocity fields. A thermo-mechanical multi-field finite element formulation consisting of the weak forms of the heat equation, the balance of linear momentum, and of the internal constraint relative to each subdomain was derived with this finite element. The total incompressibility is enforced weakly in the fluid area, while only the plastic one is enforced in the solid subdomain. Appropriate heat sources are accounted for in both fluid and solid areas, associated with the respective mechanical dissipations. The mechanical inertia terms are neglected in the solid area since it deforms in a quasi-static manner, while they are important in the fluid one. At last, convection terms appear in the fluid area in addition to inertia ones due the ALE description of the kinematics, both on the thermal and mechanical equations. The semi-discrete system of equations thus read

$$\mathbf{M}\dot{\mathbf{q}} + \left\{ \begin{array}{c} \mathbf{f}^{\text{conv}} \\ \mathbf{0} \end{array} \right\} + \mathbf{f}^{\text{int}} = \mathbf{f}^{\text{ext}} \tag{2.1}$$

where convection forces only appear in the fluid area, $\mathbf{M}$ is some generalized mass matrix, $\mathbf{q}$ is the vector of

degrees of freedom

$$\mathbf{q}^T = \{\mathbf{T} \quad \mathbf{v} \quad \mathbf{p} \quad \boldsymbol{b}\},$$

and $\boldsymbol{b}$ are the degrees of freedom of the bubble node, homogeneous to some velocity. Notice that the formulations in both fluid and solid areas are expressed in term of temperature, velocity and pressure degrees of freedom, which permits to make naturally compatible the assembly of elemental quantities of those areas. In order to provide a stable approximation to System (2.1) as the Peclet number increases, a Petrov-Galerkin method [28] is applied on thermal equations. However, since low Reynolds numbers are expected in the fluid area, a simple Galerkin method is used for mechanical equations. Furthermore, since the bubble function vanishes on the element boundary, the degrees of freedom of the bubble node $\boldsymbol{b}$ are internal to the element and are usually eliminated to save some computational cost by reducing the size of the system to be solved. However, the presence of rates in System (2.1) prevents this straighforward elimination. Such elimination was here made easy by assuming that the bubble acceleration is roughly equal to the average of those of vertex nodes, making vanishing the rates of the bubble degrees of freedom. Such approximation was anyway generating a lower numerical error than the subsequent lumping of the mass matrix. Indeed, the former restricts the acceleration to be linear on the element, while the latter enforces it to be constant per element. Finally, the semi-discrete system (2.1) is discretized in time with an implicit Euler time-stepping, and is linearized with a Newton-Raphson method at each time step. Then, a monolithic solution of the resulting linear system of equations is performed at each Newton iteration on degrees of freedom lying at vertex nodes (i.e. temperature, velocity, pressure) up to convergence.

The developments related to the formulations in the fluid and solid areas were implemented in the commercial finite element code SYSWELD [74], developed by the company ESI Group, which is dedicated to the numerical simulation of welding processes. These two formulations were first validated separately, and were the purpose of the development of analytical solutions related to a toy problem: the Couette viscometer. First, an extension of its well-known steady-state solution to the laminar flow of incompressible fluids with inertia effects and thermo-mechanical coupling was addressed in [87, 117], and served for the validation of the fluid formulation. Second, an extension was considered to solid-type elastic–plastic and thermo-elastic–plastic von Mises materials, both in small and large strains [116], and was used for the validation of the solid formulation. The latter case was obtained in the formalism of hypoelastic-plastic models, and reusing the solution developed for small strains by (i) replacing the tangential displacement u_θ by the curved arc length swept l, and (ii) neglecting the additional terms associated with the objective time derivative.

For the sake of simplicity, but also to satisfy some constraints of the code architecture, the elements of the mesh were defined as being either fluid or solid, which leads to that the fluid/solid interface passes through the faces between the elements. As the interface propagates during the simulation, elements can change of formulation. The simplest criterion for that is to define an averaged transition temperature set by the user, above which a transition from solid to fluid is performed, and below which the converse operates. Both the test on a transition temperature and the mesh updating procedure linked to the ALE description are performed at convergence. During the iterations at a given time step, the residual is computed based on the distribution of constitutive responses over elements defined at the previous time step. In the fluid area, it is computed with respect to the geometry updated at the previous time step, while the updated geometry at each iteration is considered in the solid area (updated Lagrangian). Such explicit updating procedure in the fluid area is here to ease the convergence. The update of the geometry is based on the computation of the mesh velocity, different from that of the material. On the outer boundary (actually the bead formed close to the plunging tool), it is defined as the normal component of the material one, normals at vertex nodes being computed by a weighted average of those of surface elements. Next, within the fluid area, nodes are replaced iteratively as evenly as possible by a basic barycentric positioning technique.

A simplified numerical simulation of the early stages of the plunge step of a cylindrical tool of circular cross-section into a monobloc structure is shown in Figures 2.3, 2.4 and 2.5. Especially, Figure 2.3 shows the time evolution of the fluid/solid interface, which propagates upon heating. At first relatively spread around the tool plunge, the velocity norm then increases significantly within the fluid area as it grows, as shown in Figure 2.4c. As soon as a fluid area appears, all the deformation focuses within it, leading to an elastic springback of the surrounding solid area. Finally, Figure 2.5 shows the time evolution of the Mises norm of the stresses during the simulation. During the plunge step, the tool creates stresses in the area where he presses, but these

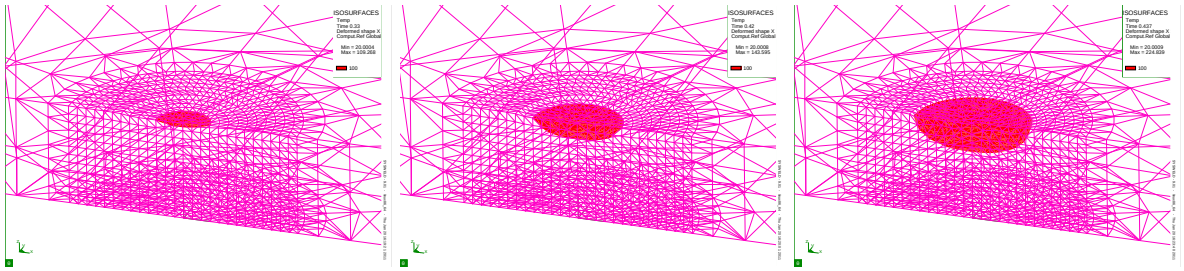

(a) $t = 0.33$ s. (b) $t = 0.42$ s. (c) $t = 0.437$ s.

Figure 2.3: Isotherm associated with the fluid/solid interface at different times. Extracted from [94].

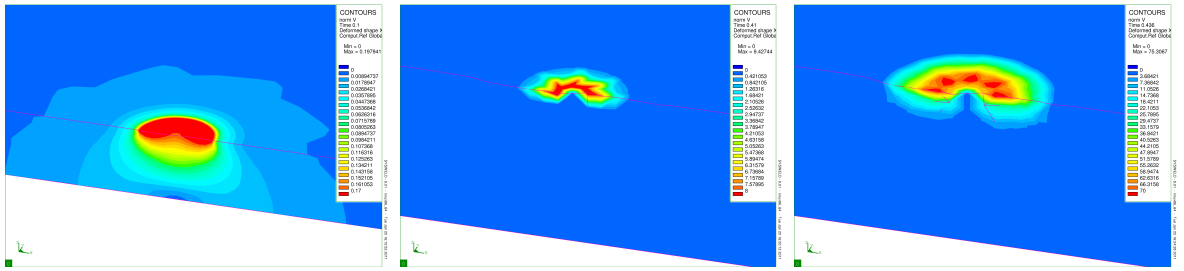

(a) $t = 0.01$ s. (b) $t = 0.42$ s. (c) $t = 0.436$ s.

Figure 2.4: Maps of the norm of the material velocity at different times. Extracted from [94].

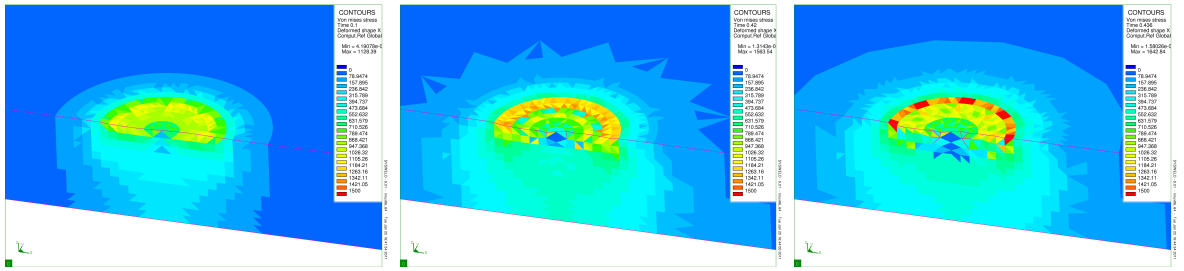

(a) $t = 0.01$ s. (b) $t = 0.42$ s. (c) $t = 0.436$ s.

Figure 2.5: Maps of the Mises norm of the stresses at different times. Extracted from [94].

stresses drop as the solid is transformed into a fluid. The maximal stresses are then reached in the solid area in the vicinity of the fluid/solid interface.

2.2.1.2 Experimental setups for FSSW

I got also the opportunity during my PhD works to carry out some experimental investigations of Friction Stir Spot Welding, at the production center of ENISE in Saint-Étienne. The global context of these experiments were on the one hand to analyze and better understand the mechanisms governing this process, and on the other hand to get macroscopic experimental data permitting the calibration of the numerical simulations. More precisely, these experiments were focused on the analysis on the influence of experimental boundary conditions upon the measured axial force and torque during the process, and on the quality of the weld. To this end, two experimental setups were designed, manufactured and mounted on a four-component force sensor. Their purpose was to study the difference induced by C-frame-like (as implemented in production lines) or plane

boundary conditions at the bottom of the lower sheet. Sheets of 2 mm thickness in AA 2024 aluminium alloy were considered. Figure 2.6 shows some pictures of the welding operation, of the weld, and of a cut of the axial stop setup, the latter aiming at mimicking C-frame boundary conditions.

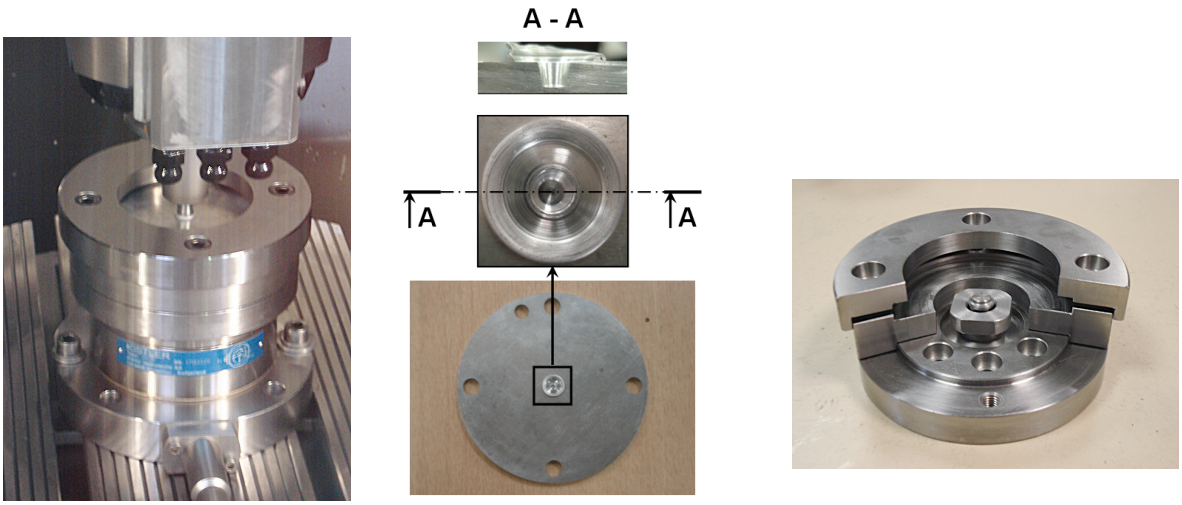

Figure 2.6: FSSW experiments, cut of the weld, and cut of a setup.

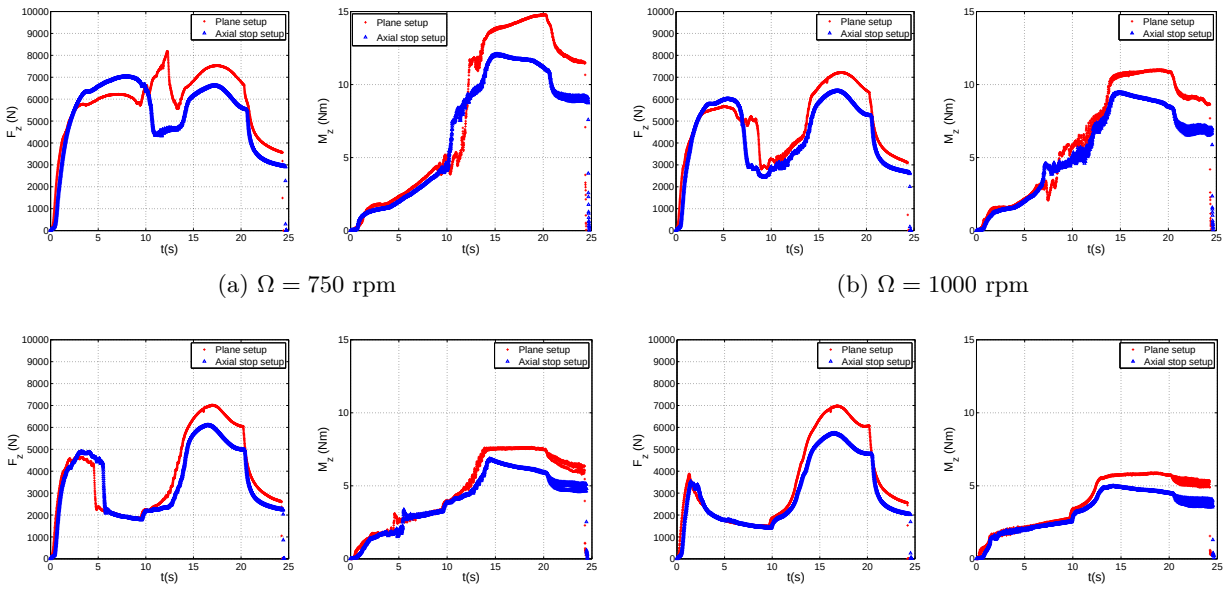

(a) $\Omega = 750$ rpm

(b) $\Omega = 1000$ rpm

(c) $\Omega = 1500$ rpm

(d) $\Omega = 2000$ rpm

Figure 2.7: Comparison of axial force and torque measured with both setups, for various rotational speeds. Extracted from [95].

Figure 2.7 shows a comparison between axial force and torque curves obtained for various roational speed of the spindle with both setups designed. A significant difference between force and torque maxima values appears between both positioning and clamping conditions. Whatever the rotational speed value, the maximum values of the axial force and torque are greater with the plane setup, which leads to that the specimen is more rigidly clamped, and can deform less.

2.2.2 High-pulsed power technologies

The basic principle of high-pulsed power technologies consists in releasing a certain amount of energy in a given medium in a very short time to generate a high power, and exploiting its effects. For convenience purpose, such energy is usually stored in an electric form, especially within a set of electrical capacitors. Various implementations of this basic principle yield particular technologies, amongst which the electromagnetic and electro-hydraulic ones, which are explained below.

2.2.2.1 Electromagnetic technology

The electromagnetic technology consists in releasing the electrical energy stored in capacitors within a coil or any kind of inductors. Following electromagnetic laws, eddy currents are generated in any electrically conductive media placed in the vicinity of the coil, hence generating repulsive Lorentz forces which can then be exploited, to form the matter, crimp or weld assemblies. This technology presents several advantages with respect to classical low speed processes, among which contact-free force application, process repeatability, and small duration can be cited. Although these technologies share some features with the explosive technology, they are more easy to handle/industrialize and involve lower pressure levels while they still benefit from processing dynamically, and does not expel any smoke or fume. This technology is actually a very old one, since we can trace it back to the 1920s [2]. Although it was used routinely in the late 1950s and early 1960s, the details of the physics were known but could not be computed effectively [55]. This is why a new gain of industrial interest for this technology has re-emerged in the late 1990s, and essentially in the 2000s with the emergence of strong computational methods, the increase of the computation power, and the marketing of dedicated commercial codes.

The École Centrale de Nantes has been hosting since the late 1970s a research activity dedicated to high pulsed power technologies. First carried out under the leadership of professor Maurice Leroy, this activity was pursued by professor Guillaume Racineux since the late 2000s, with whom I worked during my post-doc, and still continue. In that context, I had the opportunity to bring some contributions to his activities since my post-doc. They pertain either to some computational aspects of the problem, or to the analysis of dynamic phenomena of interest occurring with some particular experimental configurations via the definition of simplified modelings, which often leads to analytical solutions.

From the industrial viewpoint, the implementation of electromagnetic forming processes requires to determine and optimize many process parameters, which can be either related to the geometry of the forming device (geometries of the part and the coil) or related to the generation of the pulsed currents. These parameters are of primal importance to achieve the proper geometry of the formed part. Usual optimization procedures are often quite costly since this iterative process requires many assessments of the cost function, whose evaluation yields a computationally intensive direct analysis. In this context, a first contribution to this topic has been performed via the definition of a numerical tool dedicated to the optimization of the design of an electromagnetic compression device, focusing first only on the electromagnetic problem [125]. The objective was to take advantage of the Proper Generalized Decomposition (PGD) [85] to build a numerical chart, which can then serves to perform an optimization at a very low computational cost of this compression device. Great scientific interest and effort have been devoted to the development of PGD in the 2000s and 2010s, which has proved to be particularly effective to reduce the complexity of some particular problems exhibiting high dimensions, and circumvent the so-called 'curse of dimensionality'. The PGD enables a parametric resolution of some partial differential equation by introducing optimization parameters as extra-coordinates of the problem, and builds a tensor product approximation basis (or approximation of low rank format) in order to decouple the numerical integration of a high dimensional model in each dimension. Indeed, working with functions of one variable leads to that the computational cost scales linearly with the number of dimensions of the problem, and no more exponentially as for mesh-based methods like finite elements. Consequently, the evaluation of the cost function does not require a costly direct analysis anymore, the computational effort being previously provided upstream of the optimization step. The latter just reduces to a simple post-processing of the multidimensional numerical solution, and can be done in real time on light computing devices. PGD has been shown to be quite effective for parameter-dependent parabolic and elliptic linear problems, although extensions have been studied for non-linear and dynamic ones. For electromagnetic forming applications, the 'quasi-static' assumption of computational electromagnetism holds, meaning that the frequencies of eddy currents are quite low. This re-

sults in a linear parabolic equation written on the magnetic vector potential $\mathbf{a}$. More precisely, an axisymmetric geometrical configuration shown in Figure 2.8 was considered, neglecting the helicity of the coil windings.

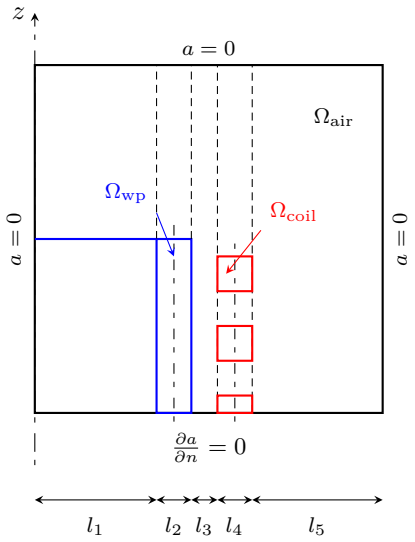

Figure 2.8: Radial parameterization of the electromagnetic compression device

The resulting scalar partial differential equation is thus written on the hoop component a of the magnetic vector potential as

$$\sigma \frac{\partial a}{\partial t} = \frac{1}{\mu}\left(\frac{\partial^2 a}{\partial r^2} + \frac{1}{r}\frac{\partial a}{\partial r} - \frac{a}{r^2} + \frac{\partial^2 a}{\partial z^2}\right) + j_0, \tag{2.2}$$

where σ, μ j_0 refer to the electrical conductivity, the magnetic permeability of the medium, and the source current density respectively. Observe that the elliptic term in Equation (2.2) reads different than that of the heat equation for instance, which comes from the double curl operator simplified for axisymmetrical problems. The PGD solution procedure is based on a greedy algorithm and proceeds by successive enrichments. Provided the solution at enrichment step n is known, the solution at enrichment step $n+1$ is sought in a separate form as

$$a^{n+1} = a^n + T(t)R(r)Z(z)\prod_{i=1}^{m} X_i(x_i) \tag{2.3}$$

where $(x_1, \ldots, x_m)$ refer to m additional coordinates, and $T(t), R(r), Z(z), X_i(x_i)$ $(1 \leq i \leq m)$ the *a priori* unknown enrichment functions. The solution at step $n+1$ is obtained by introducing the approximation (2.3) within the multidimensional weak form of Equation (2.2), and choosing test functions alternatively associated with each enrichment function the approximation (2.3) consists of. The so-called residual minimization approach [91] is then followed to compute the enrichment functions at step $n+1$. As shown in [125], the additional parameters in that context can be chosen as being the angular frequency ω and the decay time τ of the applied current density j_0 (being a damped sinusoid) appearing as a source term of Equation (2.2), which is useful to design the generator. But a parametric modeling of the geometry is also possible by considering the computational domain as a multi-layered structure, the thicknesses of all layers being accounted as optimization parameters and introduced as extra-coordinates. The keypoint to perform such parametric analysis stems from the finding of appropriate changes of variables so that a separated form of the solution be kept, allowing to preserve the efficiency of the PGD solver. Here, the domain associated with the radial coordinate Ω_r is thus mapped on a fixed parent domain for each layer, to which the coordinate s_j is associated, so that:

$$\Omega_r = \bigcup_{j=1}^{m} \Omega_{s_j} = \left[0, \sum_{j=1}^{m} s_j\right]$$

The following change of variable is thus defined in each layer of the structure:

$$r(s, l_1, \ldots, l_m) = \sum_{p<j} l_p + l_j(s - (j-1)); \quad j - 1 \leq s \leq j$$

where l_j stands for the current thickness of layer j.

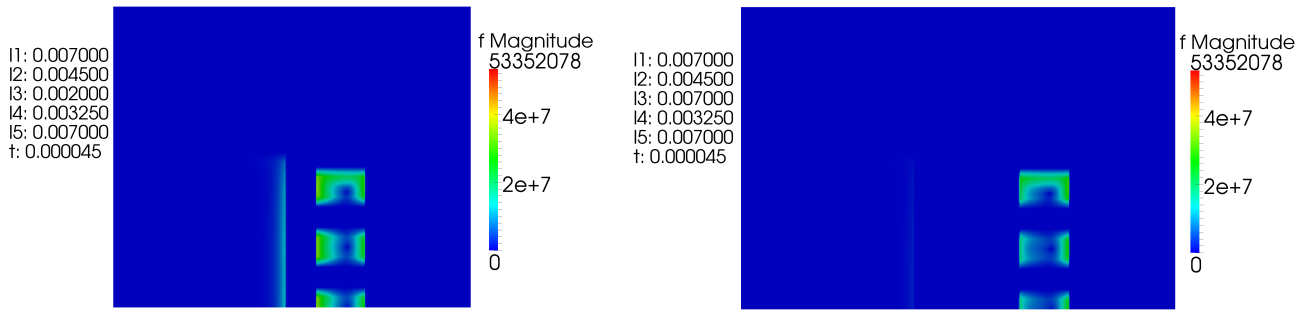

(a) $l_3 = 2 \cdot 10^{-3}$m (b) $l_3 = 7 \cdot 10^{-3}$m

Figure 2.9: Lorentz body forces (N.m^{-3}) as a function of the gap (l_3) between the workpiece and the coil. Extracted from [125].

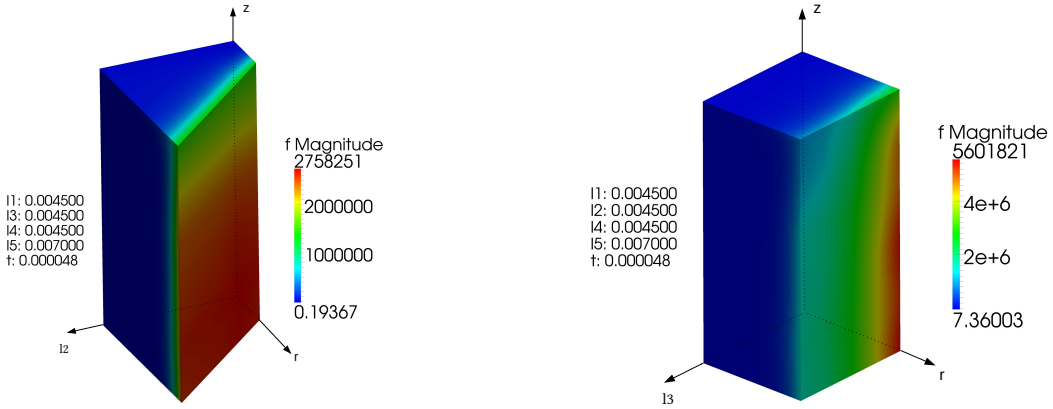

(a) l_2 (b) l_3

Figure 2.10: Lorentz body forces (N.m^{-3}) applied on the workpiece as a function of thicknesses l_2 and l_3. Extracted from [125].

Figure 2.8 shows the parameterization of the geometry of the computational domain. Next, Figure 2.9 shows the maps of the magnitude of Lorentz body forces generated on the device components at its first peak in time, for the two extremal cases of the gap value (l_3) between the workpiece and the coil windings. The results suggest as expected that their magnitude is greater when the gap is smaller. The parametric numerical solution also allows to better visualize the evolution of the Lorentz forces magnitude applied either on the workpiece or on the coil as a function of the thicknesses of the various layers. Especially, Figure 2.10 shows the evolution of these forces applied on the workpiece (at the first current peak) when varying its thickness l_2 (Figure 2.10a) and the gap magnitude l_3 (Figure 2.10b). As previously stated, the smaller l_3, the greater the magnitude of body forces reached in the workpiece. Conversely, since eddy currents only flow within a skin depth, the thickness l_2 does not seem at a first glance to have any signficative influence on body forces generated. Provided the parametric numerical solution (2.3) has been computed offline, the (online) computation of one instance of values of the parameters only involves the recombination of those enrichment functions (or 'modes'), which is a very cheap operation. Hence the evaluation of the cost function at each iteration of the optimization procedure can be

performed at a low computational cost. For instance, a brute force approach was used in [125] (hence without any intelligence) in order to find the maximal compression force over the domain of feasability.

The electromagnetic technology also allows to provide various geometrical configurations, which depart from the classical axisymmetric compression or expansion devices. This is especially the case of electromagnetic flanging, whose purpose is to bend a narrow strip at the edge of a metal sheet along a straight or curved line. Such technology may be of interest for the aeronautical industry for instance, which traditionally manufactures many components made of lightweight alloys of small and medium sizes by flexforming. However, the major difficulties to succeed in electromagnetic flanging is to master the geometrical tolerances of the formed part. Two major challenges must be met with the electromagnetic pulse technology. Firstly, a special electromagnetic inductor should be designed according to the geometry of the flange of interest. Its geometry should account for some desired spatial distribution of Lorentz forces, which should hence lead to a particular kinematics of bending of the flange. Secondly, a dedicated die should also be designed, which will give the final geometry of the flange. Such context was thus the purpose of a second contribution to the topic of electromagnetic processes. The objective of this contribution was to design a set of experiments (i) to enlighten issues related to the occurrence of some geometrical defects encountered in the formed flange, (ii) propose some physically-based explanations and (iii) propose some solutions to address these issues. A significant illustration of this work can be shown on the straight flange, which is the simplest geometry to be first considered for analysing, understanding and then correct the main defect issues occurring during the forming operation.

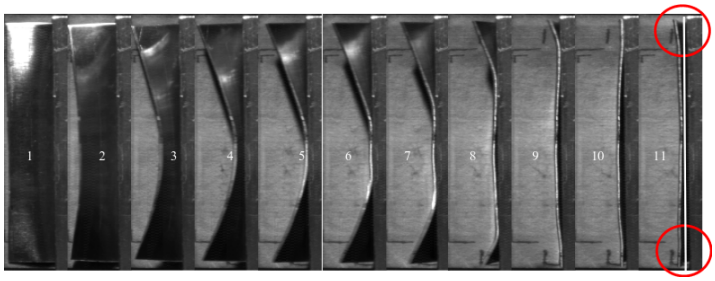

(a) Top view

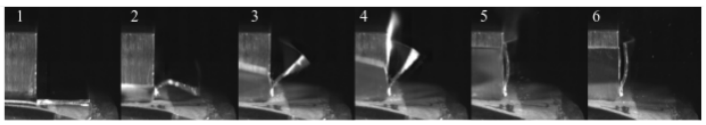

(b) Side view

Figure 2.11: First experiment: forming a straight flange with a non-optimized inductor, recorded with high speed camera (52000 frames per seconds). Extracted from [159].

(a) Top view

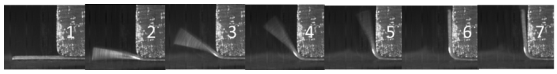

(b) Side view

Figure 2.12: Second experiment: forming a straight flange with an optimized inductor, recorded with high speed camera (45000 frames per seconds). Extracted from [159].

A first experiment of flanging is carried out on a sheet made of Aluminium alloy 1050 onto a die in steel, with a basic geometry of inductor (actually a U-shaped one). Figure 2.11 shows a sequence of pictures obtained with high speed cameras, in top and side views recorded at 52000 frames per seconds. Such experiment allows to observe that almost all the possible defects appear on the flange if no particular care is devoted to the design of the geometry of the inductor. Non-uniform bending, defects of straightness and flatness, plastic hinge, as well as a non-mastered rebound on the die occur. However, if the design of the inductor now includes the path (and the streamlines) of eddy currents flowing in the sheet, the fact that sufficient Lorentz forces should be applied at the corner of the flange so that its extremities also rotate properly about the fillet of the die, then better results can be obtained. This is the purpose of the second experiment, whose sequence of pictures is shown in

Figure 2.12. The flange is now bent much more uniformly compared to the first experiment, it does not exhibit any significant defect as previously, although a rebound is still observed in picture 7 in Figure 2.12b. An analog work can be performed on curved flanges, which essentially requires to pay attention to the particular path of unrolling the flange onto the die so that no area of compression occurs that would make the flange buckle, and hence generates wrinklings.

Regarding the rebound of the flange onto the die, a very simple one-dimensional model considering planar impacts between two bodies A and B allows to easily show that it is due to an unfavorable material impedance ratio between the flange and the die [159]. Using the method of characteristics, a closed-form solution can be obtained, either in the elastic or hydrodynamic regimes, but whose conclusions agree on the rebound. Whatever the material impedance (denoted Z_i, $i = A, B$) ratio between bodies A and B, a rebound occurs after the impact, either after one wave round-trip in the body A if $Z_A < Z_B$, or after that the transmitted pressure waves to the body B have been reflected into tensile ones via the right free boundary if $Z_A > Z_B$. From a practical viewpoint, the rebound is solved via a die compensation angle.

Figure 2.13: AA1050 formed part. Extracted from [159].

Figure 2.14: Superposition of the computed (in blue) and measured (in red) deformed shapes. Extracted from [159].

Although electromagnetic flanging of elementary geometries can be reasonably optimized in an experimental way (based on a trial and error analysis), much work remains to be provided to go for industrial components. Figure 2.13 shows a model aeronautical part consisting of several straight and curved flanges, formed simultaneously via a dedicated single inductor. Figure 2.14 shows superposed computed and experimental deformed shapes. The former is obtained with the dedicated module for electromagnetic forming of the commercial finite element code LS-DYNA, while the latter is obtained by scanning 3D. Though a correct qualitative superposition can be observed at first glance, the local examination of flanges reveals that significant defects of straightness, flatness and perpendicularity of the straight flanges is predicted by the simulation, more than those measured on the experimental part, although the latter also contains defects. The raised difficulty here is due to electromagnetic interactions between eddy currents in the different subareas of the part and the coil. Defects can appear that were not observed in each elementary experiment. The numerical simulation becomes then mandatory to predict and better understand these interactions. However, the fully resolved 3D numerical simulations carried out with commercial finite element codes require a prohibitive computational cost, and are then hardly usable in an optimization loop. Rather, a large place remains to be investigated here to design simplified and much more efficient modelings and computational methods, integrable in optimization processes.

The electromagnetic technology also allows to assemble dissimilar components, either bi-metallic assemblies [153], or even more recently hybrid structures like polymer composites to metals [167]. However, this technology may also be able to disassemble those dissimilar assemblies, which would open the door to their recycling, or that

would be useful to change a defective part, serving as a consumable for instance. The same technology would thus allow to bond and debond thin laminate structures. This idea is the purpose of a recent contribution lying within the context of the on-going PhD thesis of Benoit Lagain. This contribution aims at evaluating by analytical considerations whether or not it would be possible to use the magnetic pulse technology for disassembling laminate structures [175], without significantly damaging the debonded layers. The study involves a simple one-dimensional model in linear elastodynamics of a laminate consisting of three stacked elastic, homogeneous and isotropic layers, infinite in transverse directions, submitted to a continuous square sinus pulse applied on one of its face. It is solved with the method of characteristics for various configurations, in order to span the domain of feasability of an optimisation problem, whose purpose is to maximise the interfacial tensile stress between the first two layers with respect to layer thicknesses and acoustic impedances. One interesting feature exhibited by this optimization problem is that, after a set of assumptions, it naturally admits a decoupling between unknowns associated with the geometry, and those associated with the material wave impedances. Such decoupling holds in the sense that a two-stage staggered solution procedure of the optimization problem is naturally obtained with respect to those two subsets of unknowns. Such staggered solution scheme is reminescent of approximate partitioned schemes investigated for transient diffusion problems in Section 1.3.2, but is here performed without any modeling error. It is shown analytically that a single optimal solution exists, which is defined for a 2-layer laminate, consisting of an interfacial tensile stress of twice the maximum applied pressure asympotically reached as $\frac{Z_A}{Z_B} \to 0$. These promising results are the starting point of on-going developments of an experimental device able to disassemble multi-material assemblies which are thicker than a centimeter, as they can be found in light weight armouring plates, including a composite material on ceramic coating or on a metallic plate for instance.

2.2.2.2 Electro-hydraulic technology

In the family of high pulsed power technologies, the electro-hydraulic one can be traced back to at least the 1960s [18]. It consists in discharging the electrical energy stored in a series of capacitors between two electrodes immersed in a water tank. This discharge creates a plasma that generates a primary shock wave and secondary pressure waves, which can then be exploited. This technology presents several interests as it may also be applied for metallic materials that are not necessarily electrically conductive, it is contact-free since here water is used as a support medium for transmitting pressure waves, and it processes dynamically. One contribution to that technology was made within the framework of the PhD thesis of Cheikh Tidiane Sow [142], which I co-supervised with Guillaume Racineux, whose purpose was to develop an experimental device to perform dynamic crimping of a metallic tubes within a ring with the electro-hydraulic technology, with applications to some aeronautical components. The proposed system consists of three stages, as shown in Figure 2.15 [177]. First, the discharging

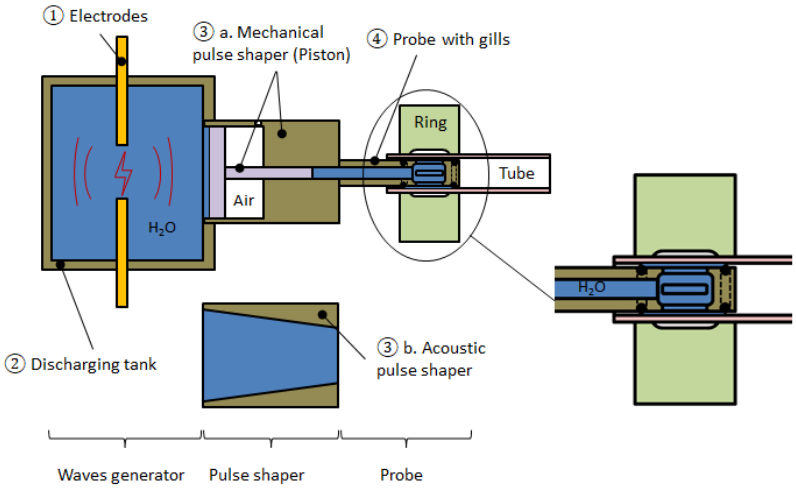

Figure 2.15: Electro-hydraulic crimping system. Extracted from [158].

tank is where the discharge occurs between the two electrodes, and pressure waves are generated. Second, the

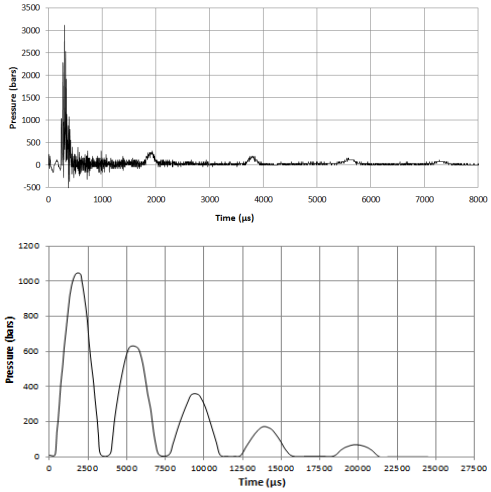

Figure 2.16: Pressure signals with acoustic (top) and mechanical (bottom) pulse shapers. Extracted from [158].

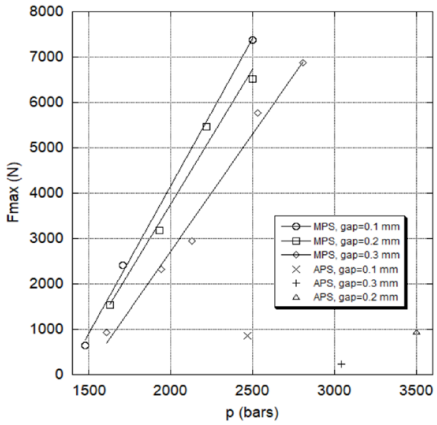

Figure 2.17: Evolution of the pullout force as a function of the measured pressure. Extracted from [158].

pulse shaper aims at transmitting and shaping the input dynamic signal as wished. Depending on the desired crimping conditions (strain rate), two pulse shapers were designed. An acoustic pulse shaper aims at amplifying the primary shock wave, while a mechanical pulse shaper allows to filter the shock wave and take advantage of the secondary waves. Third, a probe with gills permits to transmit the pressure wave to the inner surface of the tube to expand it. Figure 2.16 shows the time evolutions of the pressure measured at the output of the probe during a test at 8 kJ for an inter-electrode distance of 2.5 mm, using both acoustic and mechanical pulse shapers. The former clearly amplifies the primary shock wave, while the latter smoothes the signal and acts as a low pass filter. Figure 2.17 shows the evolution of the pullout force as a function of the measured pressure resulting from some crimping experiments performed on 316L steel assemblies. The mechanical pulse shaper permits to assemble with lower pressures than those reached with the acoustic one, the latter still requiring further work of development.

2.3 Experimental testing at high strain rates through direct impact Hopkinson bar device

Some of the aforementioned technologies profits from the so-called velocity effects to process the matter. Especially, during these operations the material is deformed at high strain rate. Typical average strain rates reached in electromagnetic forming are of the order of $10^3 s^{-1}$ [97, 159]. Those reached with the electro-hydraulic technology are of the orders of $10^2 s^{-1}$ and $10^3 s^{-1}$ with the mechanical and acoustic pulse shapers respectively [158]. However, the electromagnetic technology is also interesting for welding, giving the so-called magnetic pulse welding technics. In the latter case, a significantly higher amount of electrical energy should be stored within the capacitors in order to get a higher impact velocity (peaks of the order of 500-600 $m.s^{-1}$) that will permit to achieve a safe weld. In the later case, the material may be deformed at higher average strain rates, which are rather of the order of $10^4 s^{-1}$. Therefore, a good knowledge of the thermo-mechanical constitutive response of the material is required on a wide range of strain rate to master the feasibility of these high speed forming processes. Those constitutive responses will then feed particular database, or serve for the calibration of particular constitutive models which will then be used in numerical simulations.

Typical high strain rate experiments covering this range of strain rate are performed with the conventional Split Hopkinson Pressure Bar (SHPB) system, or compression Kolsky bar [7]. However, it is known to admit a truly upper bound of average strain rate of about 10^4 s^{-1} [52], which is a litte bit short for qualifying magnetic pulse welding. Besides, it is also known from the literature that the (increasing) evolution of the flow stress

measured with such experimental mean for strain rate sensitive metallic materials as a function of the average strain rate starts to exhibit a sort of rise in the range $[10^4, 10^5]$ s^{-1} (e.g. see [76]). Although of interest, the latter is usually not so easy to qualify since it lies between ranges of validity of conventional Kolsky bars (up to 10^4 s^{-1}) and pressure-shear plate impact (starting from 10^5 s^{-1}). The extension of the range of strain rate covered by Kolsky bars can be performed either by scaling down the size of the specimen and consequently that of the entire device, or by dispensing with the limit on the stress of the incident bar by removing it. Both have yielded the miniaturized Hopkinson bar [26] and Direct-Impact (DI) [21] devices respectively. Both approaches have been shown to achieve very high strain rates (up to 10^5 s^{-1} sometimes), although each of them presents necessarily some limits, require a specific design, and rely on some assumptions. For instance, the miniaturized system is limited by friction or by the strain gauge length, which acts as a low-pass filter. The direct impact system allows a higher velocity of the striker and hence a higher average strain rate in the specimen since the input bar has been removed. However, additional difficulties also arise in the deduction of the material constitutive response. Especially, the achievement of the force equilibrium is also usually assumed, and is used to compute the stress. However, it cannot be checked anymore. Besides, alternative techniques are requested to complete the deduction of the strain and the strain rate in the specimen.

In this context, the purpose of the PhD thesis of Xiaoli Guo was to design and set-up a direct impact Hopkinson device of reduced size (although not miniaturized) as used in the very high strain rate testing. The objective was to reach the expected levels of strain and strain rate ($\sim 10^4$ s^{-1}), while enforcing as long as possible the basic assumptions required to deduce explicitly the stress-strain curve of the specimen. Her PhD thesis was co-supervised by Guillaume Racineux and I, and was also a framework for a collaboration with Professor Ramzi Othman.

A first contribution was performed on the design of such device [115]. Indeed, the design of conventional SHPB device often relies on a set of empirical confinement equations used in order to fulfill the required assumptions. These constraints are usually classified as *system design* and *experimental design* [80]. The former involves the determination of three important length ratios, independent to the specific experiment carried out, while the latter determines the specimen dimensions, the length and the impact velocity of the projectile to deform the specimen in such a way that a given strain rate be reached at a given level of strain. However, although they allow to restrict the range of possibilities, additional constraints built on a physical basis permit to clarify and complete these empirical bounds. Moreover, the design process should be adapted to the design of a direct impact Hopkinson system of interest here. Without exhaustivity and details, the additional constraint pertain to the conservation of energy, dispersion properties of bars or to bounds linked to buckling and one-dimensional propagation of waves. In this contribution, the design of a direct impact system has been shown to be solution of an optimization problem submitted to equality ($\mathbf{h}(\mathbf{x}) = 0$) and inequality ($\mathbf{G}(\mathbf{x}) \leq 0$) type constraints of the form

$$\min_{\mathbf{x}} f(\mathbf{x}) \,; \quad \mathbf{G}(\mathbf{x}) \leq 0 \,; \quad \mathbf{h}(\mathbf{x}) = 0$$

whose unknown vector $\mathbf{x}$ consists of the length l_p of the projectile and its impact velocity v_p, the dimensions of the specimen (l_s, ϕ_s), and these of the bar (l_b, ϕ_b):

$$\mathbf{x} = \{l_p, v_p; \phi_s, l_s; \phi_b, l_b\},$$

and where the cost function $f(\mathbf{x})$ is defined as the absolute error of the difference between the predicted average strain rate $\dot{\varepsilon}_s(\mathbf{x})$ and the target one $\dot{\varepsilon}_{s_{\text{obj}}}$:

$$f(\mathbf{x}) = \left| \dot{\varepsilon}_s(\mathbf{x}) - \dot{\varepsilon}_{s_{\text{obj}}} \right| \tag{2.4}$$

Figure 2.18 shows a sketch of all equality and inequality-type constraints applied on and relating the components of the direct-impact Hopkinson device. A systematic iterative procedure is then introduced to solve this design problem [115] for testing materials like Ti-6Al-4V titanium alloy at strain rates between 5000 and 30,000 s^{-1}, by the selection of various ranges of specimen length, length and impact velocity of the projectile.

The absence of the incident bar in the direct impact device rises some difficulties in the post-process of the tests to deduce the stress-strain curve. A first difficulty is linked to that the classical equations derived to deduce the strain rate and thus the strain in the specimen for an SHPB do not work any more in the case of the

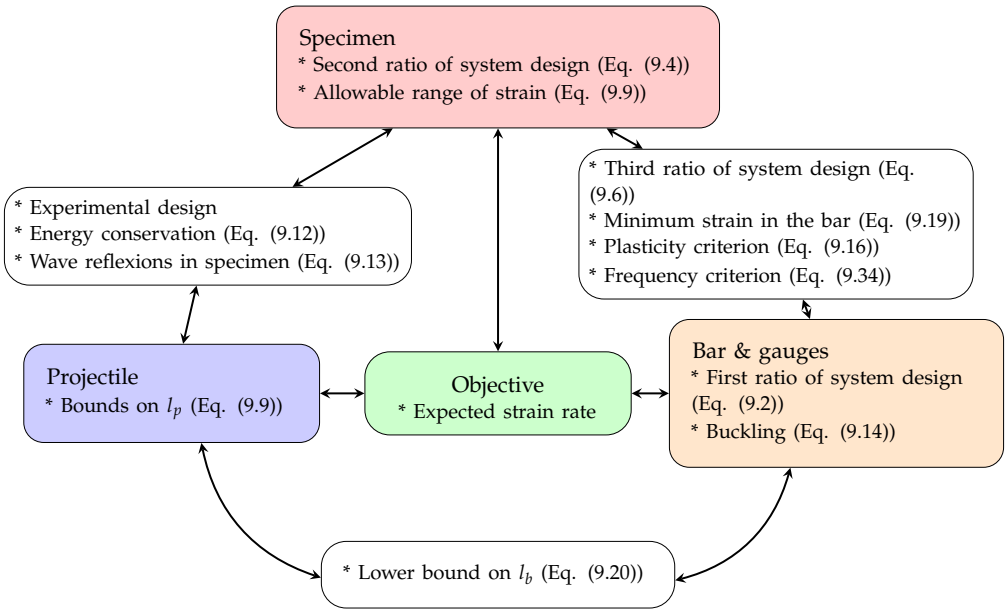

Figure 2.18: Constraints applied on and relating the components of the direct-impact Hopkinson device. Extracted from [138].

direct-impact tests. More precisely, the calculation of the strain and strain rate in a direct impact device comes down to approach the velocity of the projectile/specimen interface during the contact, either by an additional measurement or by deduction techniques. In the PhD thesis of Xiaoli Guo, two laser diodes with photodiodes were used to measure the impact velocity of the projectile v_p, the average strain rate in the specimen could thus be evaluated from Gorham's work [42] as

$$\dot{\varepsilon}_s = -\frac{v_p + \frac{A_p+A_b}{A_p} c_b \varepsilon_b(t)}{l_s}, \tag{2.5}$$

where A_p, A_b are the cross-sections of the projectile and the bar, c_b the sound speed in the bar and $\varepsilon_b(t)$ the strain measured by the strain gauge mounted on the output bar. Equation (2.5) also served to compute the predicted average strain rate of the cost function (2.4) in the design process. However, the direct-impact experiments were also equipped with a high-speed camera, which permitted to perform a tracking of the displacement of the projectile/specimen interface $u_{in}(t)$ and that of the specimen/bar interface $u_{out}(t)$, as shown in Figure 2.19. Figure 2.20 shows a comparison of both average strain and strain rate obtained either from image pro-

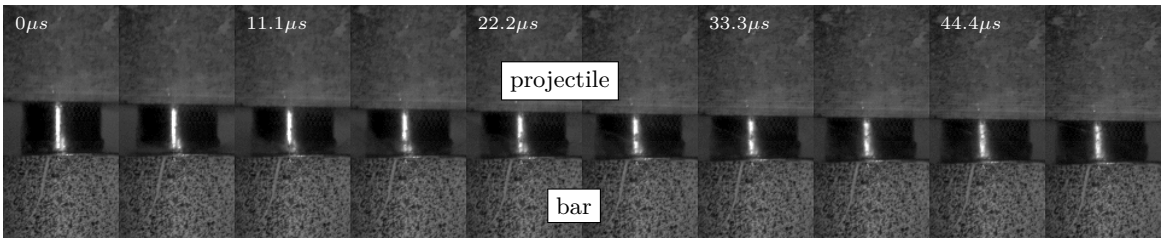

Figure 2.19: Specimen deformation capture by the high-speed camera during the test T4. Extracted from [121].

cessing or from Gorham's formula (2.5). Clearly, the two methods fit well only during one wave round trip within the projectile, also called the characteristic time, after which Equation (2.5) is clearly not valid anymore. This is a consequence of that Equation (2.5) has been built assuming the force equilibrium in the specimen. A

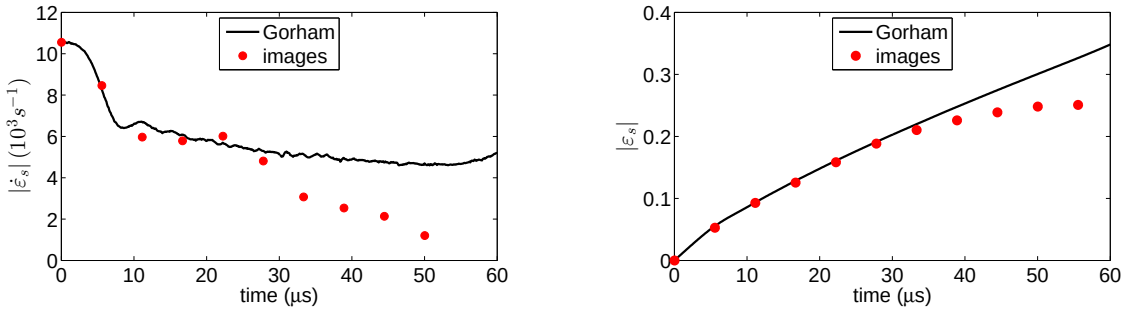

(a) Strain rate

(b) Strain

Figure 2.20: Strain rate and strain calculated in the direct-impact tests by different manner for test T4. Extracted from [121].

second difficulty of direct impact device is thus that the force equilibrium cannot be checked anymore within the specimen. On the one hand, the force equilibrium takes some time (a few wave round trips) to be achieved within the specimen. On the other hand, the return at the projectile/specimen interface of the wave reflected at the back of the projectile cancels the force equilibrium in the specimen, and hence makes Equation (2.5) not applicable. A limit of validity of explicit post-process for direct impact devices is thus reached when no sufficient wave round trips are achieved within the specimen during one occurring within the projectile. This is especially the case as the length of the projectile decreases, which goes with a higher impact velocity of the projectile in order to reach higher strain rates within the specimen. With the direct impact device designed in the PhD of Xiaoli Guo, this limit was found at about $2 \cdot 10^4 \mathrm{s}^{-1}$, above which the length of the projectile and the associated characteristic time did not permit to deform sufficiently the specimen to get a usable stress-strain curve.

One way among others to improve the assessment of the mechanical response at very high strain rate with direct impact experiments is to carry out an inverse analysis involving a dynamic numerical simulation, which is the purpose of large sections of literature. A constitutive model is hence postulated to describe the behaviour of the tested material, whose parameters are identified so that some given quantities extracted from the numerical simulation fit experimental data. This approach has been applied in [121, 115], minimizing the Euclidean norm of the difference between the simulated strain $\varepsilon_{\mathrm{sim}}(\mathbf{x}, t)$ and the recorded one $\varepsilon_{\mathrm{exp}}(t)$ over a given time duration. A basic Johnson-Cook constitutive model [30] was assumed, and calibrated for Ti-6Al-4V alloy within the range of strain rate $\dot{\varepsilon} \in [4500, 18500]\mathrm{s}^{-1}$, with numerical simulation carried out with the finite element code ABAQUS.

Thereby, inverse analyses allow to get an image of what could be the constitutive response of a material through the assumption of a constitutive model, and permits here to overcome the limits of the 'explicit' post-processing provided by Gorham's formula (2.5), by accounting for the local inertia effects within a numerical simulation. However, such inverse analysis usually raises a mountain of questions about its validity and the identified parameters. Without exhaustivity, issues can be raised related to the chosen constitutive model, cost function, uniqueness of the solution, minimization algorithm, but also about the numerical simulations carried out through the constitutive update algorithm, the time integrator, the spatial discretization, the thermo-mechanical coupling and so on. As such, the derivation of a well-derived explicit post-processing is preferable, when it is possible, with respect to inverse analysis in the sense that it is much more efficient and may yield a constitutive response which is not biased by any constitutive equations. Significant improvements have been recently introduced via image-based reconstruction of the stress field using full-field measurements techniques, with various approaches [147, 151], but which however require at least a planar surface to be valid.

2.4 Numerical simulation of impacts on dissipative solid media

2.4.1 Motivations

The numerical simulations of impacts on dissipative solids are of great importance in fast transient solid dynamics, especially in engineering applications such as crash-proof design, or high speed forming processes as introduced in Section 2.2.2. Various types of numerical simulations can be built up according to the desired objective. High resolution numerical simulations represent one such type, and are usually dedicated to the fine modeling of special effects and to their accurate representation and understanding. In this case, numerical simulations aim at rewriting the film of loading undergone by any material point, while freeing from any numerical disturbance that might impair the understanding of some physical phenomena of interest. Here, engineering applications involving impacts on structures are mainly modeled by hyperbolic initial boundary value problems, whose solutions consist of both continuous and discontinuous waves. For dissipative solid media, these waves also propagate large strains and irreversible phenomena (plastic strains, damage, cracks and so on). The accurate capturing of both wave fronts and propagation of irreversible phenomena is of primal importance in order to be able to relate the history of wave paths in the medium to its residual fields once the steady state is achieved.

The numerical simulation of impacts on dissipative solids, or what is also called Computational Structural Dynamics (CSD), has been and is again mainly performed with a Lagrangian formulation coupled to a displacement-based Galerkin approach [58], which is implemented in most industrial codes. The latter is based on the weak form of the conservation of linear momentum (actually the principle of virtual works), where the primary variable is the displacement hence yielding a second order equation in time. The classical finite element method is widely used for its spatial discretization using low order (i.e. first and second) interpolation, preferred for computational workload convenience, and coupled with explicit time integrators dedicated for second order equations such as the centered differences or Newmark finite difference schemes. This approach has been made popular since the finite element method enables an easy management of non-linear partial differential equations, especially for solid-type media for which history-dependent constitutive equations can be implemented by means of appropriate integration algorithms [71], and internal variables are stored at integration points in each element.

However, according to the phenomena the numerical simulation is expected to capture, such approach may present a series of shortcomings, which may prevent to fulfill the aforementioned objectives. A first one follows from that such approach inevitably introduces high frequency noise in the solution field in the vicinity of sharp spatial gradients. This prevents a correct capturing of discontinuous wave fronts and hence a good understanding of the relationship between wave paths and the residual state of the medium. Since the centered differences in time (for instance) provides a linear scheme for the displacement (in the sense of [112]), coupled to linear finite element shape functions providing a second-order accurate displacement approximation, this effect follows from Godunov's theorem [64] which says that *monotone linear schemes are at most of order one*. To address these spurious oscillations, artificial viscosities may be added, following for instance the old technology of von Neumann [9] or subsequent ones as reviewed in [40]. However, user-defined coefficients are not always easy to properly tune for a given application, resulting in diffusive behaviour in areas of the computational domain that do not need it, and a less oscillatory although not clean solution in the vicinity of discontinuous wave fronts. An illustration of the effects of oscillatory solutions is shown in Figure 2.21, following from the bounce problem occurring in electromagnetic flanging introduced in Section 2.2.2.1. A very simple one-dimensional model is considered which consists of a projectile (medium A, actually made of aluminium alloy) impacting a semi-infinite medium (medium B, made of steel), both following an elastic-plastic constitutive response with an isotropic linear hardening. Right after the impact (see Figure 2.21a), a finite element solution computed here without any additional viscosity exhibits strong numerical oscillations, and predicts a profile of longitudinal plastic strain which seems to decrease up to the interface. However, the analytical solution is known for that problem, at least for the first instants, and is piecewise constant. The predicted trend for the plastic strain by finite elements had therefore no physical content. Once the simulation is run until bounce occurs (see Figure 2.21b), the profile of the plastic strain computed by finite elements does not help relating the paths of plastic waves to the residual state of the medium, especially a piecewise constant profile would be expected. However, it is possible to provide non-oscillatory approximations of the solution, using numerical schemes as the one introduced in [130], but others would work also. Then, the various plateau in the profile of plastic strain clearly

appear.

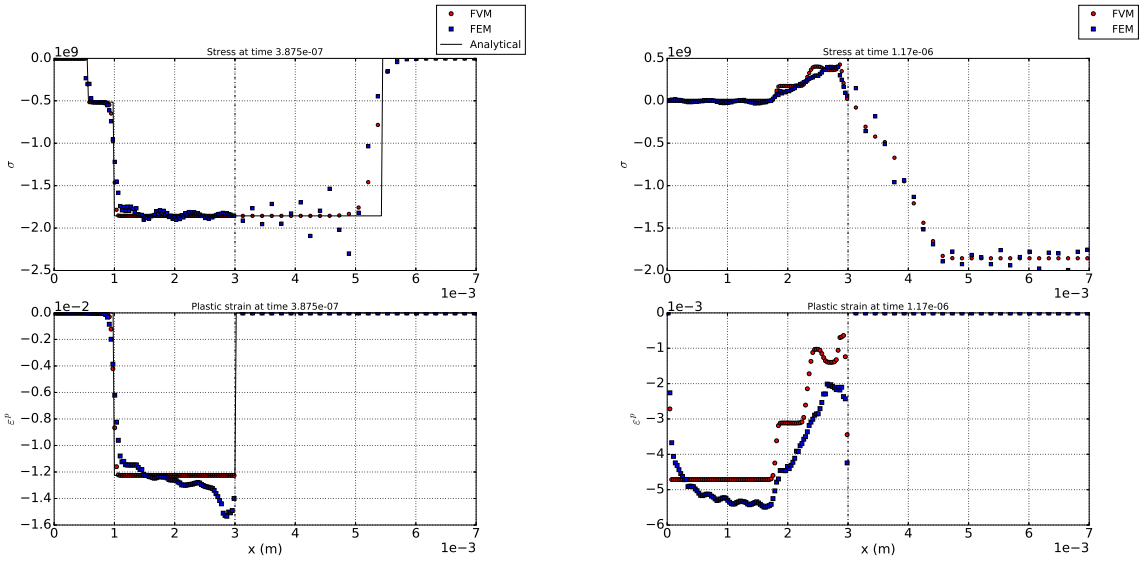

(a) (b)

Figure 2.21: Comparison of various solutions at early instants (a) and rebound time (b) of a one-dimensional projectile (A) impacting a semi-infinite medium (B), both following an elastic-plastic constitutive response, in the case $Z_A < Z_B$.

Second, displacement-based Galerkin approaches lead to that derived variables (i.e. strains and stresses) converge at one order less than the primary variables (i.e. displacements). However the former are often or primary interest, and this yields further refinement to reach a given level of error. Third, some displacement-based Galerkin approaches (as they are implemented in commercial codes) may have thermodynamic consistency problems. The weak form of the conservation of linear momentum is generally supplemented with the heat equation in structural codes for coupled thermo-mechanical problems, in which heat conduction effects are classically neglected with respect to transient ones, hence following the assumption of local adiabaticity. Thermodynamic consistency is not always properly ensured because the heat equation is generally solved (i) neglecting various thermo-mechanical couplings such thermoelastic and thermoplastic ones, and (ii) accounting for a constant Taylor-Quinney coefficient [4] (generally set at 0.9 or another close value) while it is actually not. Next, these codes are not well-suited for shock-capturing, since there is no well-defined Rankine-Hugoniot jump conditions associated with the heat equation. They are rather replaced by hydrocodes for this type of applications, for which the local balance of internal energy is integrated in time. However, since their focus is made on the thermo-mechanical coupling of the hydrostatic part of the constitutive response through an equation of state, those related to the deviatoric component is often disregarded (see e.g. [40]), or treated in an uncoupled (or time-explicit) way. Besides, enforcing the conservation of the total energy is not always straightforward, and may require some unusual definition, such as a discrete expression of the kinetic energy which may become negative (see [40, Section 2.7.2]). Related to the same issue, hypoelastic-plastic constitutive models are generally employed in commercial codes to describe the constitutive (partly irreversible) response of the structural part. However, hypoelasticity is not thermodynamically consistent, more precisely it is not true elasticity (reversibility) since a loading cycle performed on an infinitesimal element does not yield a vanishing mechanical dissipation. Morever, an objective time derivative necessarily goes with hypoelasticity which has to be chosen among an infinite amount of them, each of them yielding a different modeling in the sense that different stress levels will be achieved for one loading path. Usually, the Jaumann one is selected (for the sake of ease of implementation with respect to that of Green-Naghdi, see e.g. [40, Section 2.6.2]) which has already been shown to give oscillating shear stresses in a pure shear test as strains become large [37]. But worst, these constitutive models yields partial differential equations which are hyperbolic only conditionally [38], and give discontinuity

equations across shocks which are mathematically not well-posed [78], and hence yields wrong discrete shock speeds in the moderate range of velocities.

In that context, I was interested in a research topic whose purpose is to build numerical approximations permitting to correctly capture both continuous and discontinuous waves in dissipative solids undergoing large strains. In fast solid dynamics, besides the classification performed on time scales (or strain rate) shown in Figure 1, problems can also be classified according to the level of pressure involved. The problems of interest in these works will range from *low* to *moderate* levels of pressure, disregarding solids under *high* pressure for which the hydrodynamic approximation holds [75] and behave as compressible fluids. The interest here is focused on problems for which the shear strength is still of great importance, while the description of the increase of the pressure may eventually require a dedicated (convex) equation of state which can thus generate shock waves. More specifically, I have so far been interested in three different aspects of such kind of numerical simulations.

The first one is related to the *quality of the approximation* achieved by different numerical schemes of different aspects of the analytical solution, such as the capturing of different types of non-linear waves. Especially, the approximation should be high-order accurate in smooth areas, and non-oscillatory in the vicinity of discontinuities (such as shocks). One interest was particularly dedicated to correctly capture both continuous or discontinuous plastic waves, from which the residual state of the medium follows once the equilibrium has been reached.

The second aspect is linked to the *thermodynamic consistency* of both the formulation of the problem and its approximation. The least that can be required from these numerical simulations is to properly enforce the balance of energy as well as the second principle of thermodynamics, which is not always as easy as expected. As a part of this aspect, a contribution was made through a thermodynamically-consistent (variational) constitutive update.

The third and last aspect is linked to the *numerical approximation of the kinematics*, which addresses the issues of the description of large strains in such problems. A Lagrangian viewpoint has been adopted here, and a contribution coupling a particle-based method to a shock-capturing approximation has been made. Although the contribution has for the moment essentially focused on the approximation, it encompasses the ability to handle truly very large strains provided further works will be performed in the future.

2.4.2 On the interest of conservative formulations for computational fast transient solid dynamics

Following usual practices in Computational Fluid Dynamics (CFD) [64, 112], the system of hyperbolic equations governing the motion of dissipative solids can also be rewritten in conservative formulations. The governing equations are rewritten as a system of conservation laws, which is first order in time and embodies the divergence of a particular flux. In computational Structural Dynamics, these kinds of formulations are more recent than displacement-based (second order) Galerkin ones, and follow from the works of Plohr and Sharp [36], and of Trangenstein and Collela [38]. Under the adiabaticity conditions, without any source terms and considering the total Lagrangian description, one possible formulation among others of such system reads

$$\frac{\partial \mathcal{U}}{\partial t} + \text{DIV } \mathcal{F} = 0 \tag{2.6}$$

where the material divergence DIV is computed with respect to initial coordinates $\mathbf{X}$, and the vector of conserved variables $\mathcal{U}$ and the fluxes $\mathcal{F}$ are defined as

$$\mathcal{U} = \begin{Bmatrix} \rho_0 \mathbf{v} \\ \mathbf{F} \\ \mathcal{E} \end{Bmatrix} \; ; \quad \mathcal{F} = \begin{Bmatrix} -\mathbf{P} \\ -\mathbf{v} \otimes \mathbf{1} \\ -\mathbf{P}^T \cdot \mathbf{v} \end{Bmatrix}. \tag{2.7}$$

The first equation is still the conservation of linear momentum, but whose main unknown is now the linear momentum density $\mathbf{p} = \rho_0 \mathbf{v}$. Depending on the authors, the strain (rate) can be derived from a discrete gradient operator applied to the velocity field over a polygonal cell. For instance, this is the case in [108] following an updated Lagrangian description, which is similar to what has been done in Section 2.2.1.1 in the finite element context. But System (2.6) may also encompass some geometrical conservation laws and

therefore define a multi-field formulation. The second equation of System (2.6) expresses here the geometrical compatibility between the rate of the deformation gradient $\dot{\mathbf{F}}$ and the velocity field. However, this multi-field formulation also goes here with the following (involution) constraint

$$\text{CURL } \mathbf{F} = 0, \tag{2.8}$$

which may require special care in the discrete setting. System (2.6) can be extended if required with conservation laws written on the complementary minors of the deformation, as shown in the work of Bonet, Gil and co-workers [164, 165]. These minors consist of the deformation gradient $\mathbf{F}$, its cofactor $\mathbf{H}$ and the jacobian determinant J. Such extended system of conservation laws is then naturally compatible with polyconvex hyperelastic constitutive models. At last, the third equation of System (2.6) is the conservation of the total energy, or first principle of thermodynamics, where the density of the total energy density is defined by summing those of the internal energy and the kinetic energy, such that $\mathcal{E} = E + \frac{\rho_0 \mathbf{v}^2}{2}$.

A first obvious interest in writing the governing equations in conservative form such as System (2.6) lies in that it naturally reduces to the Rankine-Hugoniot jump conditions across any discontinuity of fields

$$S[\mathfrak{U}] = [\mathfrak{F}] \cdot \mathbf{N}, \tag{2.9}$$

where $\mathbf{N}$ is the material normal of the discontinuity surface moving at speed S, and $[\bullet]$ denotes the jump of the quantity $(\bullet)$ across the discontinuity, such that $[\bullet] = (\bullet)^+ - (\bullet)^-$. Clearly, the discretization of System (2.6) with any conservative numerical scheme [64] will ensure that the right shock speeds will be computed, since conditions (2.9) will be correctly approximated. Actually, the two first discontinuity equations in Equation (2.9) (linear momentum's jump conditions and Hadamard's compatibility conditions) will also be satisfied by a classical displacement-based Galerkin approach. However, the third one associated with the conservation of the total energy has no equivalent counterpart that could be written with the heat equation. In hydrocodes, the balance of internal energy is solved locally (usually at each integration point), but its discontinuity equation is already a linear combination of all Rankine-Hugoniot jump conditions (2.9). In addition, depending on the particular discrete scheme employed, it does not necessarily yield the analog of the discontinuity equations associated with the total energy. This is mainly due to that velocities are defined at half-time step in a centered difference scheme (discretizing in time a second order equation), while both internal energy density and stresses are defined at each time step. Particular non-trivial discrete treatment (especially of the kinetic energy as already said) may be required to ensure the conservation of the total energy (see [40, Sections 2.7.2 to 2.7.4]). Second, the writing of the conservation of the total energy in System (2.6) will enforce by definition and in a straightforward manner a proper energy balance in the discrete setting, and ensure that no energy is wasted. The numerical dissipation of the scheme will contribute to the growth of the entropy, in addition to its physical contribution. Third, once discretized in space the semi-discrete equations associated with System (2.6) can profit from any family of time integrator for first order ordinary differential equations. In particular, the family of explicit Runge-Kutta time integrators is one example among others. This avoids second order time integrator like Newmark or other dissipative ones. Fourth, when writing a multi-field formulation such as System (2.6), all unknowns contained within the vector of conserved variables $\mathfrak{U}$ will converge in the discrete setting at the same convergence rate, hence strains (then stresses) will here converge at the same rate than the velocities. The price to pay for that are (i) a larger set of conservation laws, but that does not yield a dramatic increase of computational cost since the time integration is usually made explicit, and (ii) handling the involution constraint (2.8). Next, conservative formulations profit from a well-developed literature on hyperbolic equations for its mathematical analysis [64, 112]. Especially, the hyperbolicity of System (2.6) can be directly linked to the strong ellipticity (or rank-1 convexity) of the hyperelastic energy density ψ (see e.g. [79, 48, 124])

$$\frac{\partial^2 \psi}{\partial F_{i\alpha} \partial F_{i\beta}} N_\alpha N_\beta m_i m_j > 0 \quad \forall \mathbf{N}, \mathbf{m} \in \mathbb{R}^3;\ \mathbf{N}, \mathbf{m} \neq \mathbf{0}.$$

At last, the conservative system (2.6) can be discretized in space with any type of known dedicated scheme. Especially, it is naturally compatible with all shock-capturing numerical methods providing high-order accurate non-linear and non-oscillatory approximations of the solution field. Among others, on can cite finite volume methods coupled with the Total Variation Diminishing (TVD) [64, 112, 107] or ADER-WENO [173] technologies, discontinuous Galerkin approaches (Runge-Kutta-based ones [62] or ADER-WENO [152]). Classical finite

elements can also be used, provided stabilization (actually upwinding) is made thanks to a Petrov-Galerkin method [120, 164]. Or if large strains are involved, conservative particle-based methods [165, 141] can also be used at profit.

As a final remark, notice that the two first equations of System (2.6) (namely the conservation of linear momentum and the geometrical compatibility conditions) can be derived from a variational formulation, taking the stationarity of an action integral (actually Hamilton's principle) formed with a constrained Lagrangian functional, assuming a hyperelastic constitutive response and the conservation of the entropy. The combination of the latters with the conservation of linear momentum yields the conservation of the total energy (actually the third equation of System (2.6)). Therefore the latter does not directly derive from an Euler-Lagrange equation of a variational formulation. Some analog derivation is shown in the Eulerian framework in [103]. For dissipative processes, the entropy production rate is defined so that to be positive and so that the conservation of total energy is still satisfied. Section 2.4.5 shows a variational formulation of thermo-mechanical constitutive update consistent with that.

2.4.3 Quality of the numerical approximation of plastic waves

A first set of contributions to this research topic has been dedicated to the study of the quality of the numerical approximation of plastic waves that could be provided by shock-capturing numerical methods. Indeed, the history of the propagation of plastic strains in a medium and its relation with the residual state is of primary importance for instance in high-speed forming of assembling processes. More precisely, the questions addressed were (i) to test and apply various shock-capturing technologies to elastic-plastic solids submitted to impacts, (ii) qualify what actual benefit they bring with respect to displacement-based Galerkin approaches regarding the capturing of plastic waves and the computed plastic strains, and eventually (iii) propose adaptations or extensions of some known schemes to improve the approximation of plastic waves. For the sake of simplicity, but also to perform an easier comparison with displacement-based Galerkin approaches, this first set of contributions was performed within the geometrical linearized framework and the isothermal setting.

2.4.3.1 Rate-independent elastoplasticity

A first aspect of study has been first devoted to the approximation of plastic waves when generated by *rate-independent elastic-plastic constitutive models*. Two finite volume technologies were used to this end. A first one is based on the high order wave-propagation algorithm or Flux Difference Splitting method of Leveque [64], which falls within the family of upwind cell-centered finite volume schemes. It relies on the split of interface numerical fluxes into fluctuations, which in turn are decomposed into wave contributions. Such decomposition amounts to solve a Riemann problem at each interface with a known number of waves. A higher order of accuracy is achieved by adding second order numerical fluxes, which are limited based on the Total Variation Diminishing (TVD) technology. Without going into details, the idea is to meet both high order of accuracy in smooth regions and a high resolution of discontinuity without any spurious oscillations where discontinuities arise in the solution. The latter is enforced by introducing a controlled amount of numerical viscosity locally through a non-linear approximation (actually limiters), so that to adapt to the local regularity of the solution. To carry out elastic-plastic numerical simulations with this technology, the most common solution consists in following a two-stage procedure. The first stage amounts to solve (explicitly) over the time step the discrete equations (both in space and time) associated with System (2.6) considering a *purely elastic evolution*, especially considering an *elastic* Riemann solver. The second stage then consists in projecting the obtained elastic trial stresses onto the yield locus, with any well-suited algorithm (see e.g. [71]), hence following what was initially proposed by Wilkins [16]. Although quite efficient, this approach applies limiters to the sole elastic waves. The plastic waves are not included in the Riemann solver, but emerge in the solution from the projection of elastic trial stresses onto the yield locus. It results in that the elastic precursors are well captured in very few cells, while the approximation of discontinuous plastic waves (if a linear hardening is considered) are smeared over twice as much cells. This is so even though the Courant number is set at one since the elastic precursor travels faster. Although overshoot of plastic strains are avoided, displacement-based Galerkin approaches do better and

solve plastic discontinuities with a lower number of cells. However, this approach behaves better in more general cases for which plastic waves are simple waves (for non-linear hardenings or non plane wave propagation).

Another possible solution for elastic-plastic numerical simulations is to also apply limiters to plastic waves, which should hence be included in an approximate Riemann solver. Such approximate elastic-plastic Riemann solver can easily be developed for problems involving a one-dimensional propagation of plane waves [130]. The (discontinuous) elastic waves are added additional left and/or right discontinuous plastic ones, according to the yield condition computed in both adjacent grid cells from the elastic trial stresses computed at a given interface. It results an impressive efficiency, as shown in Figure 2.21. Such approach can also be applied in order to approximate continuous plastic waves (resulting from a non-linear hardening) with an approximate elastic-plastic Riemann solver including discontinuous ones, considering either isotropic or kinematic hardenings (or both) [130]. However, the main drawback of this approach lies in that it is not generalizable in a straightforward manner to multi-dimensional stress states. In that case, the types of plastic waves occurring (and hence the loading path) also depend on the loading case, and are hence not known *a priori* for building an approximate Riemann solver. For the thin-walled tube problem, Lin and Ballman [45] overtook this difficulty by defining elementary stress paths from Clifton's results [19]. Those paths can be used in order to relate some guessed stationary state of the Riemann problem to its initial conditions through the waves involved and hence to deduce the wave pattern. By iteratively following that procedure until convergence, the Riemann problem can be solved. However, no generalization of such procedure exist for an any multi-dimensional stress state. In his PhD thesis, Adrien Renaud (co-advised by Laurent Stainier and I) made a contribution in that direction, the purpose of which was the determination of the loading paths followed inside plastic simple waves involved in two-dimensional elastic-plastic media [155, 140]. The long term idea is to identify and relate wave structures to loading paths in two-dimensional elastic-plastic media, and propose some iterative procedure analog to that of Lin and Ballman [45]. In this contribution, the characteristic analysis was addressed in a unique framework for both plane strain and plane stress cases, some properties of the loading paths for several cases were demonstrated from integral curves, then some loading paths were studied through numerical integration of characteristic equations. Basic results of Clifton [19] were retrieved for the thin-walled tube problem. But various other (and rather unusual) loading paths were also shown to occur within fast or slow plastic simple waves, either for plane stress or for plane strain cases.

One way to improve the capturing of discontinuous plastic waves while avoiding the design of elastic-plastic Riemann solvers is to consider multiple projections of trial elastic stresses onto the yield locus per time step. This can be made possible using multi-step numerical schemes. This idea was tested on the simplest (and very old) numerical scheme that can be found in this family, the Lax-Wendroff scheme [12]. On the one hand, it belongs to the class of centered schemes [112], so that no Riemann solver is required. On the other hand, its Richtmyer two-step implementation [14] allows to perform the projection of the elastic trial stresses onto the yield locus twice per time step. Two formulations of the Lax-Wendroff scheme were proposed [145] for its extension to the computation of elastic-plastic solids, respectively denoted as 'STRAIN' and 'STRESS' ones. These follow from the definition of the unknown vector which consists either of the strain or stress components in addition to the velocity ones according to the chosen formulation. The 'STRAIN' formulation is based on the system of conservation laws, and the integration of the elastic-plastic constitutive equations is performed twice per time step, first at nodes at mid-time step, then cellwise at the end of the time step. The 'STRESS' formulation is based on the quasi-linear form written in stresses, which can only be derived in the small strain framework since elastic-plastic compliances naturally appear. It amounts, for its first step, to solve a small system of equations at nodes to update the stresses nodewise, provided some effective elastic-plastic compliance moduli. Then, the stress update is performed cellwise during the Richtmyer second step and still accounts for the yield threshold. At last, the plastic strains and internal variables are updated iteratively by adjusting the elastic convex so that the updated stress state lies on its boundary, consistently with the plastic flow rule and hardening laws. Figure 2.22 shows a example of a partial impact on a plane, and a comparison between all numerical solutions. Two projections per time step improve the capture of the plastic wave with respect to a single one, and amounts to more or less fit the finite element solution, however with a little bit less noise as seen in Figure 2.22a. Other examples like dynamic ratchetting simulated with the Armstrong-Frederick non-linear kinematic hardening also allows to show the possibilities of the proposed approach.

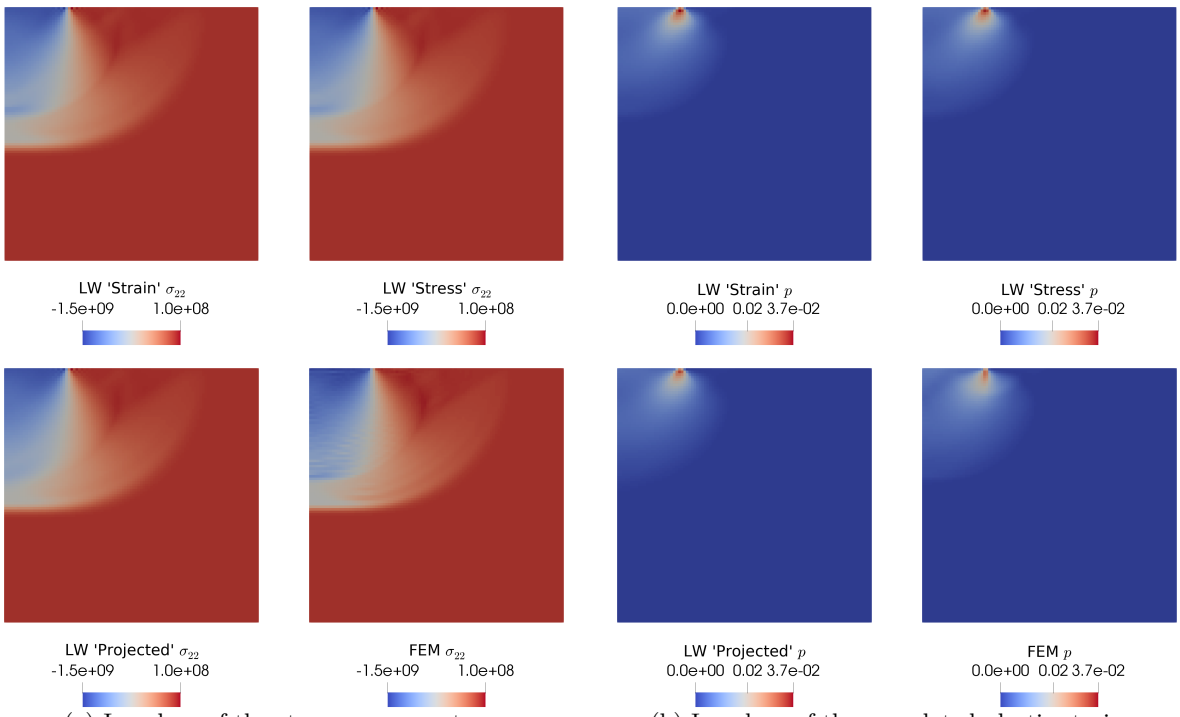

(a) Isovalues of the stress component σ_{22}

(b) Isovalues of the cumulated plastic strain p

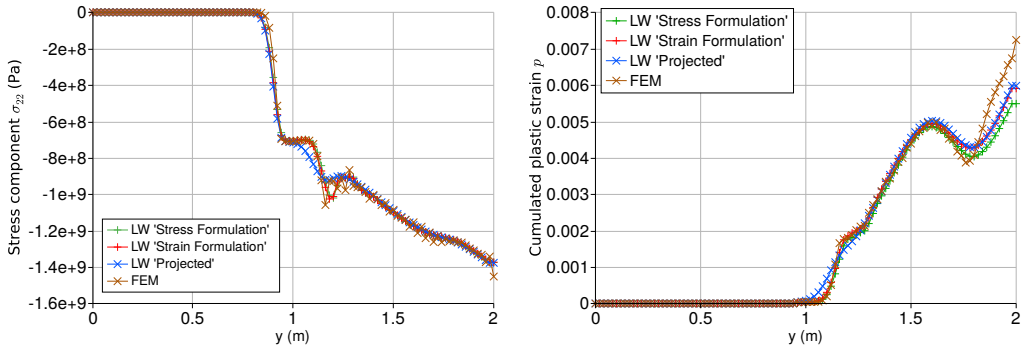

(c) Plots along the symmetry line

Figure 2.22: Comparison at time $t = 1.88 \times 10^{-4}$ seconds of the Lax-Wendroff solutions ('STRESS' and 'STRAIN' formulations), an elastic Lax-Wendroff solution projected onto the yield locus and a finite element solution. Extracted from [145].

2.4.3.2 Rate-dependent elastoviscoplasticity

A second aspect of study pertains to the approximation of the propagation of inelastic strains when generated by *rate-dependent elastic-viscoplastic constitutive models*. One possible way among others to write the governing equations of an elastic–viscoplastic system is to write its quasi-linear form, including stresses in the unknown vector $\mathbf{Q}$, which is still only possible in the small strains framework. A system of balance laws appears, including a source term $\mathbf{S}(\mathbf{Q})$

$$\frac{\partial \mathbf{Q}}{\partial t} + \mathbf{B}_i \frac{\partial \mathbf{Q}}{\partial x_i} = \mathbf{S}(\mathbf{Q}), \tag{2.10}$$

defined from the plastic flow rule which can be identified as a relaxation operator

$$\boldsymbol{\mathcal{S}}(\boldsymbol{\mathcal{Q}}) = \frac{\boldsymbol{\mathcal{R}}(\boldsymbol{\mathcal{Q}})}{\tau} \; ; \quad \frac{\partial \boldsymbol{\mathcal{R}}(\boldsymbol{\mathcal{Q}})}{\partial f} < 0,$$

with τ is the relaxation time or stiffness parameter. The relaxation term $\boldsymbol{\mathcal{R}}(\boldsymbol{\mathcal{Q}}) \equiv \boldsymbol{\mathcal{R}}(f(\boldsymbol{\mathcal{Q}}))$ is actually a decreasing function of the yield function $f(\boldsymbol{\mathcal{Q}})$, such that a relaxation of the state of the system can occur towards its equilibrium associated with the yield condition $f = 0$. The elastic-viscoplastic system can thus be identified to a *relaxation system*, that is a system of hyperbolic conservation laws with relaxation, to which a large literature is devoted [33, 47]. In particular, one can show that in the asymptotic limit $\tau \to 0$, the relaxation system (2.10) tends to an *equilibrium system*, consisting of a system of conservation laws (so without source term) of lower size. Here, an elastic–viscoplastic system tends asymtotically towards rate-independent plasticity for the limit case of vanishing viscosity, or equivalently here for a vanishing relaxation time.

Since irreversible viscoplastic effects only occur in the source term of System (2.10), the homogeneous part of the system of balance laws is governed by the sole elastic part of the elastic–viscoplastic behavior, meaning that any information in an elastic-viscoplastic system and in particular irreversible processes propagate along elastic characteristic curves. Only elastic characteristics exists, however characteristic equations now embed dissipative term linked to the viscoplastic flow rule [75].

The viscoplastic relaxation system (2.10) can be solved by means of fractional-step splitting methods, as for instance the first order accurate Godunov's splitting or the second order accurate Strang's one [112]. The convection (or homogeneous) part of System (2.10) is solved with the flux-difference splitting formalism. The latter is here extended to bidimensional non-uniform quadrilateral meshes, for which the computation of first order terms follow their classical derivation for these unstructured meshes, while second order terms are computed based on a limitation of waves which accounts for the different orientations between the current and upwind edges (see [137]). Next, the other step of the splitting method consists in solving a set of ODEs, with the source of (2.10) as a right hand side. One way to study rate-independent elastic-plastic systems is then to solve System (2.10) with a very small relaxation time τ. However, the relaxation is said to be stiff when the relaxation time τ is small compared to the time scale determined by the characteristic speeds of the system and some appropriate length scales. Practically speaking, one wants that the time step Δt is prescribed by the convection part of System (2.10) through the CFL condition, and not by its source term, which amounts to solve the latter on an underresolved time grid ($\tau << \Delta t$). Therefore, particular implicit time integrator especially satisfying the L-stability condition should be used, as for instance the implicit Euler one. But other families of time integrators like implicit-explicit IMEX Runge-Kutta schemes [68] allow to define high order schemes using an explicit time discretization for the convection part and an implicit (the DIRK one for instance) one for the relaxation operator. Other approaches like ADER-WENO schemes [152] are also available.

Figure 2.23 shows an example of a sudden velocity loading and unloading of a heterogeneous volume consisting of a an elastic-viscoplastic inclusion of circular cross-section centered within a square elastic matrix. Chaboche's viscoplastic constitutive flow rule and Prager's linear kinematic hardening are used in the inclusion. Figure 2.23 shows a comparison between an explicit finite element solution and the finite volume one, once the prescribed velocity step has almost crossed the length of the matrix. We see comparable results, but with much fewer spurious numerical oscillations in the finite volume solution thanks to limiters.

2.4.4 Lagrangian conservative particle-based methods for large strains

As the strength of impacts applied on dissipative solids increases as well as their duration (leading to an increased impulsion), problems related to the numerical approximation of the kinematics soon appear as large strains occur. Lagrangian approaches consider the mesh as sticked onto the matter. Indeed following the matter as it deforms appears natural and efficient to handle history-dependent constitutive response and apply boundary conditions. However, as the strain increases the method is less efficient and accurate when the elements are highly distorted or entangled so that re-meshing techniques, as well as costly and diffusive projection steps must be employed. Such problem will appear whatever the chosen type of formulation (i.e. displacement-based or conservative formulations) or approximation (continuous Galerkin finite elements, discontinuous Galerkin finite elements, finite volumes) as soon as the grid sticks to the matter. These issues can be avoided by using an Eulerian approach, i.e. a spatial description of the motion, computing on a fixed mesh. Dramatically large

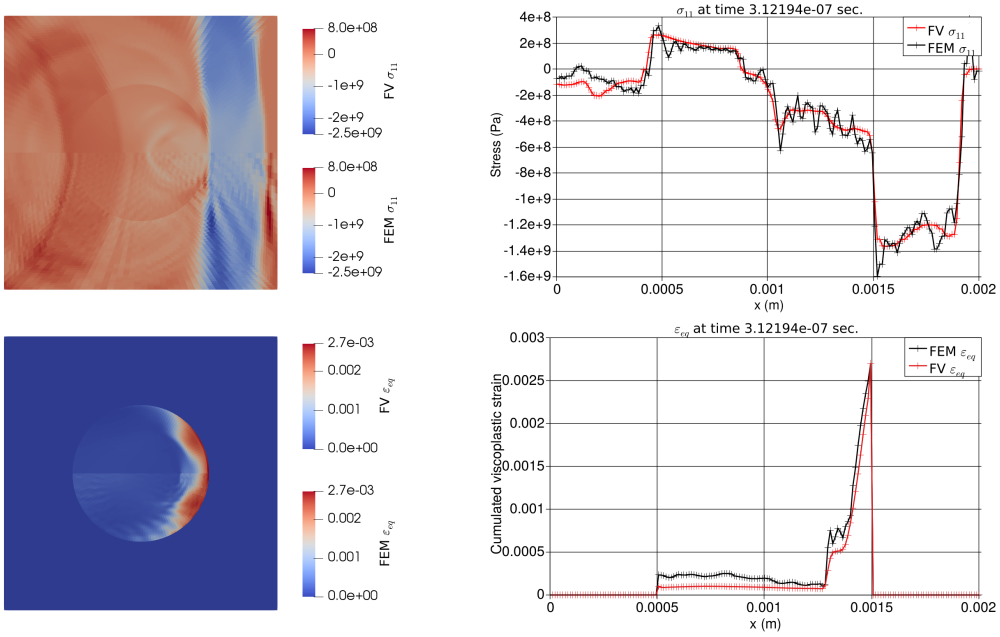

Figure 2.23: Normal stress σ_{11} and cumulated viscoplastic strains ε_{eq} at time 3.12×10^{-7} seconds, computed with finite elements (bottom-half domain) and finite volumes (top-half domain). Superposed plots are made along the symmetry line. Extracted from [137].

amounts of distortions can then be very easily simulated (see e.g. [122]). However, issues then arise on the one hand from the approximation of interfaces, which require dedicated tracking techniques and may eventually be valid for the sole very early instants of the simulation [122], and on the other hand diffusive convection steps are required in order to transport internal variables on the mesh. Alternatively, Arbitrary Lagrangian Eulerian (ALE) methods [58] aim at meeting advantages of both approaches while freeing themselves of their respective limits by distinguishing the motion of the mesh from that of the material points. However, they also combine their drawback since this type of strategy requires re-meshing or re-zoning procedures, stabilization (or upwinding) due to the appearance of convection terms, and diffusive projection steps of internal variables for solid media. Notice that the ALE approach presented in Section 2.2.1.1 took advantage of a fluid-type instantaneous constitutive response precisely to avoid such projection step.

Alternatively, mesh-free methods discretize a spatial domain by means of a collection of points that are given a support allowing them to interact with each other. A wide variety of such methods were introduced such as the Smoothed-Particle Hydrodynamics or the Element-Free Galerkin [51]. However, on the one hand these methods have their own problems (prescribing boundary conditions or others), and on the other hand their approximations were not developed for shock-capturing purpose, and give quite poor results as shown in [82].

2.4.4.1 The Discontinuous Galerkin Material Point Method

One interesting combination of all the above approaches would (i) allow to dissociate the motion of material particles from that of the computation grid, (ii) but in a lighter way than ALE approaches, and whose approximation would be of (iii) arbitrary high order and (iv) adapted for shock-capturing purpose. The two first points were already met by the Material Point Method (MPM) introduced in the 1990s [50] for solid mechanics problems. This method comes from the family of Particle-In-Cell methods (PIC) [13] developed in the 1960s, which consider particles carrying the fields of a problem that move in a computational mesh. The underlying grid is used in order to compute an approximate solution (and especially gradients) that is projected and stored at particles. Hence, one of its main advantage is that the background mesh can be discarded at each time step and re-constructed for computational convenience. The application of PIC to solid mechanics led to the MPM

in which the constitutive equations are managed at particles. As a result, MPM can be seen as a mesh-free extension of FEM with quadrature points moving in elements, which could also be viewed as a certain way to achieve a combined Euler-Lagrange approach. However, it is well-known that PIC exhibits numerical dissipation that can be reduced at the cost of spurious oscillations [41]. However, the MPM could be improved by considering a discontinuous Galerkin approximation supported by the grid mesh, which would allow to meet the two above last points.

In that context, the purpose of the PhD thesis of Adrien Renaud [140] has been to develop the Discontinuous Galerkin Material Point Method (DGMPM), coupling the two aforementioned frameworks. It aims at enabling an accurate wave path tracking in solid media undergoing large strains. The DGMPM is here derived within the large strains framework with a total Lagrangian approach, in such a way that material particles are defined in the initial configuration, as the grid also does. On the one hand, it naturally couples with hyperelastic-based constitutive responses as shown in [141], and on the other hand it permits to avoid the well-known grid-crossing instabilities [65] as material particles cross an interface between two elements. The DGMPM takes advantage of the weak form of the conservative formulation (2.6) written elementwise (although considered in the isothermal setting at first), whose integrals are computed with a particle-based quadrature, following in that the original MPM, which is based on a pointwise approximation of the initial mass density and the definition of specific quantities

$$\boldsymbol{\mathcal{U}} = \rho_0 \bar{\boldsymbol{\mathcal{U}}} \,;\, \boldsymbol{\mathcal{F}}_\alpha = \rho_0 \bar{\boldsymbol{\mathcal{F}}}_\alpha$$
$$\rho_0(\boldsymbol{X}) = \sum_{p=1}^{N_p} m_p \delta(\boldsymbol{X}^p - \boldsymbol{X})$$

which allow to change integrals into a sum over contributions associated to each material point lying within a grid cell

$$\sum_{p=1}^{N_p} m_p \left[\frac{\partial \bar{\boldsymbol{\mathcal{U}}}}{\partial t} \boldsymbol{\mathcal{V}} - \bar{\boldsymbol{\mathcal{F}}}_\alpha \frac{\partial \boldsymbol{\mathcal{V}}}{\partial X_\alpha} \right] \Bigg|_{\mathbf{X}=\mathbf{X}^p} + \int_{\partial\Omega^e} (\boldsymbol{\mathcal{F}} \cdot \boldsymbol{N}) d\Gamma = \mathbf{0} \quad \forall \boldsymbol{\mathcal{V}}. \tag{2.11}$$

Interface fluxes appearing in Equation (2.11) are computed from approximate Riemann solvers. Only one Riemann problem is defined per interface by averaging nodal values of each side. Riemann problems are defined from the quasi-linear form associated with System (2.6), hence including stresses as part of an unknown vector $\boldsymbol{\mathcal{Q}}^T = \left[\mathbf{P}^T, \mathbf{v}^T\right]$. Interface fluxes are then computed by a simple assembly

$$\boldsymbol{\mathcal{F}}_N^* = \frac{\partial \boldsymbol{\mathcal{F}}_N}{\partial \boldsymbol{\mathcal{Q}}} \boldsymbol{\mathcal{Q}}^*,$$

from the steady solution $\boldsymbol{\mathcal{Q}}^*$ of the Riemann problem. Besides, only contact waves are accounted for in the characteristic structure of the approximate Riemann solver to make its solution more efficient. Once the discontinuous Galerkin approximation [62] has been introduced in (2.11), the obtained semi-discrete equations can be discretized in time either by an explicit forward Euler algorithm or by a second order explicit Runge-Kutta scheme.

From all quantities known at material points $p = 1, \ldots, N_{mp}$ at time t_n, the computation over a time step starts by some convective phase consisting of the projection of both conserved $\bar{\boldsymbol{\mathcal{U}}}_p^n$ and auxiliary $\bar{\boldsymbol{\mathcal{Q}}}_p^n$ specific quantities to the nodes of the grid $i = 1, \ldots, N_n$. This is achieved through Shepard's functions (or Moving Least Square at order zero, see e.g. [51]), inherited from the original MPM. Next, volumic and surface discrete fluxes are computed, the latter involving the solution of approximate Riemann problems at each mesh interface. The solution is advanced in time explicitly on the grid $\bar{\boldsymbol{\mathcal{U}}}_i^{n+1}$, and then mapped back to material points. The back mapping is here performed by a simple interpolation involving the finite element shape functions defined on the grid, which amounts to follow the PIC [13]. Knowing the updated deformation gradient from $\bar{\boldsymbol{\mathcal{U}}}_p^{n+1}$ (see Equation (2.7)), a constitutive update allows to compute stresses $\mathbf{P}_p^{n+1}$ and internal variables $\mathbf{Z}_p^{n+1}$ at material point p, and to build the updated specific auxiliary vector $\bar{\boldsymbol{\mathcal{Q}}}_p^{n+1}$. Especially, a variational constitutive update [56] is used in [157] for hyperelastic-plastic constitutive models based on a hyperelasticity of Hencky. Once the state of material points has been updated, the grid can be discarded if required, before a next time step.

Figure 2.24 shows an example of comparison of numerical solutions obtained with the DGMPM (1 and 4 ppc (ppc stands for particles per cell)) coupled to a forward Euler explicit time integration, explicit FEM and MPM (1ppc) on a test case close to the LAser Shock Adhesive Test (LASAT) [66]. An overall correct agreement is observed between the solutions. The DGMPM appears sligthly more diffusive than FEM and MPM, which are clearly more noisy.

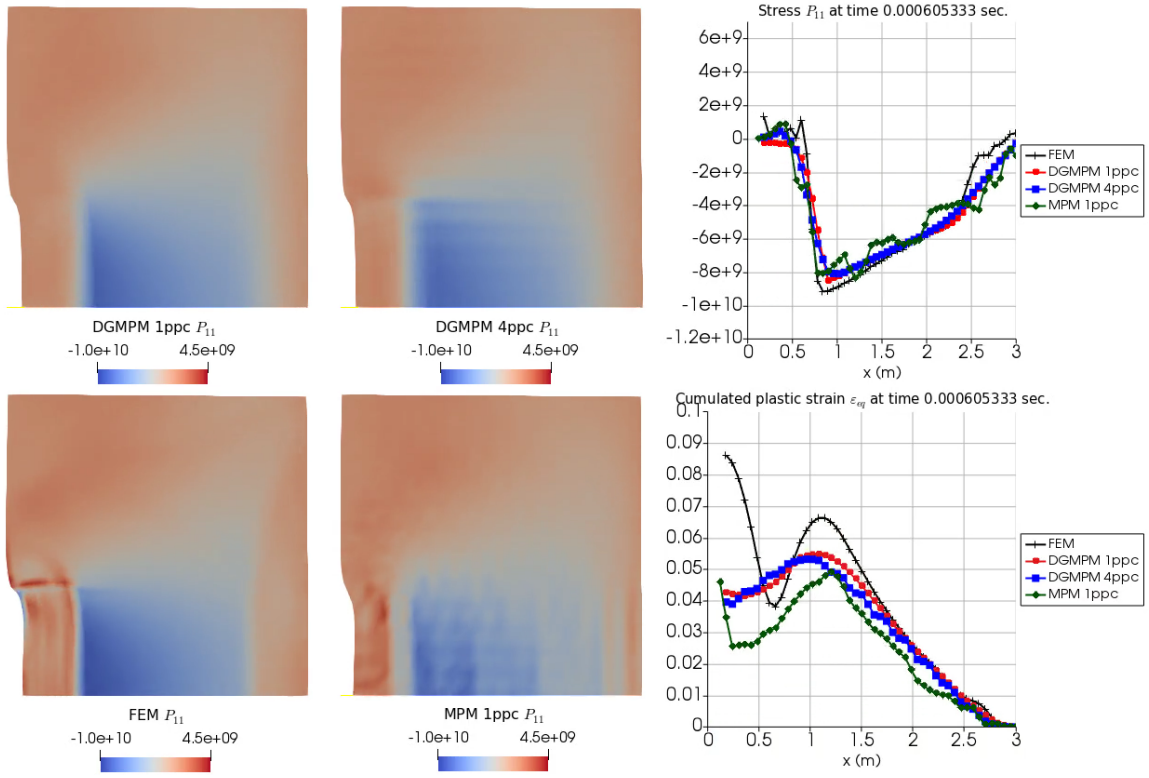

Figure 2.24: Comparison of the normal stress component P_{11} computed with various numerical solutions on a LASAT-like test [66].

The stability but also the numerical diffusion (as shown in Figure 2.24) of the DGMPM highly depends on the number and the distribution of particles inside the computational grid. The derivation of stability conditions for the DGMPM is then crucial in order to fully exploit (later) the arbitrariness of the grid. Especially, stability conditions allows to (i) ensure the stability of the scheme while minimizing the numerical diffusion; (ii) adapt the Courant number when the grid is reconstructed; (iii) adapt the grid so that a given CFL condition is satisfied. Provided linear finite element shape functions, stability conditions of the DGMPM have been studied on a scalar linear advection equation. A first analysis carried out in the one-dimensional case coupled to a forward Euler explicit time integration [141] has allowed to write the discrete update equation of the form

$$\bar{Q}_{\alpha}^{n+1} = f(\bar{Q}_{\mu}^{n}) \quad \mu = 1, \ldots, P.$$

The obtained scheme equations depends on the Courant number $a\Delta t/\Delta x$, a being the celerity, and on the position of materials points within the grid mesh. Next, a von Neumann linear (A-) stability analysis allows to study the consequences of various positions and numbers of material points in a cell onto the critical time step. As a special case, considering only one particle per cell allows to recover the well-known first order accurate upwind scheme, or Godunov's scheme [112], for which the maximum Courant number can reach unity. Increasing the number of material points per cell leads to a decrease of the maximum Courant number, whose various configurations are studied in [141]. Actually, the DGMPM in this version will be first order accurate, whatever the number of particles per cell and their relative positions. The latter will only have an influence on the amount of numerical diffusion and on the critical time step. This stability analysis was then extended to a second-order

Runge-Kutta (RK2) explicit time integrator for one-dimensional problems, and to two-dimensional problems coupled to a forward Euler explicit time integration in [156]. Various configurations (number/positions) were studied assuming the distribution of particles is the same in every cells of the computational grid, and allow to draw some trend of evolution of CFL. Especially, the RK2 time discretization provides higher critical CFL to the DGMPM. Moreover, for both the forward Euler and the RK2 time integrators, moving all the particles upstream (resp. downstream) leads to less restrictive (resp. more restrictive) stability conditions. In addition, for distributions of particles satisfying the symmetry with respect to the cell centers, the RK2 algorithm yields the optimal CFL number, whereas it is not the case for the forward Euler. Similar results have been emphasized for two-dimensional problems.

The developments of the first version of the DGMPM has focused on the construction of its approximation for low order of accuracy. Although the arbitrariness of the polynomial order provided by the discontinuous Galerkin framework has not been exploited so far since only linear finite element shape function were considered, the first study permitted to study limit cases of low order approximation of the method, and the associated consequences of the number of particles and their positions on stability conditions. Next, it is of real interest to extend the method to truly high order of approximation. This is the purpose of the on-going PhD thesis of Alaa Lakiss, which is a collaboration between the Lebanon International University (with advisors Mikael Tannous and Bakri Abdul-Hay) and Centrale Nantes (with advisors Laurent Stainier and I). Several issues should be overcomed to extend the first-order DGMPM to high order approximations. First, the low regularity of Shepard's functions inherited from the MPM used to make the projection of quantities from particles to grid prevents to increase the level of accuracy of the DGMPM. Second, the reverse projection from the grid to particles using PIC is too much diffusive, and should be improved, especially its coupling with limiters would be relevant. Third, the material points-based numerical integration generates too much error and cannot be afforded to increase the order of accuracy. Last but not least, the crucial point the method should meet to address history-dependent constitutive models is to ensure that internal variables always lie at material points, in order to avoid diffusive projection steps of the loading history. Unfortunately, explicit Runge-Kutta-type integrators cannot satisfy this last condition. For instance, the second stage of a RK2 requires the computation of the stresses at mid-time step at nodes, which would require somehow a projection of internal variables to grid nodes.

The extension of the first-order DGMPM to arbitrary high-order accurate approximations is performed by adapting the ADER (Arbitrary high order schemes using DERivatives) approach [152] to the particular spatial discretization of the DGMPM. To put it in short and without going into details, the ADER approach amounts to make a time integration of System (2.6) through some Gauss time-quadrature. An approximate solution is then provided to each sub-instants the quadrature needs by the construction at each time step of a space-time approximation of the solution defined on $\Omega_e \times [t_n, t_{n+1}]$. The latter can be obtained from a dedicated time discontinuous Galerkin approach formulated on a space-time slab $\Omega_e \times [t_n, t_{n+1}]$ (see [152]). The ADER method can thus be thought as a predictor-corrector approach. The work of Alaa Lakiss brings two novelties to the DGMPM. First, the degrees of freedom of the ADER-predictor fields are now defined at material points (and not at interpolation points as for ADER-DGFEM, see [152]), hence the computation of the constitutive response of the material is ensured to be always performed at these material points. Internal variables are never changed of geometrical support [176]. Second, Shepard's functions are replaced by a Moving Least Square (MLS) approximation (see e.g. [51]) for the projection of quantities from particles to integration points for the numerical integration of integrals of the weak form. The order of the MLS approximation is of arbitrary order of accuracy, the latter should therefore be chosen in a consistent manner with the polynomial order of both the ADER space-time predictor and the discontinuous Galerkin approximation lying on the grid. Thanks to the total Lagrangian framework of the formulation, both the discontinuous Galerkin approximation and the particle to grid mapping are computed once for all at the beginning of the computation, until the grid is discarded.

Figure 2.25 shows a comparison of the normal stress component σ_{11} computed with various numerical solutions on a test case consisting of a normal velocity prescribed on the right side of a multi-holed medium following a hyperlastic neo-Hookean constitutive response. Second order accurate solutions in both space and time are computed with TVD-RK2 DGFEM, ADER-DGFEM and ADER-DGMPM, 'S1' denoting bilinear shape functions and 'T1' a linear approximation over the time step. The post-process is performed pointwise either at interpolation points (Gauss-Legendre ones here) or at material points. A good agreement is observed

between the three solutions.

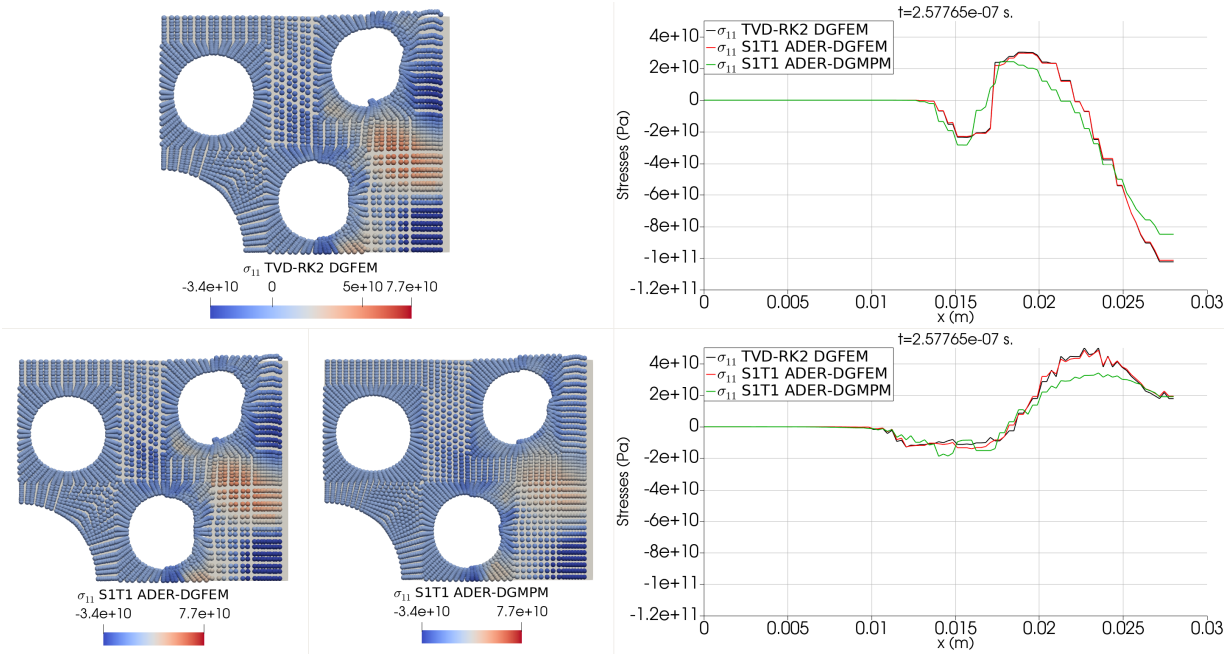

Figure 2.25: Comparison of the normal stress component σ_{11} computed with various numerical solutions on a multi-holed medium submitted to a normal velocity loading on its right side, of continuous time profile. Extracted from [176].

2.4.4.2 Conservative Smooth Particle Hydrodynamic (SPH)

The approximation of some well-known mesh-free methods developed in the 1980s and the 1990s are still the topic of adaption for shock-capturing purpose. This is especially the case also of the Smooth Particle Hydrodynamics (SPH) method [25, 43], which has been the purpose of intense developements over several decades, then tested and extended for shock problems [59]. However, it is still the object until recently of much work in that direction [113, 134, 170]. Although these works were much devoted to fluid mechanics problems, some extension based on some enlargement of the conservative formulation (2.6) was proposed by Lee et *al.* [146] for isothermal solid mechanics problems. Its extension to the case of large strain thermo-elasticity was the purpose of a joint collaboration between the Swansea college of enginerring (involving Chun Hean Lee, Antonio Gil and Javier Bonet) and Centrale Nantes (Laurent Stainier and I). One subpart of the PhD work of Ataollah Ghavamian has been devoted to the extension to large strain thermo-elasticity of an entropy-stable Smooth Particle Hydrodynamics algorithm [165], whose contribution was mainly supported by the Swansea team. A total Lagrangian conservative multi-field formulation $\{\mathbf{p}, \mathbf{F}, \mathbf{H}, J, \mathcal{E}\}$ coupled to a polyconvex hyperelastic constitutive response and a Mie-Grüneisen equation of state was considered. The conservative SPH relies on the weak form of the conservative multi-field formulation, and its discretization uses a corrected kernel approximation. The scheme is stabilized solving approximate Riemann problems between particles, and is integrated in time with a basic second-order accurate explicit TVD Runge-Kutta time integrator. Comparison was successfully performed with respect to a node-centered finite volume method.

2.4.5 A variational formulation of thermo-mechanical constitutive update for hyperbolic conservation laws

The conservative formulation (2.6) can be of interest to carry out thermo-mechanical numerical simulations in solid mechanics related to areas of applications already covered by both structural codes and hydrocodes. Indeed, it permits to easily ensure the conservation of the total energy, and can be coupled with quite various

kinds of approximations for both continuous and discontinuous solutions. However, the definition of the vector of conserved quantities (2.7) leads to that the constitutive update should therefore be driven from updated values of some strain measure ($\mathbf{F}$) and the internal energy density E as input data. The same situation already applies for Lagrangian hydrocodes [40]. However depending on the particular code (see e.g. [129, Chapter 6] or [70, Chapter 18]), the thermo-mechanical coupling of both deviatoric and hydrostatic components of the stresses may be computed in an uncoupled way. More precisely, fixed point iterations are performed on the internal energy density to compute the updated pressure, while accounting for already updated deviatoric stresses through some constitutive update embedding plasticity. Eulerian formulations may also often consider that only the hydrostatic contribution of the internal energy density depends on the entropy density (see e.g. [122, 149]).

As already mentioned in Section 1.1, the variational framework has allowed to build variational constitutive updates [56] which are numerically efficient and thermodynamically consistent. The thermo-mechanically coupled variational constitutive updates developed first by Yang et al. [72], then by Mosler and co-workers [93, 123], both rely on a formulation using displacements and temperature fields on a mesh, since they were developed in order to be couplable with structural codes. In addition, they also both rely on a two-field temperature formulation (an external temperature T appearing in the heat equation, and an internal temperature θ obtained through a state law). The idea of the contribution [174] was to propose one extension of these variational constitutive updates so that (i) it is couplable with the conservative formulation (2.6) and therefore with any conservative scheme, (ii) thermo-mechanical coupling can be naturally accounted for on both hydrostatic (through an equation of state or not) and deviatoric (for thermal softening) components of the stresses. Notice that it is therefore also compatible with more traditional Lagrangian (displacement-based) hydrocodes thanks to its input variables.

The variational formulation of the thermo-mechanical local constitutive problem in the continuous setting is based on a Lagrangian functional consisting on the one hand of the functional already introduced in [72], and on the other hand on the residual of the rate of the Legendre transform of Helmholtz's free energy density $W(\mathbf{F}, T, \mathbf{Z})$, enforced to vanish through a Lagrange multiplier:

$$\mathcal{L}(\dot{\mathbf{q}}, \lambda; \mathbf{q}) = \dot{E} - T\dot{\eta} + \phi(\dot{\mathbf{F}}, \dot{\mathbf{Z}}; \mathbf{F}, \mathbf{Z}, T) + \lambda \frac{d}{dt}(T\eta + W(\mathbf{F}, T, \mathbf{Z}) - E) \tag{2.12}$$

where the following state vector $\mathbf{q} = \{E, \mathbf{F}, \eta, \mathbf{Z}, T\}$ has been introduced, *which is assumed to be known and fixed here*, λ denotes the Lagrange multiplier, η the entropy density and $\mathbf{Z}$ a set of internal variables. Provided both the rate of deformation gradient $\dot{\mathbf{F}}$ and the rate of internal energy density $\dot{E}$ are given and known from the set of conservation laws (2.6), the optimization problem reads

$$\mathcal{W} = \underset{\dot{\eta}, \dot{T}, \lambda}{\text{stat}} \ \inf_{\dot{\mathbf{Z}}} \ \mathcal{L}(\dot{\mathbf{q}}, \lambda; \mathbf{q}) \tag{2.13}$$

where the variable with respect to which the stationarity conditions are computed are the rate of entropy density $\dot{\eta}$, the temperature rate $\dot{T}$, the Lagrange multiplier λ, and the rate of internal variables $\dot{\mathbf{Z}}$. The Euler-Lagrange equations associated with the optimization problem (2.13) allow to get the definition of the entropy, the evolution equations of internal variables and a Lagrange multiplier equal to unity. Substitution of the Lagrange multiplier within the functional (2.12) would permit to retrieve that used in [111], however *the whole point of this work is to keep this Lagrange multiplier as an independent unknown* since the input known data are $\{\dot{\mathbf{F}}, \dot{E}\}$. Notice that this variational formulation does not require the two-field temperature formulation of [72, 93, 123] anymore, which becomes useless. In the discrete setting, an incremental functional $\mathcal{I}(\mathbf{q}_{n+1}, \lambda_{n+1}; \mathbf{q}_n)$ is sought in such a way that it approximates the integral of the Lagrangian functional $\mathcal{L}$ (2.12) over the time increment Δt:

$$\mathcal{I}(\mathbf{q}_{n+1}, \lambda_{n+1}; \mathbf{q}_n) = \Delta E - T_n \Delta\eta + \Delta t \phi\left(\frac{\Delta \mathbf{F}}{\Delta t}, \frac{\Delta \mathbf{Z}}{\Delta t}; \mathbf{F}_{n+\alpha}, \mathbf{Z}_{n+\alpha}, T_{n+\alpha}\right) + \lambda_{n+1}\Delta(T\eta + W(\mathbf{F}, T, \mathbf{Z}) - E)$$

yielding a semi-implicit incremental variational update

$$\mathcal{W}_{n+1} = \underset{(\eta, T, \lambda)_{n+1}}{\text{stat}} \quad \inf_{\mathbf{Z}_{n+1}} \ \mathcal{I}(\mathbf{q}_{n+1}, \lambda_{n+1}; \mathbf{q}_n).$$

The stationarity with respect to the entropy density gives the updated value of the Lagrange multiplier

$$\lambda_{n+1} = \frac{T_n}{T_{n+1}},$$

which is not equal to unity anymore, but is close to it. Such ratio is reminescent of that introduced in former versions of variational constitutive update in thermo-mechanics [72, 93, 123] (especially see Equations (1.1) and (1.3)), but is introduced in a different manner here, and brings some consistent approximations within the discrete Euler-Lagrange equations, as well as in the computation of the reversible part of stresses.

Next, an application to thermo-hyperelastic-viscoplastic solid media is proposed, following the parameterization of the flow rule direction based on pseudo-stresses introduced in the work of Mosler and co-workers [89, 100, 90]. For a fully isotropic medium (both elastically and plastically) with a sole isotropic hardening, the discrete Euler-Lagrange equations amount to solve a non-linear system of three scalar equations on the unknown vector $\mathbf{q} = \{T, \Delta\lambda, \psi\}$, where $\Delta\lambda$ stands for the increment of the plastic multiplier, and ψ is an angle following from the parameterization of pseudo-stresses on spherical coordinates, see [100]. Although the input data of the variational constitutive update are $\{\mathbf{F}, E\}_{n+1}$, the solution process is performed in particular on the temperature T, which permits to use all well-known and already developed thermo-mechanically coupled constitutive models formulated with Helmholtz's free energy density $W(\mathbf{F}, T, \mathbf{Z})$. The physical content and the types of thermo-mechanical couplings acouunted for in the modeling can thus be directly enforced on the definition of the various contributions to the expression of Helmholtz's free energy density since its Legendre transform is solved numerically. This is the case for instance for the hydrostatic contribution (yielding an equation of state for the pressure) as well as for deviatoric contribution including plasticity and thermal softening effects. Furthermore, the non-linear system of equations written on the unknown vector $\mathbf{q}$ was solved in a

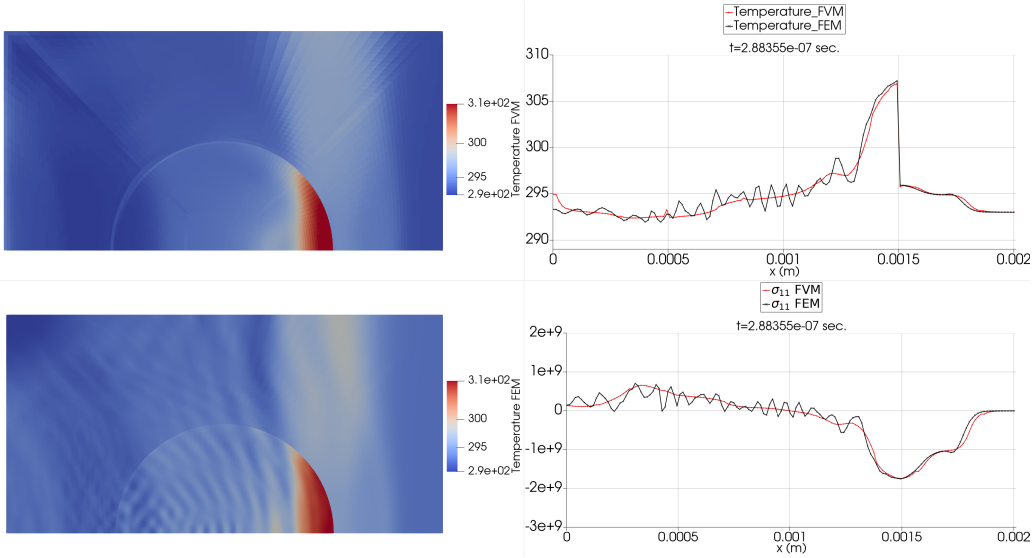

Figure 2.26: Comparison of the numerical solutions computed with the finite volume method (FVM) and the finite element method (FEM). Maps on the left part show the temperature fields computed with the two methods. Graphs on the right part show the superposed plots for the two solutions of the temperature and of the longitudinal stress component σ_{11}, both plotted along the symmetry line. Extracted from [174].

monolithic manner in [174]. However, partitioned schemes can also be derived from that system, analog to those introduced in the context of diffusion (see Section 1.3.2), that would permit to ease the solution process. But these partitioned schemes would therefore be consistent with a variational framework, and even define some particular consistent physically-based block-preconditioner applied to the monolithic system, which is not the case of integration algorithms already implemented in hydrocodes [70].

Figure 2.26 shows the comparison of two numerical solutions on the same test case than that shown in Figure 2.23. The simulations are here carried out with a thermo-elastic-viscoplastic inclusion (following a Johnson-Cook flow rule [30]) embedded in a thermoelastic matrix, both in small strains. A first solution is obtained with the Flux-Difference Splitting scheme (FVM) coupled to the proposed variational constitutive update. The second solution is computed with the the finite element method (FEM) with Q1 finite elements, coupled with an explicit central difference time integrator, and to a variational constitutive update driven in both strain $\boldsymbol{\varepsilon}$

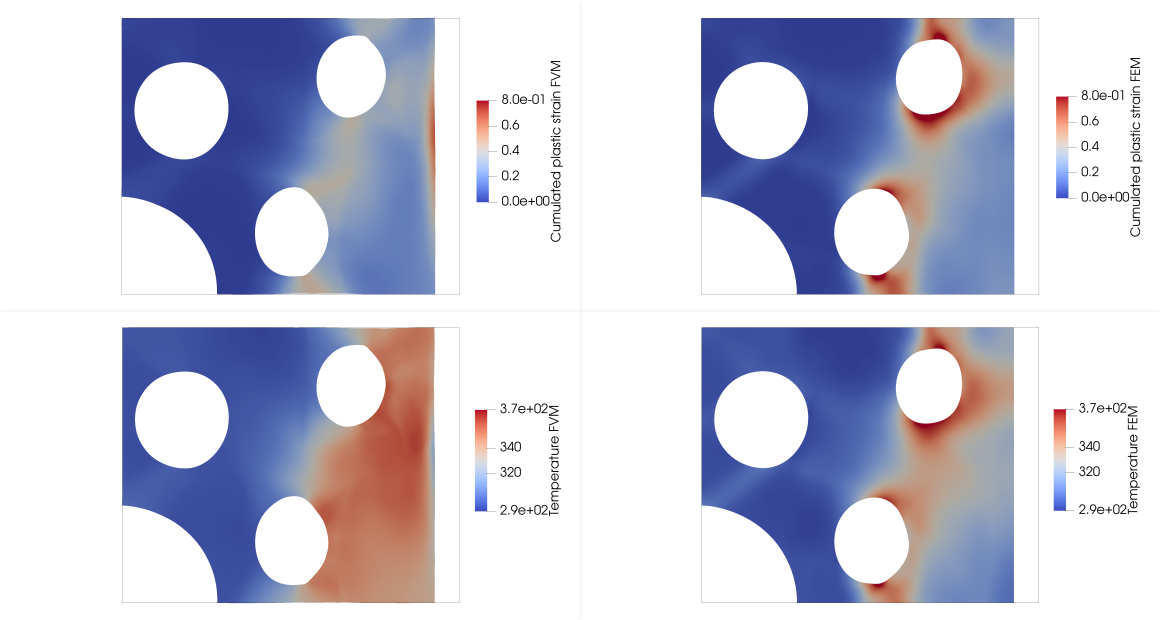

Figure 2.27: Maps of the cumulated plastic strain and the temperature plotted in the current configuration of the multi-holed elementary cell at time $t = 1.4 \times 10^{-5}$ seconds, computed with the finite volume method (FVM) and the finite element method (FEM). Extracted from [174].

and temperature T [168]. The details of such formulation can be found in [111]. A good correlation can be seen between the two solutions, up to spurious numerical oscillations occurring in the finite element solution which are removed from the finite volume one thanks to limiters.

Figure 2.27 shows a comparison between finite volume and finite element solutions on the multi-holed test case, involving here large strains. The comparison is here essentially qualitative since hyperelastic laws are different, in addition to the spatial and time discretizations, the constitutive update and the handling of quasi-incompressibility. But a correct comparison can be observed up to that FVM predicts higher temperatures and lower cumulated plastic strain than those given by the FEM.

2.4.6 Software aspects

The numerical methods involved in Section 2.4 (except Section 2.4.4.2) were the purpose of the development of a home-made library called HypLib, dedicated to the numerical simulation of two-dimensional hyperbolic problems. The main objective of this library is to be as modular as possible in order to make compatible all hyperbolic systems with all available numerical schemes for comparison purpose. More precisely, the objective is to ease the implementation of a new set of equations, immediately compatible with all discretizations, or the implementation of a new scheme, compatible with all sets of equations. This library has been written in an oriented-object manner, using the langage Python, and takes advantage of all the associated packages and libraries this langage allows to profit. Unfortunately, such modularity is obtained at the price of a computationally less efficient library.

Meshes are performed with the free software Gmsh, and the viewing operation of the post-processing is done with Paraview. All other pre-processing, computation, and post-processing operations are coded within the library. The library has approximately 25,000 lines of codes of definitions of objects and functions, and a large set of test cases which gather approximately 150,000 lines of codes. These test cases are of primal importance and serve on the one hand for validating elementary aspects of the solution while implementing a new features, involving usually very few degrees of freedom, and on the other hand for running more complex simulations on structures. A small sketch of the architecture of the library is given below, giving an idea of implemented functionalities as well as the categories in which several classes are defined:

* Hyperbolic conservation laws: Euler equations, conservative system (2.6) in both small and large strains, including or not the equation on the total energy.
* Parabolic systems: transient heat transfer, 'quasi-static' electromagnetism in potential form.
* Constitutive models: (hyper-)elasticity, (hyper-)elasto(visco)plasticity in both small and large strains, in a variational framework or not, and thermo-mechanically coupled or not; a few equations of states; available coupling with the library of constitutive equations MatLib [168].
* Numerical schemes: time discretizations (explicit and implicit time-stepping), space discretizations (finite volumes, continuous and discontinuous Galerkin finite elements, Material Point Method), space-time discretization (ADER predictor), splitting schemes to treat source terms.
* Riemann solvers: both exact and approximate ones.
* Utilities: Computation supports, material points, meshes, exports to Paraview.

As all library supporting research developments, it is still in current evolution. Its purpose is also to constitute a digital platform for the common developments with collaborators, and PhD students.

Chapter 3

Conclusions and perspectives

3.1 Conclusions

This document has presented a (hopefully) concise resume of my research works carried out over the years, from my PhD thesis up to now. The manuscript has focused on the presentation and the ordering of the main ideas of contributions performed over those years, while avoiding to go into the details which can be found in the associated papers.

The *objects of analysis* in these works have pertained to some coupled systems. Primarily, the coupling between thermal and mechanical effects has been studied in various scenarios. In a sense, these works allowed me to take a (very) short walk through the large class of thermo-mechanical problems and their applications, which have been ordered for convenience in this manuscript according to the characteristic time at which the deformation process occurs. Diffusion-type processes, whatever related to heat transfer or diffusion of species, as well as fast transient dynamics were the purpose of a set of contributions. However, other kinds of coupling like the one between thermo-mechanics and electromagnetism has also been of interest, especially for applications related to electromagnetic forming processes, although related computational aspects are rather parts of perspectives.

These works have been carried out by employing various *methods of analysis*. First, regarding the modeling and computational aspects, methods associated with variational calculus, conservative formulations, and multi-scale analysis (to just cite a few) have been employed to treat various coupled systems, ranging from slow and diffusive coupled mechanics systems to fast transient solid dynamics. These methods of analysis are usually well-suited mathematically, and yield or are easily connected with consistent approximations: incremental variational principles, shock-capturing methods, model order reduction through various approaches. The study of both slow and fast thermo-mechanical systems may sometimes share some common method of analysis, as it was the case with variational calculus. The variational constitutive updates connected with a set of conservation laws for fast transient dynamics was inspired from works previously developed for slow systems. Second, following those developed during my PhD thesis, the development (when possible) of analytical solutions is of great interest since they provide much valuable informations. On the one hand, they may serve for the validation of some approximation, as it was the case for fluid and solid enriched finite elements, or for the computation of (visco-)plastic or hyperelastic waves. On the other hand, a closed-form solution of simplified modelings can be used for the understanding a particular phenomenon, or for restricting the range of possibilities when designing magnetic pulse disassembly for instance. Third, although less numerous, experimental approaches have also been followed and were the purpose of various collaborations. They were applied either for high strain rate testing with Hopkinson bars, or for dynamic material processing encompassing Friction Stir Spot Welding and high pulsed power processes.

Practically speaking, the contributions brought by these works can be summarized as follows:

1. *the development of the modeling and/or computational aspects of transient diffusion coupled quasi-static mechanics via multi-field variational approaches.* A first instance pertains to the implementation of variational h-adaption methods for thermo-mechanical problems during the PhD thesis of Rohit Pethe, each

physics being associated its own mesh, with applications to linear friction welding or the generation of shear band by thermal softening in a hat-shaped test specimen. A second example follows from the PhD thesis of Jorge de Anda Salazar with variational approaches applied to transient diffusion of species. More specifically, the main contributions of this PhD are (i) an original way of deriving multi-field variational principles based on Onsager's principle, (ii) the derivation of partitioned schemes through the introduction of explicit dependencies between the various fields during the computation of stationary points then reinterpreted as consistent physically-based block-preconditionners, (iii) the extension of the variational approach to the electrochemical coupling and its illustration on a cathode-electrolyte system of a lithium-ion electrical battery.

2. *the development of efficient computational approaches for multi-scale analysis of transient diffusion systems coupled mechanics*, especially the content of the PhD thesis of Abdullah Waseem. The definition of reduced models for numerical homogenization allowed on the one hand to dramatically reduce the computational cost provided an assumed regime of relaxed separation of scales and a linear constitutive response of constituents, and on the other hand to define enriched continua at the macroscale, embedding only a limited number enrichment variables accounting for local transient effects, easing the two-scale solution process. Illustrations were also performed on a cathode-electrolyte system of a lithium-ion battery with active particles, simulating their swelling and shrinking through diffusion of species. An opening of former works to a framework encompassing non-linear constitutive responses was also carried out through the definition of a so-called data-driven reduced homogenization.

3. *the analysis and the development of mechanical processes dedicated to the assembly or the disassembly of heterogeneous structures.* Contributions in this area were related on the one hand to Friction Stir Spot Welding during my PhD thesis, through the development of a fully implicit monolithic thermo-mechanically coupled fluid/solid solver in an Arbitrary Lagrangian Eulerian context plus some experimental devices. On the other hand, some research actions were pursued around high pulsed power technologies, and more specifically via the electromagnetic and electro-hydraulic technologies. Contributions are (i) the development of a reduced order modeling of eddy current equations for an electromagnetic compression device, (ii) the analysis of electromagnetic flanging, (iii) an opening towards the electromagnetic disassembly of laminate hybrid structures via an analytical solution, and (iv) the design of an electro-hydraulic crimping device for dynamic ring/tube assemblies.

4. *the development of means for experimental testing at high strain rates.* The purpose of the PhD thesis of Xiaoli Guo was to design a direct impact Hopkinson device of reduced size, devoted to testing compression specimen at strain rates of the order of $10^4 s^{-1}$, in order to qualify the constitutive responses of some metallic alloys in those ranges, with applications to magnetic pulse welding technologies.

5. *the exploitation and the development of the framework defined by conservative formulations for computational fast solid dynamics.* These formulations widely used in Computational Fluid Dynamics are very little used and known in the community of solid mechanics, mainly only within a niche market related to shock-capturing simulations. However, their interest can be wider than that since they allow to unify into a well-posed mathematical framework coupled thermo-mechanical analyses in solid mechanics related to areas of applications already covered by both structural codes and hydrocodes. Contributions in that domain were related to

    i. the exploitation and the extension of existing shock-capturing methods for the approximation of plastic waves,

    ii. the completion of the thermodynamic consistency of the approach by introducing a variational principle and an associated constitutive update whose input data is the internal energy density in addition to a strain measure, which perfectly couples with the solution of the conservation of the total energy embedded in the framework of conservative formulations, or with existing hydro-codes (i.e. solving the balance of internal energy),

    iii. the proposition of Lagrangian conservative particle-based shock-capturing methods dedicated to large strains problems, especially the development of first versions of the Discontinuous Galerkin Material Point Method (DGMPM), but also a collaboration with Swansea university regarding the conservative Smooth Particle Hydrodynamics (SPH) method.

3.2 A few perspectives

Natural extensions of previous works are associated with *diffusive systems*, *conservative formulations* for fast solid dynamics, and *dynamic assembly processes*.

Diffusive systems coupled mechanics Works carried out on diffusive systems reported in Chapter 1 took advantage from both phenomenological approach at the macroscopic level and advanced averaging theories, which constitute two complementary approaches to address the modeling and numerical simulation of these systems. The two above approaches admit many further areas of investigation. Especially, they are expected to be extended to the coupling with dissipative effects in mechanics, but also with other physics (electrical, thermal effects). They can both profit from variational calculus, in order to build well-posed modelings of multi-field and multi-physic problems, as well as naturally derive consistent and efficient computational methods. At last, the reduced order modeling for multi-scale problems should readily be extended to embody various kinds of non-linearities, such as a non-linear diffusion response, or a non-linear response of the mechanical part (large strains, plasticity, micro-cracks developed at the microscale). A first attempt based on *data-driven reduced homogenization* has been presented in Section 1.4.4, which appears as one route among others for such extension. However, the challenge of this extension lies in the extraction of a reduced bases set, since an eigenvalue problem is not at hand in the non-linear case.

Conservative formulations and shock-capturing schemes Further developments of the research topic associated with fast transient solid dynamics (summarized in Section 2.4) may follow two main areas of investigation.

A first area of investigation pertains to the *Discontinuous Galerkin Material Point Method (DGMPM)*, whose development is very far from being fixed. Generally speaking, its development revolves around (i) the development of its approximation, (ii) its coupling with various physics, and (iii) the development and the exploitation of its capabilities of adaptivity. So far, only a few items of point (i) have been addressed, although many features of its approximation are still lacking and are parts of perspectives. The point (ii) involves various couplings with other systems of equations like different physics, which may be of interest for several applications. Its extension to coupled thermo-mechanics can profit from developments shown in Section 2.4.5. Further, a coupling with electromagnetism would permit to connect with applications of electromagnetic forming (see Sections 2.2.2.1 and 3.2), taking advantage of the arbitrary grid as a geometrical support for the approximation of electromagnetic equations in their eddy current formulation. The last point (iii) regarding the capabilities of adaptivity of the method has even not started to be addressed so far. The DGMPM should indeed be able to combine p-adaption, and h-adaption taking advantage of the arbitrary grid. But the combination of both should yield ppc-adaption (ppc stands for particle per cell), since there is a one-to-one relation between the number of particle per cell, the local order of approximation, and the type and order of the numerical integration.

A second area of investigation is associated with *the exploitation of variational calculus for fast transient solid dynamics*. Various extensions of the coupled variational principle recalled in Section 2.4.5 are envisaged. Especially its mechanical content can be enriched, for instance accounting for non-linear kinematic hardening as initiated by Mosler [90] in another framework, or accounting for other physical phenomena. Next, there would be a great interest in finding a unified functional, gathering both non-rate and rate-type variational principles, whose Euler-Lagrange equations would yield both conservation laws (2.6) and (dissipative) constitutive equations.

Dynamic assembly processes Mechanical processes dedicated to the assembly or the disassembly of heterogeneous structures appears as a great playground for the study of thermo-mechanical systems. A first area of investigation pertains to *the exploitation of their principles*. Considering high pulse power processes, many new geometrical configurations or functions dedicated to particular industrial applications can be proposed. For instance, the on-going PhD thesis of Benoit Lagain aims at performing both magnetic pulse assembly and disassembly of hybrid metal/composite structures. The exploitation of high pulse power technolgies may allow to perform in the future strong advances in dynamic assembly or disassembly of hybrid structures, of various geometries and related to various industrial applications.

A second area of investigation is associated with *a better understanding of some (thermo-mechanical) physical phenomena occurring at fine scale*, and to try to relate them to macroscopic process parameters. Indeed various phenomena occur at fine scale during Magnetic Pulse Welding (MPW), like jetting, wavy pattern and so on, which yet known in principle still require more experimental data and informations on their magnitude, triggering effects or chronology of events. They especially require quantitative in situ observations at very fine space and time scales, in order to better understand the role of interface phenomena with the welded joint, and establish what precise relationship can be drawn between the electromagnetic loading, the path of waves in the structure, the propagated mechanical states and the modification of the interface geometry. Besides, these observations should not only be kinematical ones, but conducting local energy balance at these scales could allow to better understand thermally-induced mechanisms of change of microstructure.

A third area of investigation is *to propose various kinds of modeling of all or part of these processes*. Three types of relevant modelings and/or simulations can be associated with these processes. The first one consists in *defining simple modelings*, usually one-dimensional, which admit analytical solutions, and whose purpose is to explain one particular phenomenon, or to find a range for its occurrence by restricting the range of possibilities. These solutions are usually much valuable, and allow to better orientate the subsequent research work. The last last example pertains to finding electromagnetic disassembly conditions [175]. However, others related to oblique impacts and associated shear instability of an interface may be of interest in the future. Second, at the opposite of the previous light models, high-resolution numerical simulations of impacts on dissipative solids may be required to relate the history of wave paths to the residual state, while considering more complex geometries and physical content. This is the purpose of the on-going development of numerical methods based on conservative formulations (see Section 2.4). Provided this approach is much more computationally intensive than the former one, it should only be applied to describe well-defined objectives, such as these related to the second area of investigation. A third kind of approach can involve simplified modelings via the definition of homogenized equivalent media in dynamics. Indeed, the welding occurs at some microscopic scale close to the interface, while the overall motion can be observed at a macroscopic one, leading to a multi-scale problem. An efficient description could indeed take advantage of the construction of homogeneous equivalent media to address such interface two-scale problem while preventing huge computational cost.

References

[1] A. Fick. "On liquid diffusion." In: *Philosophical Magazine Series 4* 10.63 (1855), pp. 30–39.

[2] P.L. Kapitsa. "A method for producing strong magnetic fields." In: *Proceedings of Royal Society Serine A* 105 (1924), pp. 691–710.

[3] Lars Onsager. "Reciprocal relations in irreversible processes. I." In: *Physical review* 37.4 (1931), p. 405.

[4] Geoffrey Ingram Taylor and H Quinney. "The latent energy remaining in a metal after cold working." In: *Proceedings of the Royal Society of London. Series A, Containing Papers of a Mathematical and Physical Character* 143.849 (1934), pp. 307–326.

[5] Lars Onsager. "Theories and problems of liquid diffusion." In: *Annals of the New York Academy of Sciences* 46 (1945), pp. 241–265.

[6] Horatio Scott Carslaw and John Conrad Jaeger. *Conduction of heat in solids*. Oxford, Clarendon press, 1947.

[7] Herbert Kolsky. "An investigation of the mechanical properties of materials at very high rates of loading." In: *Proceedings of the physical society. Section B* 62.11 (1949), p. 676.

[8] Cornelius Lanczos. *The variational principles of mechanics*. Oxford University Press, 1949.

[9] John Von Neumann and Robert D. Richtmyer. "A method for the numerical calculation of hydrodynamic shocks." In: *Journal of applied physics* 21.3 (1950), pp. 232–237.

[10] Maurice Anthony Biot. "Thermoelasticity and irreversible thermodynamics." In: *Journal of applied physics* 27.3 (1956), pp. 240–253.

[11] MA Biot. "Linear thermodynamics and the mechanics of solids. Proceedings of the third US National Congress of Applied Mechanics." In: *Published by ASME* (1958).

[12] P. Lax and B. Wendroff. "Systems of conservation laws." In: *Communications on Pure and Applied mathematics* 13.2 (1960), pp. 217–237.

[13] Francis H. Harlow. *The particle-in-cell method for numerical solution of problems in fluid dynamics*. Tech. rep. Los Alamos Scientific Lab., N. Mex., 1962.

[14] R.D. Richtmyer. *A survey of difference methods for non-steady fluid dynamics*. Tech. rep. Technical Notes 63-2. National Center for Atmospheric Research, 1962.

[15] George Herrmann. "On variational principles in thermoelasticity and heat conduction." In: *Quarterly of Applied Mathematics* 21.2 (1963), pp. 151–155.

[16] M.L. Wilkins. "Methods in computational physics." In: vol. 3. Academic Press, 1964. Chap. Calculation of elastic-plastic flow, pp. 211–263.

[17] M. Ben-Amoz. "On a variational theorem in coupled thermoelasticity." In: *Journal of Applied Mechanics* 32 (1965), pp. 943–945.

[18] K. Kojima. "Formage par décharge dans un liquide." In: *B. of the Japan Institute of Metals* 4.3 (1965), pp. 205–213.

[19] R.J. Clifton. *An analysis of combined longitudinal and torsional plastic waves in a thin-walled tube*. Tech. rep. TR-5. Brown university Providence R.I, Division of Engineering, 1966.

[20] R. Craig and M. Bampton. "Coupling of substructures for dynamic analyses." In: *AIAA journal* 6.7 (1968), pp. 1313–1319.

[21] C.K.H. Dharan and F.E. Hauser. "Determination of stress-strain characteristics at very high strain rates." In: *Experimental Mechanics* 10.9 (1970), pp. 370–376.

[22] Michael Berliner Bever, David Lewis Holt, and Alan Lee Titchener. "The stored energy of cold work." In: *Progress in materials science* 17 (1973), pp. 5–177.

[23] Bernard Halphen and Quoc Son Nguyen. "Sur les matériaux standard généralisés." In: *Journal de mécanique* 14 (1975), pp. 39–63.

[24] John M. Ball. "Convexity conditions and existence theorems in nonlinear elasticity." In: *Archive for rational mechanics and Analysis* 63.4 (1976), pp. 337–403.

[25] Leon B. Lucy. "A numerical approach to the testing of the fission hypothesis." In: *The astronomical journal* 82 (1977), pp. 1013–1024.

[26] D. A. Gorham. "Measurement of stress-strain properties of strong metals at very high rates of strain." In: *Institute of Physics Conference Series*. 47. 1979, pp. 16–24.

[27] A. Maewal. "Homogenization for Transient Heat Conduction." In: *Journal of Applied Mechanics* 46 (1979), pp. 945–946.

[28] Alexander N. Brooks and Thomas J.R. Hughes. "Streamline upwind/Petrov-Galerkin formulations for convection dominated flows with particular emphasis on the incompressible Navier-Stokes equations." In: *Computer methods in applied mechanics and engineering* 32.1-3 (1982), pp. 199–259.

[29] G. Francfort. "Homogenization and rapid Oscillations in Linear Thermoelasticity." In: *CRAS Série I* 295 (1982), pp. 367–370.

[30] G. R. Johnson and W. H. Cook. "A constitutive model and data for metals subjected to large strains, high strain rates and high temperatures." In: *Proceedings of the 7th International Symposium on Ballistics* (1983), pp. 541–547.

[31] Douglas N. Arnold, Franco Brezzi, and Michel Fortin. "A stable finite element for the Stokes equations." In: *Calcolo* 21.4 (1984), pp. 337–344.

[32] A. Chrysochoos. "Bilan énergétique en élastoplasticité grandes déformations." In: *Journal de Mécanique théorique et appliquée* 4.5 (1985), pp. 589–614.

[33] Tai-Ping Liu. "Hyperbolic conservation laws with relaxation." In: *Communications in mathematical physics* 108 (1987), pp. 153–175.

[34] A. Molinari and M. Ortiz. "Global viscoelastic behavior of heterogeneous thermoelastic materials." In: *International journal of solids and structures* 23.9 (1987), pp. 1285–1300.

[35] Frank J. Zerilli and Ronald W. Armstrong. "Dislocation-mechanics-based constitutive relations for material dynamics calculations." In: *Journal of applied physics* 61.5 (1987), pp. 1816–1825.

[36] Bradley J. Plohr and David H. Sharp. "A conservative Eulerian formulation of the equations for elastic flow." In: *Advances in Applied Mathematics* 9.4 (1988), pp. 481–499.

[37] László Szabó and Mihály Balla. "Comparison of some stress rates." In: *International journal of solids and structures* 25.3 (1989), pp. 279–297.

[38] J.A. Trangenstein and P. Collela. "A higher-order Godunov method for modeling finite deformation in elastic-plastic solids." In: *Communications in Pure Applied mathematics* 47 (1991), pp. 41–100.

[39] F. Armero and J.C. Simo. "A new unconditionally stable fractional step method for non-linear coupled thermomechanical problems." In: *International Journal for numerical methods in Engineering* 35.4 (1992), pp. 737–766.

[40] David J. Benson. "Computational methods in Lagrangian and Eulerian hydrocodes." In: *Computer Methods in Applied Mechanics and Engineering* 99 (1992), pp. 235–394.

[41] D. Burgess, D. Sulsky, and J.U. Brackbill. "Mass matrix formulation of the FLIP particle-in-cell method." In: *Journal of Computational Physics* 103.1 (1992), pp. 1–15.

[42] D. A. Gorham, P. H. Pope, and J. E. Field. "An improved method for compressive stress-strain measurements at very high strain rates." In: *Philosophical Transactions of the Royal Society of London. Series A. Mathematical and Physical Sciences* 438.A (1992 1992), pp. 153–170.

[43] Joe J. Monaghan. "Smoothed particle hydrodynamics." In: *Annual review of astronomy and astrophysics* 30 (1992), pp. 543–574.

[44] J.C. Simo and C. Miehe. "Associative coupled thermoplasticity at finite strains: Formulation, numerical analysis and implementation." In: *Computer Methods in Applied Mechanics and Engineering* 98.1 (1992), pp. 41–104.

[45] X. Lin and J. Ballman. “A Riemann solver and a second-order Godunov method for elastic-plastic wave propagation in solids.” In: *International Journal of Impact Engineering* 13 (1993), pp. 463–478.

[46] Venkata S. Balanethiram and Glenn S. Daehn. “Hyperplasticity: Increased forming limits a high workpiece velocity.” In: *Scripta Metallurgica et Materialia;(United States)* 30.4 (1994).

[47] G.Q. Chen, C.D. Levermore, and T.P. Liu. “Hyperbolic conservation laws with stiff relaxation terms and entropy.” In: *Communications on pure and applied mathematics* 47.6 (1994), pp. 787–830.

[48] Jerrold E. Marsden and Thomas J.R. Hughes. *Mathematical foundations of elasticity*. Courier Corporation, 1994.

[49] J.J. Mason, A.J. Rosakis, and G. Ravichandran. “On the strain and strain rate dependence of the fraction of plastic work converted to heat: an experimental study using high speed infrared detectors and the Kolsky bar.” In: *Mechanics of Materials* 17.2-3 (1994), pp. 135–145.

[50] Deborah Sulsky, Zhen Chen, and Howard L. Schreyer. “A particle method for history-dependent materials.” In: *Computer methods in applied mechanics and engineering* 118.1-2 (1994), pp. 179–196.

[51] T. Belytschko, Y. Krongauz, D. Organ, M. Fleming, and P. Krysl. “Meshless methods: An overview and recent developments.” In: *Computer Methods in Applied Mechanics and Engineering* 139.1 (1996), pp. 3–47.

[52] Han Zhao and Gérard Gary. “The testing and behaviour modelling of sheet metals at strain rates from 10- 4 to 104 s- 1.” In: *Materials Science and Engineering: A* 207.1 (1996), pp. 46–50.

[53] M. Rivara. “New longest edge algorithm for the refinement and/or improvement of unstructured triangulations.” In: *International Journal for Numerical Methods in Engineering* 40 (1997), pp. 3313–3324.

[54] M. Rivara and P. Inostroza. “Using longest-side bisection techniques for the automatic refinement of delaunay triangulations.” In: *International Journal for Numerical Methods in Engineering* 40 (1997), pp. 581–597.

[55] Gregg K. Fenton and Glenn S. Daehn. “Modeling of electromagnetically formed sheet metal.” In: *Journal of Materials Processing Technology* 75.1-3 (1998), pp. 6–16.

[56] Michael Ortiz and Laurent Stainier. “The variational formulation of viscoplastic constitutive updates.” In: *Computer methods in applied mechanics and engineering* 171.3-4 (1999), pp. 419–444.

[57] Daniel Rittel. “On the conversion of plastic work to heat during high strain rate deformation of glassy polymers.” In: *Mechanics of Materials* 31.2 (1999), pp. 131–139.

[58] T. Belytschko, W.K. Liu, and B. Moran. *Nonlinear finite elements for continua and structures*. Wiley, 2000.

[59] B. Ben Moussa and J.P. Vila. “Convergence of SPH method for scalar nonlinear conservation laws.” In: *SIAM Journal on Numerical Analysis* 37.3 (2000), pp. 863–887.

[60] Sia Nemat-Nasser. “Introduction to high strain rate testing.” In: *ASM handbook* 8 (2000), pp. 427–428.

[61] P. Rosakis, A.J. Rosakis, G. Ravichandran, and J. Hodowany. “A thermodynamic internal variable model for the partition of plastic work into heat and stored energy in metals.” In: *Journal of the Mechanics and Physics of Solids* 48.3 (2000), pp. 581–607.

[62] Bernardo Cockburn and Chi-Wang Shu. “Runge–Kutta discontinuous Galerkin methods for convection-dominated problems.” In: *Journal of scientific computing* 16.3 (2001), pp. 173–261.

[63] R. Sakano, K. Murakami, K. Yamashita, T. Hyoe, M. Fujimoto, M. Inuzuka, U. Nagao, and H. Kashiki. “Development of spot FSW robot system for automobile body members.” In: *Third International Symposium of Friction Stir Welding*. Kobe, Japan, 2001.

[64] R.J. Leveque. *Finite volume methods for hyperbolic problems*. Cambridge University Press, 2002.

[65] Scott G. Bardenhagen and Edward M. Kober. “The generalized interpolation material point method.” In: *Computer Modeling in Engineering and Sciences* 5.6 (2004), pp. 477–496.

[66] Sophie Barradas, Michel Jeandin, C. Bolis, L. Berthe, M. Arrigoni, M. Boustie, and G. Barbezat. “Study of adhesion of PROTAL® copper coating of Al 2017 using the laser shock adhesion test (LASAT).” In: *Journal of materials science* 39.8 (2004), pp. 2707–2716.

[67] Jean-Claude Michel and Pierre Suquet. "Computational analysis of nonlinear composite structures using the nonuniform transformation field analysis." In: *Computer methods in applied mechanics and engineering* 193.48-51 (2004), pp. 5477–5502.

[68] L. Pareschi and G. Russo. "Implicit-Explicit Runge-Kutta schemes and applications to hyperbolic systems with relaxation." In: *Journal of scientific computing* 25 (2005), pp. 129–155.

[69] Mala Seth, Vincent J. Vohnout, and Glenn S. Daehn. "Formability of steel sheet in high velocity impact." In: *Journal of materials processing technology* 168.3 (2005), pp. 390–400.

[70] John O. Hallquist et al. "LS-DYNA theory manual." In: *Livermore software Technology corporation* (2006).

[71] Juan C. Simo and Thomas J.R. Hughes. *Computational inelasticity*. Vol. 7. Springer Science & Business Media, 2006.

[72] Qiang Yang, Laurent Stainier, and Michael Ortiz. "A variational formulation of the coupled thermo-mechanical boundary-value problem for general dissipative solids." In: *Journal of the Mechanics and Physics of Solids* 54.2 (2006), pp. 401–424.

[73] J. Mosler and M. Ortiz. "Variational h-adaption in finite deformation elasticity and plasticity." In: *International Journal for Numerical Methods in Engineering* 72.5 (2007), pp. 505–523.

[74] *SYSWELD®*. User's manual, ESI Group. 2007.

[75] L. Wang. *Foundations of stress waves*. Elsevier, 2007.

[76] R.W. Armstrong and S.M. Walley. "High strain rate properties of metals and alloys." In: *International Materials Reviews* 53.3 (2008), pp. 105–128.

[77] Blaise Bourdin, Gilles A. Francfort, and Jean-Jacques Marigo. "The variational approach to fracture." In: *Journal of elasticity* 91.1 (2008), pp. 5–148.

[78] Sergey L. Gavrilyuk, Nicolas Favrie, and Richard Saurel. "Modelling wave dynamics of compressible elastic materials." In: *Journal of computational physics* 227.5 (2008), pp. 2941–2969.

[79] Gilles Kluth and Bruno Després. "Perfect plasticity and hyperelastic models for isotropic materials." In: *Continuum Mechanics and Thermodynamics* 20.3 (2008), pp. 173–192.

[80] K. T. Ramesh. "Part D: Chapter 33. High strain rate and impact experiments." In: *Springer handbook of experimental solid mechanics*. Springer, 2008, pp. 1–31.

[81] Nicolas Ranc, L. Taravella, Vincent Pina, and Philippe Hervé. "Temperature field measurement in titanium alloy during high strain rate loading—adiabatic shear bands phenomenon." In: *Mechanics of Materials* 40.4-5 (2008), pp. 255–270.

[82] S Ma, X Zhang, and XM Qiu. "Comparison study of MPM and SPH in modeling hypervelocity impact problems." In: *International journal of impact engineering* 36.2 (2009), pp. 272–282.

[83] J Mosler and M Ortiz. "An error-estimate-free and remapping-free variational mesh refinement and coarsening method for dissipative solids at finite strains." In: *International Journal for Numerical Methods in Engineering* 77.3 (2009), pp. 437–450.

[84] I. Negreanu, G. Gary, and D. Mohr. "Enhanced infrared radiation method for temperature measurement in dynamic experiments." In: *Society for Experimental Mechanics - SEM Annual Conference and Exposition on Experimental and Applied Mechanics 2009* 1 (Jan. 2009), pp. 86–88.

[85] Francisco Chinesta, Amine Ammar, and Elias Cueto. "Recent advances and new challenges in the use of the proper generalized decomposition for solving multidimensional models." In: *Archives of Computational methods in Engineering* 17.4 (2010), pp. 327–350.

[86] Marc G.D. Geers, Varvara G. Kouznetsova, and W. Brekelmans. "Multi-scale computational homogenization: Trends and challenges." In: *Journal of computational and applied mathematics* 234.7 (2010), pp. 2175–2182.

[87] Thomas Heuzé, Jean-Baptiste Leblond, Jean-Michel Bergheau, and Éric Feulvarch. "A finite element for laminar flow of incompressible fluids with inertia effects and thermomechanical coupling." In: *European Journal of Computational Mechanics/Revue Européenne de Mécanique Numérique* 19.1-3 (2010), pp. 293–304.

[88] F. Larsson, K. Runesson, and F. Su. "Variationally consistent computational homogenization of transient heat flow." In: *International Journal for Numerical Methods in Engineering* 81 (2010), pp. 1659–1686.

[89] J. Mosler and O.T. Bruhns. "On the implementation of rate-independent standard dissipative solids at finite strain–Variational constitutive updates." In: *Computer Methods in Applied Mechanics and Engineering* 199.9-12 (2010), pp. 417–429.

[90] Jörn Mosler. "Variationally consistent modeling of finite strain plasticity theory with non-linear kinematic hardening." In: *Computer Methods in Applied Mechanics and Engineering* 199.45-48 (2010), pp. 2753–2764.

[91] Anthony Nouy. "A priori model reduction through proper generalized decomposition for solving time-dependent partial differential equations." In: *Computer Methods in Applied Mechanics and Engineering* 199.23-24 (2010), pp. 1603–1626.

[92] Laurent Stainier and Michael Ortiz. "Study and validation of a variational theory of thermo-mechanical coupling in finite visco-plasticity." In: *International Journal of Solids and Structures* 47.5 (2010), pp. 705–715.

[93] M. Canadija and Jörn Mosler. "On the thermomechanical coupling in finite strain plasticity theory with non-linear kinematic hardening by means of incremental energy minimization." In: *International Journal of Solids and Structures* 48.7-8 (2011), pp. 1120–1129.

[94] Thomas Heuzé, Jean-Baptiste Leblond, and Jean-Michel Bergheau. "Modélisation des couplages fluide/solide dans les procédés d'assemblage à haute température." In: *Mechanics & Industry* 12.3 (2011), pp. 183–191.

[95] Thomas Heuzé, Joël Rech, F. Dumont, Jean-Baptiste Leblond, and Jean-Michel Bergheau. "Two experimental set-ups designed for investigation of friction stir spot welding process." In: *Science and Technology of Welding and Joining* 16.8 (2011), pp. 735–744.

[96] R. Neugebauer, K.D. Bouzakis, B. Denkena, F. Klocke, A. Sterzing, A.E. Tekkaya, and R. Wertheim. "Velocity effects in metal forming and machining processes." In: *CIRP annals* 60.2 (2011), pp. 627–650.

[97] Verena Psyk, D. Risch, Brad L. Kinsey, A. Erman Tekkaya, and M. Kleiner. "Electromagnetic forming—a review." In: *Journal of Materials Processing Technology* 211.5 (2011), pp. 787–829.

[98] Laurent Stainier. "Consistent incremental approximation of dissipation pseudo-potentials in the variational formulation of thermo-mechanical constitutive updates." In: *Mechanics research communications* 38.4 (2011), pp. 315–319.

[99] J.L. Auriault. "Wave propagation and transient heat transfer in thermoelastic composites." In: *International Journal of Heat and Mass Transfer* 55 (2012), pp. 5972–5978.

[100] Nikolaus Bleier and Jörn Mosler. "Efficient variational constitutive updates by means of a novel parameterization of the flow rule." In: *International journal for numerical methods in engineering* 89.9 (2012), pp. 1120–1143.

[101] Violette Brulliard, Erwan Verron, and Steven Le Corre. "Derivation of a New Model Including the Effect of Swelling on Finite Strain Properties for Polymeric Gels." In: *Engineering Systems Design and Analysis*. Vol. 44878. American Society of Mechanical Engineers. 2012, pp. 403–412.

[102] Camille Chauvin, Jacques Petit, and Frederic Sinatti. "An application of the emissive layer technique to temperature measurement by infrared optical pyrometer." In: *AIP Conference Proceedings*. Vol. 1426. 1. American Institute of Physics. 2012, pp. 368–371.

[103] Francesco Dell'Isola and Sergey Gavrilyuk. *Variational models and methods in solid and fluid mechanics*. Vol. 535. Springer Science & Business Media, 2012.

[104] John Newman and Karen E. Thomas-Alyea. *Electrochemical systems*. John Wiley & Sons, 2012.

[105] J. M. Bergheau and R. Fortunier. *Finite element simulation of heat transfer*. John Wiley & Sons, 2013.

[106] David E. Keyes, Lois C. McInnes, Carol Woodward, William Gropp, Eric Myra, Michael Pernice, John Bell, Jed Brown, Alain Clo, Jeffrey Connors, et al. "Multiphysics simulations: Challenges and opportunities." In: *The International Journal of High Performance Computing Applications* 27.1 (2013), pp. 4–83.

[107] C.H. Lee, A.J. Gil, and J. Bonet. "Development of a cell centred upwind finite volume algorithm for a new conservation law formulation in structural dynamics." In: *Computers and Structures* 118 (2013), pp. 13–38.

[108] P.H. Maire, R. Abgrall, J. Breil, R. Loubère, and B. Rebourcet. "A nominally second-order cell-centered Lagrangian scheme for simulating elastic-plastic flows on two dimensional unstructured grids." In: *Journal of Computational Physics* 235 (2013), pp. 626–665.

[109] K. Pham, V. G. Kouznetsova, and M. G. D. Geers. "Transient computational homogenization for heterogeneous materials under dynamic excitation." In: *Journal of the Mechanics and Physics of Solids* 61.11 (2013), pp. 2125–2146.

[110] Rian Seghir, Jean-Francois Witz, Laurence Bodelot, Eric Charkaluk, and Philippe Dufrenoy. "An improved lagrangian thermography procedure for the quantification of the temperature fields within polycrystals." In: *Quantitative InfraRed Thermography Journal* 10.1 (2013), pp. 74–95.

[111] Laurent Stainier. "A variational approach to modeling coupled thermo-mechanical nonlinear dissipative behaviors." In: *Advances in Applied Mechanics* 46 (2013), pp. 69–126.

[112] E.F. Toro. *Riemann solvers and numerical methods for fluid dynamics*. Springer, 2013.

[113] Diego Avesani, Michael Dumbser, and Alberto Bellin. "A new class of Moving-Least-Squares WENO–SPH schemes." In: *Journal of Computational Physics* 270 (2014), pp. 278–299.

[114] Violette Brulliard. "Etude du comportement du Nucleus pulposus à l'aide d'un modèle couplant grandes déformations et diffusion." available at https://hal.archives-ouvertes.fr/tel-01224563. PhD thesis. Ecole Centrale de Nantes (ECN), 2014.

[115] Xiaoli Guo, Thomas Heuzé, Ramzi Othman, and Guillaume Racineux. "Inverse Identification at Very High Strain Rate of the Johnson–Cook Constitutive Model on the Ti-6Al-4 V Alloy With a Specially Designed Direct-impact Kolsky Bar Device." In: *Strain* 50.6 (2014), pp. 527–538.

[116] Thomas Heuzé, Hussein Amin-El-Sayed, Jean-Baptiste Leblond, and Jean-Michel Bergheau. "Benchmark tests based on the Couette viscometer—II: Thermo-elasto-plastic solid behaviour in small and large strains." In: *Computers & Mathematics with Applications* 67.8 (2014), pp. 1482–1496.

[117] Thomas Heuzé, Jean-Baptiste Leblond, and Jean-Michel Bergheau. "Benchmark tests based on the Couette viscometer—I: Laminar flow of incompressible fluids with inertia effects and thermomechanical coupling." In: *Computers & Mathematics with Applications* 67.10 (2014), pp. 1925–1937.

[118] Christian Miehe, Steffen Mauthe, and H. Ulmer. "Formulation and numerical exploitation of mixed variational principles for coupled problems of Cahn–Hilliard-type and standard diffusion in elastic solids." In: *International journal for numerical methods in engineering* 99.10 (2014), pp. 737–762.

[119] Alexander Bartels, Thorsten Bartel, M. Canadija, and Jörn Mosler. "On the thermomechanical coupling in dissipative materials: a variational approach for generalized standard materials." In: *Journal of the Mechanics and Physics of Solids* 82 (2015), pp. 218–234.

[120] Javier Bonet, Antonio J. Gil, Chun Hean Lee, Miquel Aguirre, and Rogelio Ortigosa. "A first order hyperbolic framework for large strain computational solid dynamics. Part I: Total Lagrangian isothermal elasticity." In: *Computer Methods in Applied Mechanics and Engineering* 283 (2015), pp. 689–732.

[121] Xiaoli Guo. "On the direct impact Hopkinson system for dynamic tests at very high stain rates." PhD thesis of École Centrale de Nantes, 2015.

[122] S. Ndanou, N. Favrie, and S. Gavrilyuk. "Multi-solid and multi-fluid diffuse interface model: Applications to dynamic fracture and fragmentation." In: *Journal of Computational Physics* 295 (2015), pp. 523–555.

[123] M. Canadija and Jörn Mosler. "A variational formulation for thermomechanically coupled low cycle fatigue at finite strains." In: *International Journal of Solids and Structures* 100 (2016), pp. 388–398.

[124] S Gavrilyuk, S Ndanou, and S Hank. "An example of a one-parameter family of rank-one convex stored energies for isotropic compressible solids." In: *Journal of Elasticity* 124.1 (2016), pp. 133–141.

[125] Thomas Heuzé, Adrien Leygue, and Guillaume Racineux. "Parametric modeling of an electromagnetic compression device with the proper generalized decomposition." In: *International Journal of Material Forming* 9.1 (2016), pp. 101–113.

[126] T. Kirchdoerfer and M. Ortiz. "Data-driven computational mechanics." In: *Computer Methods in Applied Mechanics and Engineering* 304 (2016), pp. 81–101.

[127] Quoc-Son Nguyen. "Quasi-static responses and variational principles in gradient plasticity." In: *Journal of the Mechanics and Physics of Solids* 97 (2016), pp. 156–167.

[128] A. Sridhar, V. G. Kouznetsova, and M. G. D. Geers. "Homogenization of locally resonant acoustic metamaterials towards an emergent enriched continuum." In: *Computational Mechanics* 57.3 (2016), pp. 423–435.

[129] Xiong Zhang, Zhen Chen, and Yan Liu. *The material point method: a continuum-based particle method for extreme loading cases*. Academic Press, 2016.

[130] Thomas Heuzé. "Lax–Wendroff and TVD finite volume methods for unidimensional thermomechanical numerical simulations of impacts on elastic–plastic solids." In: *Journal of Computational Physics* 346 (2017), pp. 369–388.

[131] G. R. Ramos, T. dos Santos, and R. Rossi. "An extension of the Hill–Mandel principle for transient heat conduction in heterogeneous media with heat generation incorporating finite RVE thermal inertia effects." In: *International Journal for Numerical Methods in Engineering* 111.6 (2017), pp. 553–580.

[132] Reza Adibi-Asl and R Seshadri. "Variational method in limit load analysis—a review." In: *Journal of Pressure Vessel Technology* 140.5 (2018).

[133] Laurence Brassart and Laurent Stainier. "Effective transient behaviour of inclusions in diffusion problems." In: *ZAMM-Journal of Applied Mathematics and Mechanics/Zeitschrift für Angewandte Mathematik und Mechanik* 98.6 (2018), pp. 981–998.

[134] Anthony Collé, Jérôme Limido, and Jean-Paul Vila. "An accurate SPH scheme for dynamic fragmentation modelling." In: *EPJ Web of Conferences*. Vol. 183. EDP Sciences. 2018, p. 01030.

[135] Rui Fang, Philipp Farah, Alexander Popp, and Wolfgang A Wall. "A monolithic, mortar-based interface coupling and solution scheme for finite element simulations of lithium-ion cells." In: *International Journal for Numerical Methods in Engineering* 114.13 (2018), pp. 1411–1437.

[136] Volker Fohrmeister, Alexander Bartels, and Jörn Mosler. "Variational updates for thermomechanically coupled gradient-enhanced elastoplasticity—implementation based on hyper-dual numbers." In: *Computer Methods in Applied Mechanics and Engineering* 339 (2018), pp. 239–261.

[137] Thomas Heuzé. "Simulation of impacts on elastic–viscoplastic solids with the flux-difference splitting finite volume method applied to non-uniform quadrilateral meshes." In: *Advanced Modeling and Simulation in Engineering Sciences* 5.1 (2018), pp. 1–32.

[138] Thomas Heuzé, Xiaoli Guo, and Ramzi Othman. "Very high strain rate range." In: *The Kolsky-Hopkinson Bar Machine*. Springer, 2018, pp. 249–272.

[139] S. Kaessmair and P. Steinmann. "Computational first-order homogenization in chemo-mechanics." In: *Archive of Applied Mechanics* 88.1-2 (2018), pp. 271–286.

[140] Adrien Renaud. "Discontinuous Galerkin Material Point Method: application to hyperbolic problems in solid mechanics." Available at https://hal.archives-ouvertes.fr/tel-02052066. PhD thesis of École Centrale de Nantes, 2018.

[141] Adrien Renaud, Thomas Heuzé, and Laurent Stainier. "A Discontinuous Galerkin Material Point Method for the solution of impact problems in solid dynamics." In: *Journal of computational physics* 369 (2018), pp. 80–102.

[142] Cheikh Tidiane Sow. "Étude et développement du procédé de sertissage électrohydraulique." PhD thesis of École Centrale de Nantes, 2018.

[143] Jorge de Anda Salazar. "Development of variational models & algorithmic strategies for coupled problems." Available at https://hal.archives-ouvertes.fr/tel-02944072. PhD thesis of École Centrale de Nantes, 2019.

[144] Laurence Brassart and Laurent Stainier. "Effective transient behaviour of heterogeneous media in diffusion problems with a large contrast in the phase diffusivities." In: *Journal of the Mechanics and Physics of Solids* 124 (2019), pp. 366–391.

[145] Thomas Heuzé. "Lax-Wendroff schemes for elastic-plastic solids." In: *Journal of Computational Physics* 396 (2019), pp. 89–105.

[146] Chun Hean Lee, Antonio J. Gil, Ataollah Ghavamian, and Javier Bonet. "A Total Lagrangian upwind Smooth Particle Hydrodynamics algorithm for large strain explicit solid dynamics." In: *Computer Methods in Applied Mechanics and Engineering* 344 (2019), pp. 209–250.

[147] Adrien Leygue, Rian Seghir, Julien Réthoré, Michel Coret, Erwan Verron, and Laurent Stainier. "Non-parametric material state field extraction from full field measurements." In: *Computational Mechanics* 64.2 (2019), pp. 501–509.

[148] Yihuan Li, Wenyu Lai, and Yongxing Shen. "Variational h-adaption method for the phase field approach to fracture." In: *International Journal of Fracture* 217.1-2 (2019), pp. 83–103.

[149] Ilya Peshkov, Walter Boscheri, Raphaël Loubère, Evgeniy Romenski, and Michael Dumbser. "Theoretical and numerical comparison of hyperelastic and hypoelastic formulations for Eulerian non-linear elasto-plasticity." In: *Journal of Computational Physics* 387 (2019), pp. 481–521.

[150] Rohit Pethe, Thomas Heuzé, and Laurent Stainier. "Variational h-adaption for coupled thermomechanical problems." In: *Engineering Computations* (2019).

[151] Rian Seghir, Fabrice Pierron, and Lloyd Fletcher. "Image-based stress field reconstruction in complex media." In: *Residual Stress, Thermomechanics & Infrared Imaging, Hybrid Techniques and Inverse Problems, Volume 7*. Springer, 2019, pp. 101–104.

[152] Saray Busto, Simone Chiocchetti, Michael Dumbser, Elena Gaburro, and Ilya Peshkov. "High order ADER schemes for continuum mechanics." In: *Frontiers in Physics* 8 (2020), p. 32.

[153] Chady Khalil, Surendar Marya, and Guillaume Racineux. "Magnetic pulse welding and spot welding with improved coil efficiency—Application for dissimilar welding of automotive metal alloys." In: *Journal of Manufacturing and Materials Processing* 4.3 (2020), p. 69.

[154] Rohit Pethe, Thomas Heuzé, and Laurent Stainier. "Remapping-free variational h-adaption for strongly coupled thermo-mechanical problems." In: *Finite Elements in Analysis and Design* 176 (2020), p. 103435.

[155] Adrien Renaud, Thomas Heuzé, and Laurent Stainier. "On loading paths followed inside plastic simple waves in two-dimensional elastic-plastic solids." In: *Journal of the Mechanics and Physics of Solids* 143 (2020), p. 104064.

[156] Adrien Renaud, Thomas Heuzé, and Laurent Stainier. "Stability properties of the Discontinuous Galerkin Material Point Method for hyperbolic problems in one and two space dimensions." In: *International Journal for Numerical Methods in Engineering* 121.4 (2020), pp. 664–689.

[157] Adrien Renaud, Thomas Heuzé, and Laurent Stainier. "The discontinuous Galerkin material point method for variational hyperelastic–plastic solids." In: *Computer Methods in Applied Mechanics and Engineering* 365 (2020), p. 112987.

[158] C.T. Sow, R. Lementec, T. Heuzé, and G. Racineux. "Development and optimization of the electrohydraulic crimping process." In: *International Conference on High Speed Forming (ICHSF)*. Dortmund, Sept. 2020.

[159] Cheikh Tidiane Sow, Grégoire Bazin, Thomas Heuzé, and Guillaume Racineux. "Electromagnetic flanging: from elementary geometries to aeronautical components." In: *International Journal of Material Forming* 13.3 (2020), pp. 423–443.

[160] Abdullah Waseem, Thomas Heuzé, Laurent Stainier, M.G.D. Geers, and V.G. Kouznetsova. "Model reduction in computational homogenization for transient heat conduction." In: *Computational Mechanics* 65.1 (2020), pp. 249–266.

[161] Abdullah Waseem, Thomas Heuzé, Laurent Stainier, Marc G.D. Geers, and Varvara G. Kouznetsova. "Enriched continuum for multi-scale transient diffusion coupled to mechanics." In: *Advanced Modeling and Simulation in Engineering Sciences* 7.1 (2020), pp. 1–32.

[162] Yuzhe Xiao, Chenghao Wan, Alireza Shahsafi, Jad Salman, and Mikhail A Kats. "Depth thermography: noninvasive 3D temperature profiling using infrared thermal emission." In: *ACS Photonics* 7.4 (2020), pp. 853–860.

[163] Jorge de Anda Salazar, Thomas Heuzé, and Laurent Stainier. "Multifield variational formulations of diffusion initial boundary value problems." In: *Continuum Mechanics and Thermodynamics* 33.2 (2021), pp. 563–589.

[164] Javier Bonet, Chun Hean Lee, Antonio J. Gil, and Ataollah Ghavamian. "A first order hyperbolic framework for large strain computational solid dynamics. Part III: Thermo-elasticity." In: *Computer Methods in Applied Mechanics and Engineering* 373 (2021), p. 113505.

[165] Ataollah Ghavamian, Chun Hean Lee, Antonio J. Gil, Javier Bonet, Thomas Heuzé, and Laurent Stainier. "An entropy-stable Smooth Particle Hydrodynamics algorithm for large strain thermo-elasticity." In: *Computer Methods in Applied Mechanics and Engineering* 379 (2021), p. 113736.

[166] Elizabeth M.C. Jones, Amanda R. Jones, and Caroline Winters. "Combined thermographic phosphor and digital image correlation (TP+ DIC) for simultaneous temperature and strain measurements." In: *Strain* (2021), e12415.

[167] Chady Khalil, Surendar Marya, and Guillaume Racineux. "Magnetic Pulse Hybrid Joining of Polymer Composites to Metals." In: *Metals* 11.12 (2021), p. 2001.

[168] L. Stainier. *ZorgLib*. User's manual. 2021.

[169] Adrien Vinel, Rian Seghir, Julien Berthe, Gérald Portemont, and Julien Réthoré. "Metrological assessment of multi-sensor camera technology for spatially-resolved ultra-high-speed imaging of transient high strain-rate deformation processes." In: *Strain* 57.4 (2021), e12381.

[170] Ping-Ping Wang, A-Man Zhang, Zi-Fei Meng, Fu-Ren Ming, and Xiang-Li Fang. "A new type of WENO scheme in SPH for compressible flows with discontinuities." In: *Computer Methods in Applied Mechanics and Engineering* 381 (2021), p. 113770.

[171] A Waseem, T Heuzé, L Stainier, M.G.D. Geers, and V.G. Kouznetsova. "Two-scale analysis of transient diffusion problems through a homogenized enriched continuum." In: *European Journal of Mechanics-A/Solids* 87 (2021), p. 104212.

[172] Abdullah Waseem, Thomas Heuzé, Marc G.D. Geers, Varvara G. Kouznetsova, and Laurent Stainier. "Data-driven reduced homogenization for transient diffusion problems with emergent history effects." In: *Computer Methods in Applied Mechanics and Engineering* 380 (2021), p. 113773.

[173] Walter Boscheri, Raphaël Loubère, and Pierre-Henri Maire. "A 3D cell-centered ADER MOOD Finite Volume method for solving updated Lagrangian hyperelasticity on unstructured grids." In: *Journal of Computational Physics* 449 (2022), p. 110779.

[174] Thomas Heuzé and Laurent Stainier. "A variational formulation of thermomechanical constitutive update for hyperbolic conservation laws." In: *Computer Methods in Applied Mechanics and Engineering* 394 (2022), p. 114893.

[175] Benoit Lagain, Thomas Heuzé, Guillaume Racineux, and Michel Arrigoni. "An analytical approach of design for recycling of laminate structures by the use of magnetic pulse disassembling." In: *International Journal of Solids and Structures* 275 (2023), p. 112290.

[176] Alaa Lakiss, Thomas Heuzé, Mikhael Tannous, and Laurent Stainier. "ADER Discontinuous Galerkin Material Point Method." In: *submitted to International Journal for Numerical Methods in Engineering* (2023).

[177] R. LeMentec, C. Sow, Thomas Heuzé, P. Rozycki, and G. Racineux. “Electrohydraulic crimping of tubes within rings.” In: *Metals* 13.8 (2023), p. 1382.